Gesellschaft für Anlagen- und Reaktorsicherheit (GRS) mbH

The DEBORA-Project: Development of Borehole Seals für High-Level Radioactive Waste - Phase II

Final Report

GRS - 161

Gesellschaft für Anlagen- und Reaktorsicherheit (GRS) mbH

The DEBORA-Project: Development of Borehole Seals for High-Level Radioactive Waste – Phase II

Final Report

T. Rothfuchs
H.-K. Feddersen
K.-P. Kröhn
R. Miehe
K. Wieczorek

With contributions of
A. Poley (NRG – Petten/NL)

Braunschweig
December 1999

Anmerkung:

Die diesem Bericht zugrundeliegenden Arbeiten wurden mit Mitteln des Bundesministeriums für Wirtschaft und Technologie (BMWi) unter dem Förderkennzeichen 02E8715 gefördert.

Die Verantwortung für den Inhalt dieser Veröffentlichung liegt allein bei den Autoren.

GRS - 161

Deskriptoren:
Endlager, Experiment, Geosphäre, Hochaktiver Abfall, Labor, Langzeitsicherheit, Modell, Salz, Technische Barriere

Foreword

During the phase I (1991 - 1995) of the DEBORA ("**De**velopment of **Bo**rehole Seals for High-Level **Ra**dioactive Waste") project a theoretical desk study was performed to identify the requirements for and the tasks of high-level waste (HLW) borehole seals. Crushed salt was identified as the most suitable sealing material. According to model calculations the crushed salt in the HLW disposal boreholes reaches the properties of the surrounding undisturbed rock mass by convergence induced compaction within very few years (< 10 years).

This report describes experimental and theoretical work performed within phase II of the project to confirm and further improve the material models used to predict the compaction behaviour of crushed rock salt in long-term safety analyses.

Two in-situ experiments simulating the relevant conditions in disposal boreholes were performed in the Asse mine in Germany. The experiments were designed, installed and evaluated by GRS-Braunschweig in co-operation with the Dutch Nuclear Research and Consultancy Group (NRG).

The DEBORA project was part of the "**B**ackfill **a**nd **M**aterial **B**ehaviour in an **U**nderground **S**alt Repository (BAMBUS)" project. Within the framework of the BAMBUS project NRG and the Universidad Polytécnica de Cataluna in Barcelona (UPC) contributed to the DEBORA project by performing relevant thermomechanical modelling.

The DEBORA project was funded under contract No. 02E8715 by the German Bundesministerium für Wirtschaft und Technologie (BMWi) and co-sponsored within the BAMBUS project under contract No. FI4W-CT95-0009 by the Commission of the European Communities.

Abstract

The long-term safety of a repository for radioactive waste in deep geological formations is to be ensured by a sealing system consisting of natural and technical barriers. Each component of the technical barrier system has to meet specific requirements depending on the layout of the repository.

Already in the early eighties, research and development works have been started to investigate the sealing capability of crushed salt backfill in underground salt repositories. Laboratory investigations served to investigate the compaction behaviour and to determine the mechanical and hydrological material parameters. Material models to be implemented in computer codes were developed on basis of the obtained laboratory results. First numerical simulations of the long-term sealing behaviour of crushed salt backfill in disposal boreholes containing heat producing high-level waste have been performed in phase I of the DEBORA project.

The major objective of the project phase II was to confirm the obtained modelling results by comparison with representative experimental data. Two in-situ experiments in 15 m deep boreholes with a diameter of 0.6 m were thus performed in the Asse mine. The experiment DEBORA 1 served for the investigation of the compaction behaviour of crushed salt backfill in the annulus between the heat producing waste canisters and the surrounding rock. In the experiment DEBORA 2 the crushed salt compaction in the seal region above the canister stack was investigated. By electrical heating maximum temperatures of 185 °C and 135 °C were achieved at the end of the experiments. In both experiments a maximum backfill pressure of about 15 MPa was measured. The convergence induced borehole closure amounted to 15.5 mm and 42.5 mm, respectively.

The general agreement between the measured and predicted compaction behaviour was comparably good in both experiments but, the long-term relevant low compaction rates in the final stage of both experiments were predicted even better. It is thus concluded that the material models developed so far allow a satisfactory prediction of the long-term sealing behaviour of crushed salt backfill. Hence, further large scale in-situ experiments are not considered necessary. However, some more laboratory investigations are considered useful in order to investigate discrepancies between measurements and predictions observed in particular in the early compaction stage at porosities above 20 %.

The hydraulic behaviour of the compacting crushed salt was investigated too. The relation $k = 1.9 \cdot 10^{-8}\ \phi^{5.27}\ m^2$ between the permeability k and the porosity ϕ was derived from an evaluation of all in-situ and laboratory data. Former laboratory results are very well confirmed by this relation.

In addition to the in-situ investigations brine intrusion and propagation of gas in sealed disposal boreholes were investigated using geometrically simplified, numerical models. The calculations show a complex displacement behaviour of the fluid phases which cannot be captured by single-phase flow models. The results are sensitive to almost all parameters. Thus, special attention should be paid to the material laws and the model geometry for site specific predictions.

Kurzfassung

Die Langzeitsicherheit eines geologischen Endlagers soll nach internationaler Übereinkunft durch ein System aus natürlichen und technischen Barrieren gewährleistet werden. Dementsprechend wurde in Deutschland in den "Sicherheitskriterien für die Endlagerung radioaktiver Abfälle in einem Bergwerk" des Bundesministers des Innern aus dem Jahr 1983 als Maßnahme zur Verwirklichung der Schutzziele ein Mehrbarrierenkonzept gefordert. Dabei muss jedes Teilsystem - zum Beispiel Kammer- und Streckenverfüllungen, Bohrloch-, Schacht- oder Kavernenverschlüsse - seinen spezifischen Beitrag liefern.

Forschungsarbeiten zur Untersuchung der Eignung von Salzgrus als Verschlussmaterial für Endlagerhohlräume wurden bereits in den achtziger Jahren mit der Aufnahme erster Laboruntersuchungen zur Ermittlung der relevanten mechanischen und hydraulischen Stoffparameter begonnen. Auf Basis der Laborergebnisse wurden erste Materialmodelle entwickelt, mit deren Hilfe dann in der Phase I des DEBORA-Projektes Prognoserechnungen zum Langzeitverhalten des Versatzmaterials Salzgrus in Endlagerbohrlöchern für hochradioaktive Abfälle aus der Wiederaufarbeitung bestrahlter Brennelemente (high-level waste (HLW)) durchgeführt wurden.

Das Ziel der Phase II des DEBORA-Projektes bestand darin, die Belastbarkeit der in der Phase I gewonnenen theoretischen Ergebnisse durch geeignete In-situ-

Experimente mit begleitenden Laboruntersuchungen zu überprüfen, um das vorgeschlagene Verschlusskonzept entweder zu bestätigen oder Hinweise auf eventuell erforderliche Modifikationen zu ermitteln.

In den DEBORA-Versuchen wurde das Kompaktionsverhalten und die Durchlässigkeit von Salzgrus im Ringspalt zwischen den wärmeproduzierenden Kokillen und dem Gebirge (DEBORA 1) und im Verschlussbereich (DEBORA 2) oberhalb der Kokillensäule untersucht. Beide Experimente wurden in 0,6 m durchmessenden ca. 15 m tiefen Bohrlöchern in einer Strecke auf der 800-m-Sohle der Asse durchgeführt. Bei DEBORA 1 wurden die wärmeproduzierenden Kokillen durch eine beheizte Verrohrung innerhalb des Bohrloches simuliert, während der Wärmeeintrag in den Verschlussbereich bei DEBORA 2 durch vier außerhalb des Bohrloches bei 1,1 m Radius installierte Erhitzer erfolgte. Innerhalb der jeweiligen Versuchsdauer von 12 bzw. 15 Monaten wurden maximale Salzgrustemperaturen von 185 °C bzw. 135 °C erreicht. Die gemessenen maximalen Versatzdrücke lagen in beiden Versuchen bei etwa 15 MPa. Die Bohrlochkonvergenz betrug im Versuchszeitraum maximal 25,5 mm bzw. 42,5 mm.

Die Übereinstimmung der prognostizierten und gemessenen Ergebnisse ist in beiden Experimenten etwa gleich gut. Insbesondere die für das Langzeitverhalten des kompaktierenden Versatzes relevanten geringeren Kompaktionsraten gegen Ende der Versuche wurden vergleichsweise gut prognostiziert, woraus der Schluss gezogen wird, dass mit den verwendeten Materialmodellen für relativ homogenen Versatz eine befriedigende Vorhersage des Kompaktionsverhaltens möglich ist. Weitere großmaßstäbliche Untersuchungen werden daher nicht mehr als erforderlich betrachtet. Einige weiterführende Laboruntersuchungen zur Klärung der Diskrepanzen im Porositätsbereich oberhalb 20 % wären jedoch im Hinblick auf eine weitere Verbesserung der Modelle wünschenswert.

Das Durchlässigkeitsverhalten des kompaktierenden Salzversatzes wurde im Rahmen des DEBORA-Projektes erstmals in situ untersucht. Damit wurde ein wesentlicher Beitrag zur Absicherung der in Langzeitsicherheitsanalysen verwendeten Modellansätze geleistet. Aus allen im Labor und in situ gewonnenen Daten wurde zwischen der Permeabilität k und der Porosität ϕ die für Langzeitsicherheitsanalysen wichtige Relation $k = 1.9 \cdot 10^{-8}\ \phi^{5.27}\ m^2$ abgeleitet, womit bereits früher ermittelte Labordaten gut bestätigt werden.

Anhand von Prinzipmodellen wurden ergänzend modelltheoretische Untersuchungen zum Laugenzutritt und zur korrosionsbedingten Gasbildung in Endlagerbohrlöchern für hochradioaktive Abfälle im Salz angestellt. Die Rechnungen lassen erwarten, dass die gegenseitige Verdrängung der Fluide ein komplizierter Vorgang ist, der nicht mehr durch Einphasenströmungsmodelle erfasst werden kann. Die Ergebnisse hängen dabei empfindlich von praktisch allen Eingangsparametern ab, was besonders hohe Anforderungen an die Genauigkeit stellt, mit der die Materialgesetze und die Geometrie für solche Modelle beschrieben werden.

Table of Contents

1 Introduction

1.1 Background

The long-term safety of a repository for radioactive waste in deep geological formations is to be ensured by a sealing system consisting of natural and technical barriers. Each component of the technical barrier system has to meet specific requirements depending on the layout of the repository.

According to the German radioactive waste management concept steel canisters containing vitrified High-Level Waste (HLW) originating from reprocessing of spent fuel are to be disposed of in disposal boreholes located in deep geological salt formations.

As known from earlier investigations small amounts of natural fluids will be released from the salt into the disposal boreholes because of heating and irradiation of the salt. If the borehole would be sealed gastight this would lead to an increase in gas pressure. The fluids may cause corrosion of the waste canisters thus increasing the generation of gases and gas pressures. For reasons of safety, the borehole seals are to be designed in such a manner that an unacceptable increase of the borehole gas pressure and an uncontrolled release of gases and radionuclides into the repository are avoided. These requirements seem contradictory in principle but have to be considered during the development of borehole seals.

During the phase I of the DEBORA-project the conditions of state (gas pressure increase, mechanical stresses in the salt formation, deformation of the salt formation) in and around a disposal borehole have been analyzed in detail in order to quantify the requirements of a borehole seal (Rothfuchs et al., 1996). Additionally, the suitability of different sealing materials was analyzed.

Crushed salt was identified as the most suitable sealing material. The initial permeability of crushed salt is high (ca. 10^{-12} m^2) but as a consequence of the thermally induced salt convergence it finally reaches very small values which are comparable to those of the undisturbed surrounding rock mass (10^{-21} – 10^{-22} m^2). Because of this behaviour the amounts of fluids released into the borehole shortly after waste emplacement can escape from the borehole thereby avoiding the development of high gas pressures in the borehole. The long-term permeability, however, is low and limits a

possible escape of radionuclides on the one hand and a inrush of brine from the repository on the other hand.

Because of the limited mechanical strength of the HLW waste canisters, the distribution of their weight load is required in case of disposal in deep boreholes (Barnert et al., 1994). This can be obtained by backfilling the annulus between the waste canisters and the borehole wall with crushed salt during the emplacement procedure. Hence, sealing of the disposal borehole will be performed simultaneously with canister emplacement. After completion of the emplacement of the waste canisters and crushed salt in a borehole, the remaining part between the uppermost canister and the disposal drift - the seal region - will also be sealed with crushed salt.

In borehole seals the backfill material consists of crushed salt as received by drift excavation, i.e., a coarsely grained material with a maximum grain size of 60 mm. The backfill material used in the borehole annulus will be fine grained crushed salt with a maximum grain size of 10 mm.

In the phase I of the DEBORA-project model calculations had been performed to analyze the compaction and permeability behaviour of crushed salt. According to these calculations the crushed salt in the annulus of HLW disposal boreholes reaches the properties of the surrounding undisturbed rock mass within very few years (< 10 years). However, the level of confidence in these numerical predictions was comparably low because the used constitutive models were only based on some few laboratory experiments. No in-situ experiments suitable for the validation of the models had been performed so far.

In Phase II, the DEBORA project was one part of the project BAMBUS (**B**ackfill **a**nd **M**aterial **B**ehaviour in **U**nderground **S**alt Repositories) that was undertaken as a joint project by BGR (DE), ENRESA (ES), FZK (DE), G.3S (FR), GRS (DE), NRG (NL), and UPC (ES) between January 1996 and December 1998. The project was funded by the European Commission and the national governments and authorities (Bechthold, et al., 1999).

1.2 Issues and Objectives

The main issue at the beginning of the DEBORA project was, therefore, in how far the models developed so far would be suitable to describe the mechanical and hydraulical behaviour of crushed salt being used as a sealing material in nuclear repositories, especially in heated high-level waste disposal boreholes. From the laboratory investigations and the models developed it had been known that parameters as for instance the temperature, the deformation rate, the grain size, and the moisture contained in the material might have an impact on the compaction behaviour. Not all of these parameters, however, were considered in the existing models, e.g., (Hein, 1991), (Zhang et al., 1993), (Spiers et al., 1993).

The main objective of phase II of the DEBORA-project was, therefore, to perform in-situ experiments with accompanying laboratory investigations in order to:

- to increase the data base on important phenomena and processes in backfilled disposal boreholes,

- to expand the knowledge required for repository design and performance assessments, and

- to test and refine Thermo-Hydro-Mechanical (THM) models for predicting the long-term repository performance.

1.3 Work Programme

In order to enable the investigation of the impact of the different parameters, two independent in-situ experiments were planned to represent the expected conditions in sealed HLW boreholes.

The experiment DEBORA 1 focused on investigating the backfill behaviour in the borehole annulus whereas in the experiment DEBORA 2 the backfill in the borehole seal was investigated. It was considered necessary to carry out two separate experiments because the boundary conditions in the two borehole regions differ considerably. In comparison to the seal region above the canister stack, the higher temperatures in the vicinity of the waste canisters lead to much faster compaction in

the borehole annulus. A further difference is caused by the fact that only fine-grained crushed salt with a maximum grain size of about 10 mm can be used to fill the narrow annulus, whereas crushed salt with maximum grain diameters of 60 mm - as received from drift excavation - can be used as backfill in the seal region.

Thermomechanical and hydraulical design calculations (see Chapters 4.1 and 4.2) were performed to determine the experimental conditions with regard to temperature, stress, deformation, and gas flow in the rock and the crushed salt backfill.

The in-situ-investigations were accompanied by laboratory investigations necessary to determine the material parameters of the backfill used in the experiments. With the determined parameters the thermomechanical calculations were repeated and the results of which were compared with the observed in-situ measuring data.

According to the design calculations of the phase I, the DEBORA experiments were suitable to investigate the compaction of crushed salt and the resulting permeability decrease over a fairly wide parameter range. Both experiments were performed in the former HLW test field (Figure 1-1) at the 800-meter level of the Asse mine.

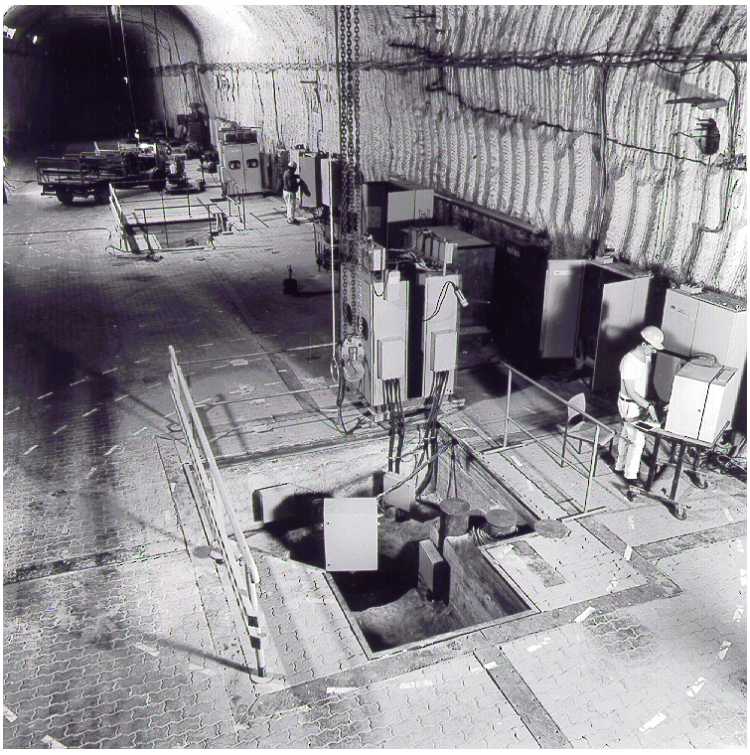

Figure 1-1 View into the former HLW test field at the 800-meter level of the Asse mine. The DEBORA-2 test site is located in the foreground.

In addition to the experimental investigation of crushed salt compaction, hydraulical model calculations (see Chapter 5) were performed within the framework of the project in order to analyze brine intrusion and two-phase flow of brine and gas in sealed HLW disposal boreholes. The calculations were done with the help of the two-phase flow code MUFTE (Helmig et al., 1994). The main objective of this work was to analyze the sensitivity of the considered processes in view of the high material parameter contrasts at discontinuities like for instance shaft-drift interface or seal-drift-interface. Also the dynamics of the processes were to be analysed in order to improve the understanding of the principal mechanisms and the significance of the two-phase flow in a sealed disposal borehole.

2 In-situ Investigations

2.1 DEBORA 1

2.1.1 Design

As mentioned above, the DEBORA-1 experiment was designed to simulate the conditions in the annulus of an HLW disposal borehole.

The DEBORA-1 borehole (Figure 2-1) was equipped with a liner to enable the investigation of the compaction and the remaining porosity of fine grained crushed salt backfill in the borehole annulus. The borehole liner contained four electrical heaters. Both, the liner and the heaters together represented the waste canisters in an HLW disposal borehole. The initial borehole diameter was 600 mm and the borehole depth was about 15 m. The liner diameter was 420 mm and its wall thickness was 25 mm. The heaters inside the liner produced 9 kW of electric power. In the experiment, the temperature, the radial stress, and the borehole closure were measured at three levels and three azimuthal directions 10.5 m, 12 m, and 13.5 m below the drift floor. The permeability of the compacted crushed salt was determined by periodic flow tests using nitrogen which was injected via an injection tube into the gas injection volume. The gas flowed through the backfill and was collected in the gas collection volume at the upper end of the test interval.

The measurements of pressures and temperatures of the crushed salt were performed with the same type of sensors for both DEBORA experiments. All pressure/temperature sensors (Figure 2-2) had a stainless steel membrane coupled through silicon oil with a semiconductor measuring element. In this measuring element a full rectifier bridge was implemented, thereby converting the strain caused by the pressure on the membrane into an electrical signal. The rectifier bridge was temperature-compensated by some resistors, and one of these resistors was used to generate a temperature signal. The signals were both amplified into a 4-20 mA output with external amplifiers.

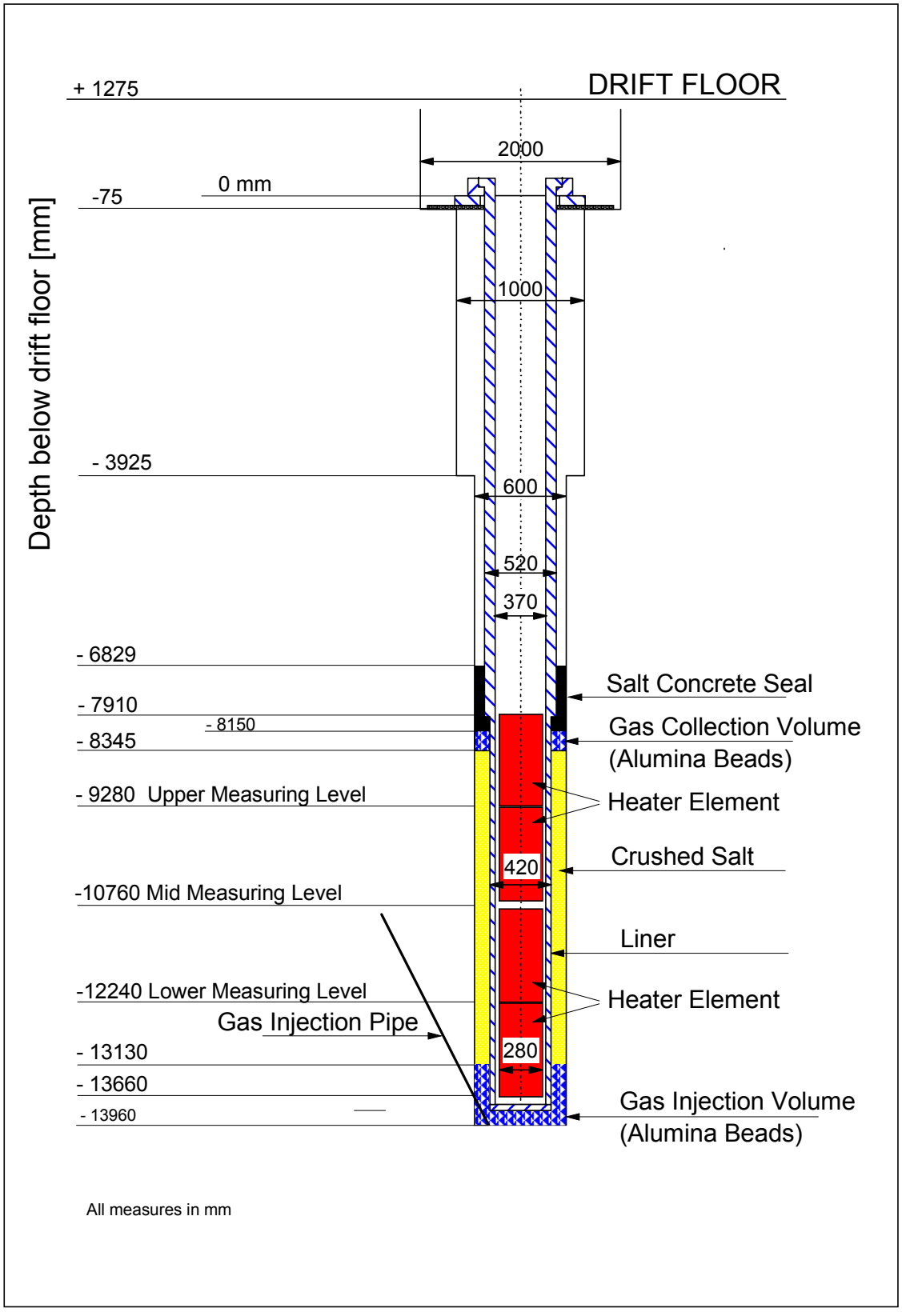

Figure 2-1 Layout of the experiment DEBORA 1 for the investigation of crushed salt compaction in the annulus between waste canisters and borehole wall.

Figure 2-2 Pressure and temperature sensor.

The measuring range of the pressure sensor was 0 to 200 bar pressure and of the temperature sensor 20 to 200 °C. The calibration accuracy was ± 2 bar for the hydrostatic pressure and typically ± 3 °C for the temperature, respectively. The sensors were delivered by Kulite Benelux B.V. The sensors were screwed in a frame with the head of the sensor directed towards the pressure of the crushed salt. The sensor itself could withstand temperatures up to 260 °C, the connecting cable up to 500 °C.

The displacement gauges (Figure 2-3), delivered by NRG's subcontractor ECN (Netherlands Energy Research Foundation), consisted of a fixed cylindrical part connected to the frame in which a moving part can slide. After mounting of the frame to which the sensors were connected, a spring was released pushing the moving part against the borehole wall. Inside each gauge, a metal plate was connected to the moving part. In this plate a five row pattern of rectangular holes was cut. Five pairs of contact pins mounted on the fixed part of the sensor slided over the pattern only making contact if there was no hole on that position.

The five contact pins together formed a digital gray-code (contact = 1; no contact = 0). This code has the characteristic that only one of the contacts changes from one position to the following. With an external DA-converter, the gray-code was converted into an analogue signal. The diameter of the sensor was about 75 mm. Calibration was performed for all the sensors at room temperature and for one sensor, additionally, at maximum specification temperature.

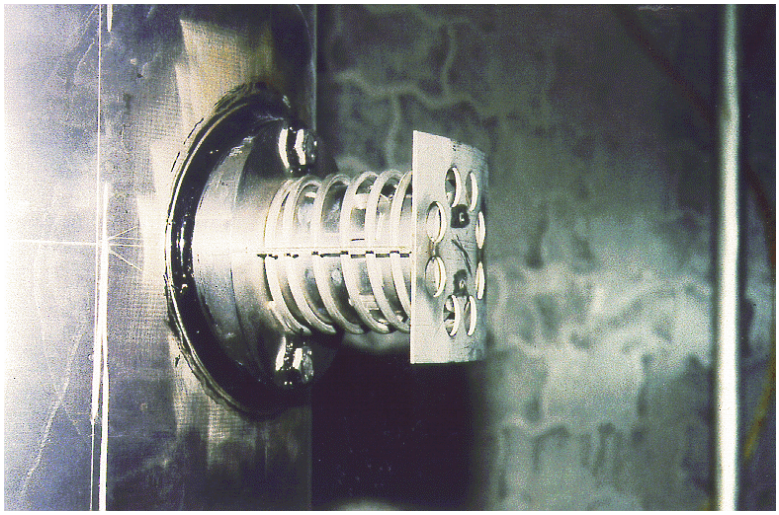

Figure 2-3 Displacement gauge.

The displacement gauges for DEBORA 1 could measure a displacement range of 65 to 97 mm with an accuracy of ± 0.2 mm for the switching moments and a resolution of 1.25 mm. The maximum design temperature was 175 °C and the maximum design pressure 200 bar.

Instruments for measuring the inlet and the outlet gas flows were installed in a gas measuring station (Figure 2-4) in the test drift. In the gas injection and the gas collection volume temperature resistant gas pressure transducers were placed for monitoring the pressure gradient over the test interval. When stationary gas flow was achieved, the permeability of the crushed salt could be calculated according to the generalized Darcy's law for compressible media (compare Section 2.1.3):

Design calculations for the gas flow tests and an estimation of measuring errors regarding the results of the flow tests had been performed within the framework of the hydraulical analyses of the project (for further details see Chapter 4.2).

The analysis yielded an error of little more than 5 % for the permeability. Since the displacement gauges worked with a constant error, the total error in the porosity using the geometric approach grew exponentially during the experiment. The error was approximately 2 % at the beginning and increased to 5 % for a porosity between 10 % and 15 %.

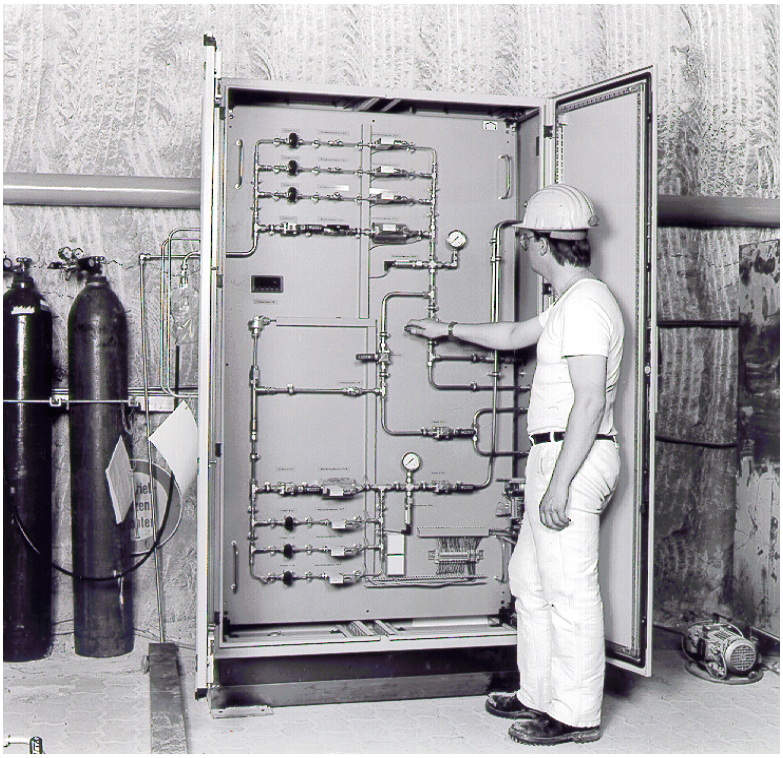

Figure 2-4 DEBORA 1; gas measuring station.

Before the liner equipped with instruments (Figure 2-5) was installed in the borehole, the gas injection volume was filled with ceramic alumina beads. After installation of the liner, the gap between liner and borehole wall was filled with crushed salt with a maximum grain size of 8 mm. The gas collection volume was also filled with ceramic alumina beads. To seal the test volume, a 1.3 m long concrete plug was poured on top of the gas collection volume.

2.1.2 Performance

Heating in DEBORA 1 was started on 17 February 1997 and terminated on 13 March 1998. During the first two days of the heating period, the measurement data were collected every ten minutes. After two days, when the temperature increase became more moderate, the collection frequency was reduced to two hours and finally, after one and a half month, to one measurement per four hours.

Figure 2-5 DEBORA 1; borehole liner equipped with instruments.

Especially in May 1997, thunderstorms in the area of the Asse mine caused several interruptions of the heater power. On 18 May 1997 a lightning led to a severe damage of the main power station in the mine so that an emergency operation took place for approximately one month until the repair work could be finished. The heater power interruptions can be clearly seen in the Figures showing the temperature and stress development (compare Figure 2-6 and Figure 2-7 in Section 2.1.3).

A few weeks after the start of the heating phase of DEBORA 1, some pressure/temperature sensors started to show erroneous readings. Since the same types of transducers would be used in DEBORA 2, which was already partially built at that time, it was imperative to understand the possible reasons in order to improve either the transducers or their immediate environment to prevent future malfunctions. Later on in DEBORA 2, small bags filled with fine grained salt were placed in front of the pressure sensors as a measure for protecting the pressure membranes against sharp edged salt grains.

In the course of the experiment also some displacement gauges showed an irregular behaviour. Since during the first gas flow tests minor amounts of water were observed that obviously had been released from the backfill, it was assumed that water vapour together with some salt dust had intruded the displacement gauges and precipitated on

the electrical contacts, thus obscuring their signals. This assumption was supported by the observation that the displacement gauges located in the upper borehole section suffered more than those in the lower section. Furthermore, an immediately started nitrogen flushing of DEBORA 1 led to an improvement of the performance of the distance gauges.

The permeability measurements were carried out monthly or, in the later stage of the experiment, each time when a sufficiently large progress of crushed salt compaction was observed from the borehole wall displacement measurements. Each permeability measurement was performed at different gas pressure levels of about 2, 4, 6 and 8 bars. This procedure enabled a Klinkenberg correction of the measured permeability values.

2.1.3 Results

Heating of the DEBORA-1 borehole led to a rapid increase of the backfill temperature up to about 185 °C (Figure 2-6). During the further course of the experiment only a slight further temperature rise was observed. The measured temperatures were considerably lower than the predicted ones (see Section 4.1.1.3). As additional model calculations showed, the observed deviation of the backfill temperature by about 20 % can partly be explained by a heat flow via the neighbouring displacement gauges. Other reasons for the discrepancy may be the underestimated vertical heat conduction in the liner and the neglected vertical convective heat transport inside the non-backfilled liner.

The development of the radial stress is shown in Figure 2-7. Like the temperatures, the measured stresses were significantly lower than the predicted ones (see Section 4.1.1.3). Possible reasons for this are again the neglected vertical heat transport in and inside the liner and concentration of stresses at the protruding metallic sensor surface around the measurement membrane. Laboratory calibrations of the stress sensors were therefore performed under consideration of the actual situation in the borehole. The calibration curves (Figure 2-8) show that the measured value starts to decrease immediately after the applied uniaxial stress is being kept constant. The final stress value is by about a factor of 2 smaller than the prevailing stress.

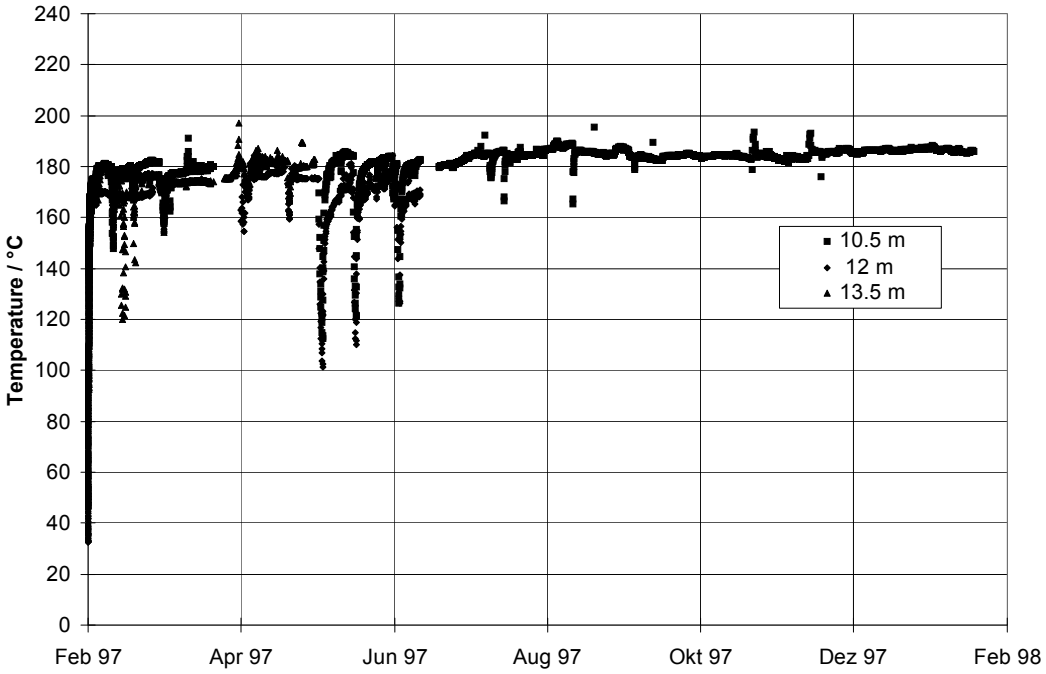

Figure 2-6 Development of backfill temperature in DEBORA 1.

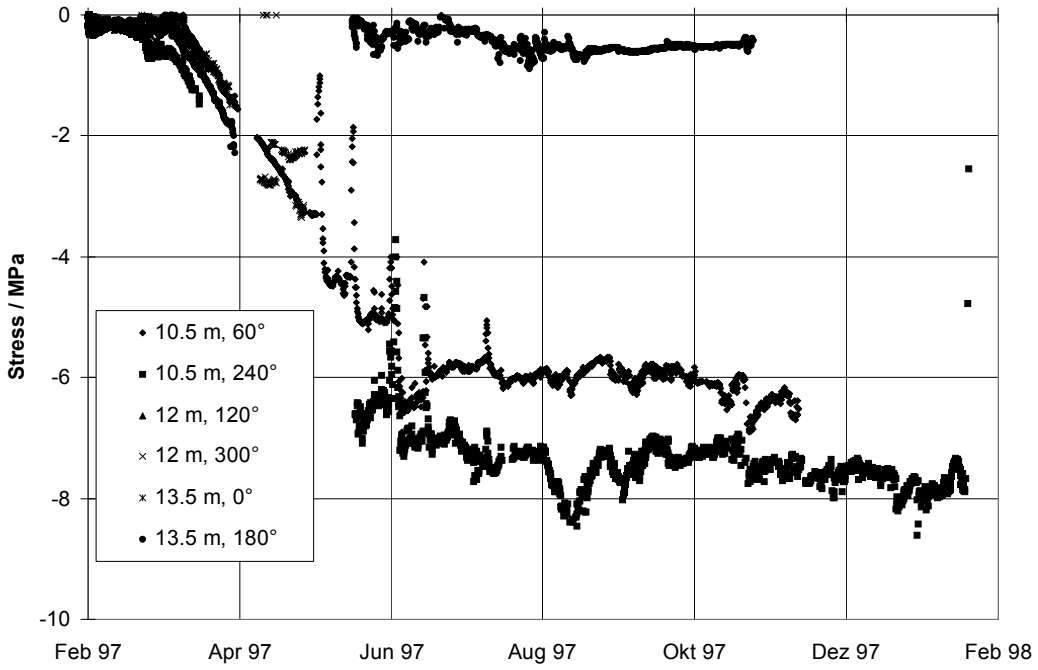

Figure 2-7 Development of radial stress in the backfill of DEBORA 1.

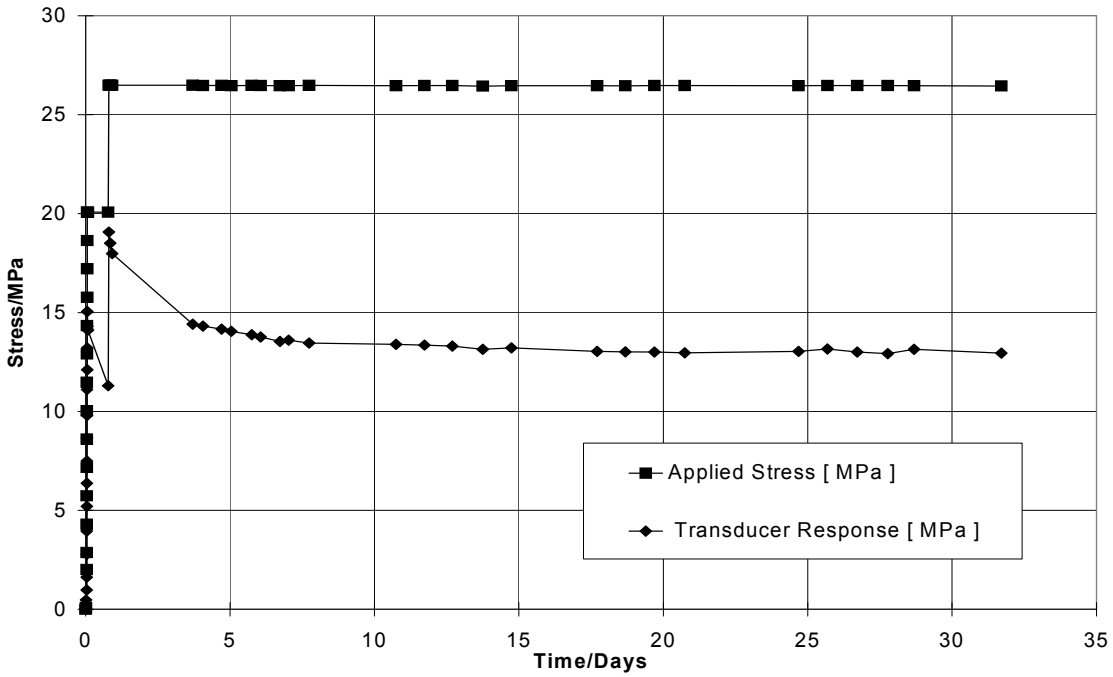

Figure 2-8 Calibration results of a reference pressure transducer.

Thus, the assumption of stress concentration around the membrane seems to be confirmed. Consequently, the stress values shown in Figure 4-13 in Section 4.1.1.3 are multiplied by a factor of 2.

Figure 2-9 shows the development of the gap width versus time as evaluated from the readings of the displacement gauges (compare Section 2.1.1). The respective displacement rates can be seen in Figure 2-10. Already after seven months of heating only very small displacement rates were observed. Therefore, although originally a heating period of 18 months was envisaged, the test was shut down after about 13 months of heating on 13 March 1998.

The porosity of the crushed salt backfill in the borehole annulus was determined by a volumetric evaluation of the borehole wall displacement measurements and additionally by inverse modelling of the flow tests. Figure 2-11 shows the respective development of the porosity at the three measurement levels. The porosity values determined by inverse modelling show a faster compaction rate for the first five months than the geometrically derived data. The changes after that time are minimal and could not be demonstrated by this method. The same two phases of compaction can be recognized

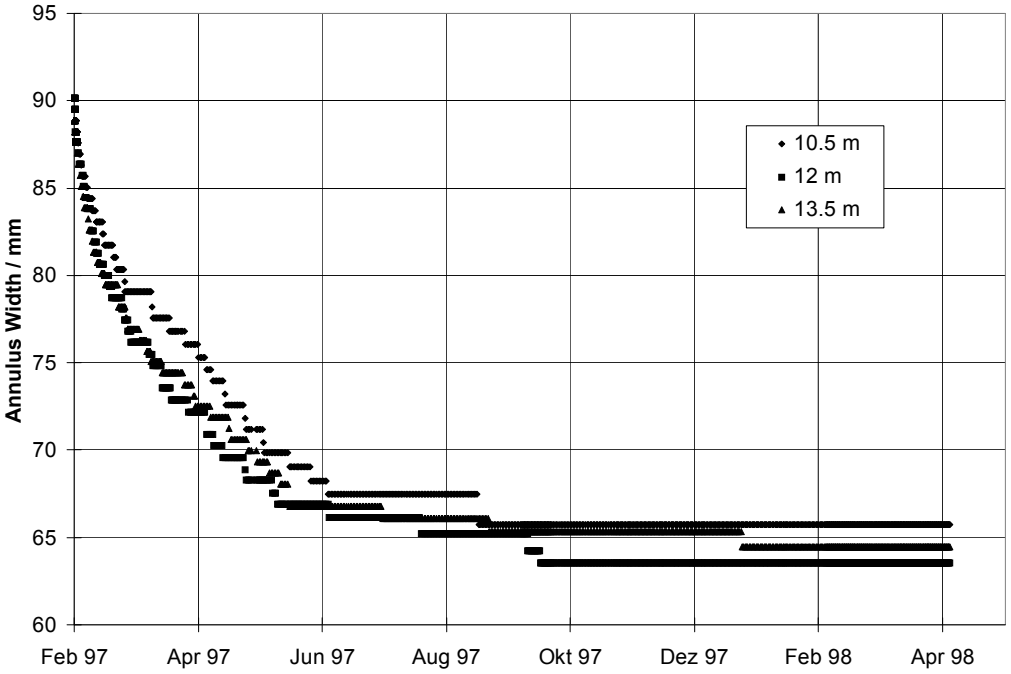

Figure 2-9 Development of the annulus width in DEBORA 1.

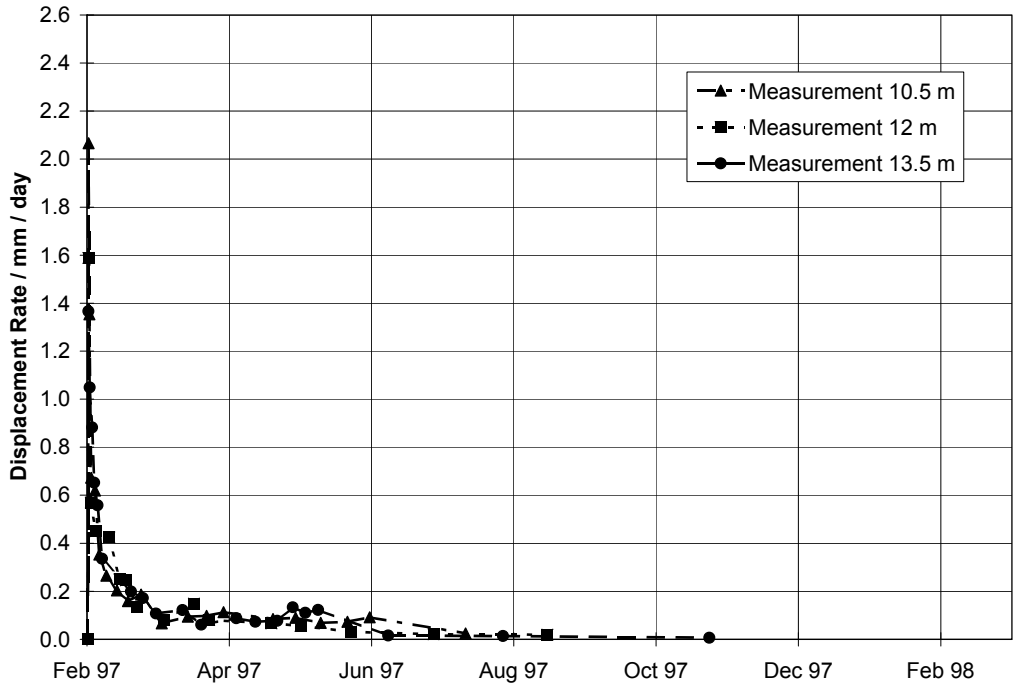

Figure 2-10 Development of the displacement rates in DEBORA 1.

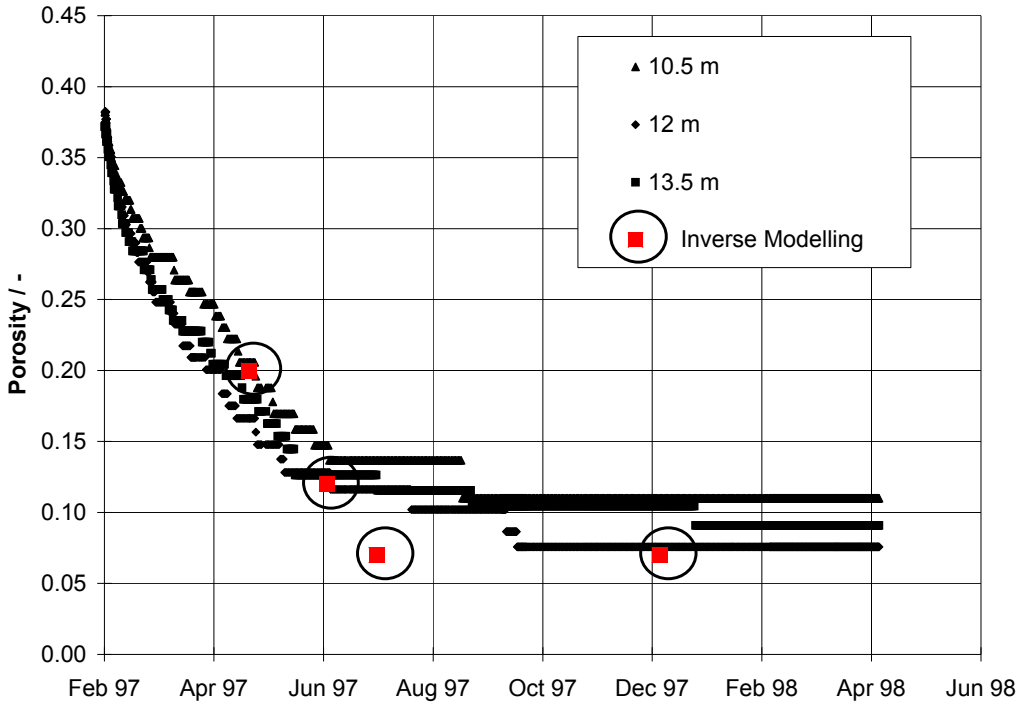

Figure 2-11 Development of backfill porosity in DEBORA 1.

in the displacement data, but the change into slow compaction is observed some three months later. The final porosity value at the end of DEBORA 1 determined by inverse modelling lies slightly below the displacement-derived value.

In order to clarify the reasons for the observed discrepancies in the porosity determination, a post test analysis of the compacted crushed salt was performed. The required samples were obtained in connection with the retrieval of metal specimens which had been attached to the borehole liner for corrosion investigations (Bechthold et al., 1999). Figure 2-12 shows cutting of samples out of the compacted crushed salt and Figure 2-13 shows the uncovered DEBORA-1 liner partly still covered with remaining crushed salt.

The porosity distribution along the test interval (Figure 2-14) achieved at the end of the experiment was determined by post-test laboratory investigations of the retrieved crushed-salt samples. The distribution shows noticeable peaks at the locations of the

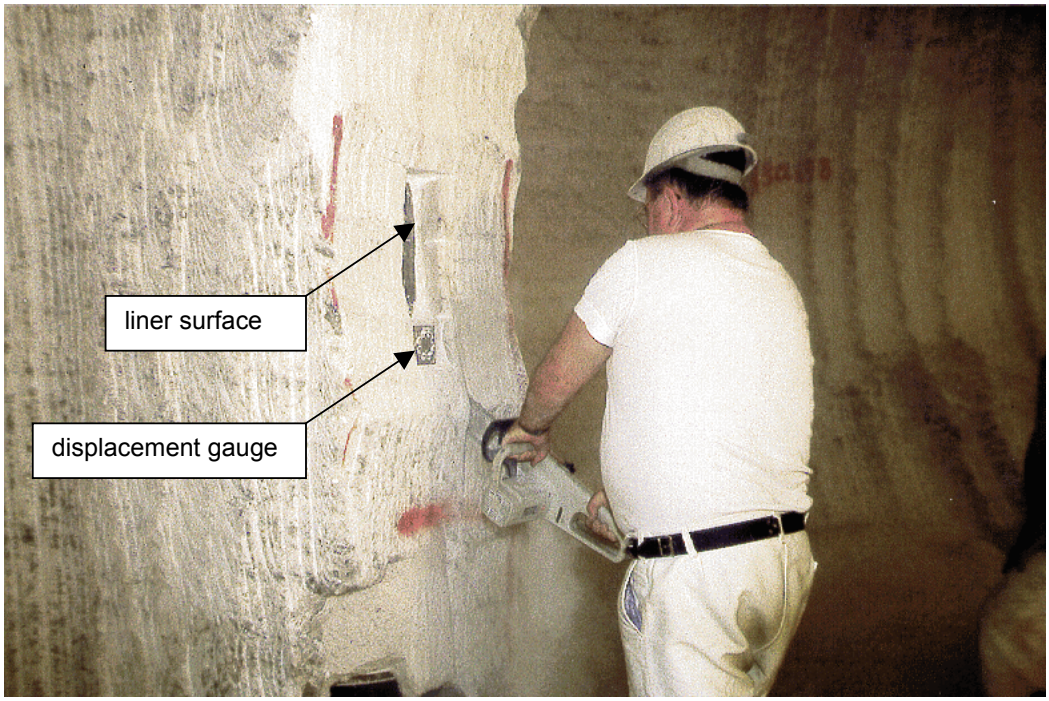

Figure 2-12 Sawing of samples from the compacted crushed salt sticking at the uncovered DEBORA-1 liner.

Figure 2-13 Uncovered DEBORA-1 liner.

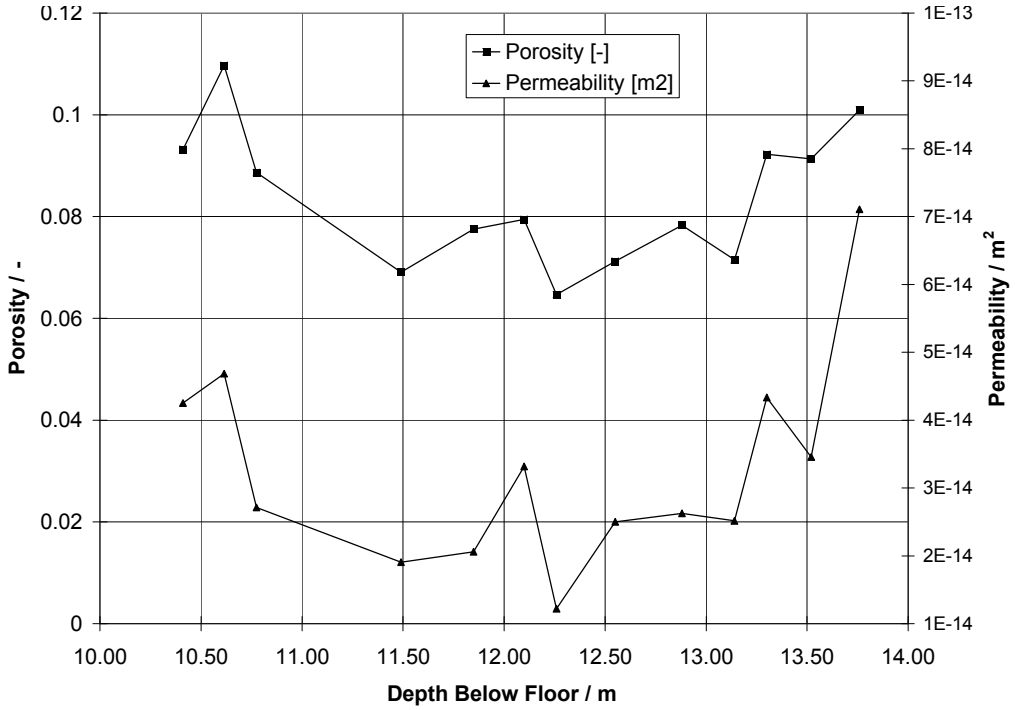

Figure 2-14 Final porosity and permeability distribution along the test interval determined by post-test investigations.

displacement transducers. The average porosity, however, appears to be about two percent points lower than the peak value which is consistent with the results of the inverse modelling.

Backfill permeability measurements were carried out periodically when the borehole wall displacement measurements indicated a sufficient progress in the compaction of the crushed salt. In the flow tests, stationary gas flow was established so that the permeability could be calculated according to the generalized Darcy's law for compressible media:

$$k = q \cdot (T/T_{norm}) \cdot \eta(T) \cdot p_{norm} \cdot 2 \cdot h \,/\, (A \cdot (p_{in}^2 - p_{out}^2)) \qquad (2\text{-}1)$$

where

- k permeability (m^2)
- q volume flow of the gas ($m^3 \cdot s^{-1}$)
- T temperature of flowing gas in the crushed salt (K)
- T_{norm} normal temperature = 273,15 K

$\eta(T)$ temperature dependent dynamic viscosity of the test gas (Pa·s)

p_{norm} normal gas pressure = 101325 (Pa)

h length of the crushed salt interval (m)

A actual cross section of the crushed salt (m^2)

p_{in} gas pressure at the gas injection volume (Pa)

p_{out} gas pressure at the gas collection volume (Pa).

In DEBORA 1, the first reliable measurement was possible two months after start-up of heating when a backfill porosity of 0.25 had been reached. Figure 2-15 shows the decrease of the permeability over time. Within the experimental period, the permeability decreased by almost two orders of magnitude from $4.7 \cdot 10^{-12}$ m^2 to $7.24 \cdot 10^{-14}$ m^2.

A compilation of the porosity and permeability data obtained in DEBORA 1 is shown in Figure 2-16. The regression analysis of these data resulted in the relationship $k = 4.74 \cdot 10^{-9} \phi^{4.63}$ between the permeability k and the porosity ϕ.

2.2 DEBORA 2

2.2.1 Design

In the experiment DEBORA 2 (Figure 2-17) the backfill behaviour in the borehole seal was investigated. As mentioned in Section 1.3, this experiment was considered to be necessary in addition to DEBORA 1 firstly, because the temperature and thus the rock convergence differ markedly in the borehole annulus and the seal region, and, secondly, because the grain sizes of the backfill material differ significantly in the borehole sections.

The experiment was carried out in a 600-mm-diameter and about 15-m-deep borehole located 15 m away from the DEBORA-1 borehole. Crushed salt was filled into the lower 5.5 m of the borehole. This part, simulating the seal of an HLW disposal borehole, was heated by four external peripheral heaters producing 3.5 kW each (14 kW in total). The measurements in this experiment focused on the interrelationships between temperature, rock convergence, backfill compaction, backfill pressure, and remaining backfill permeability.

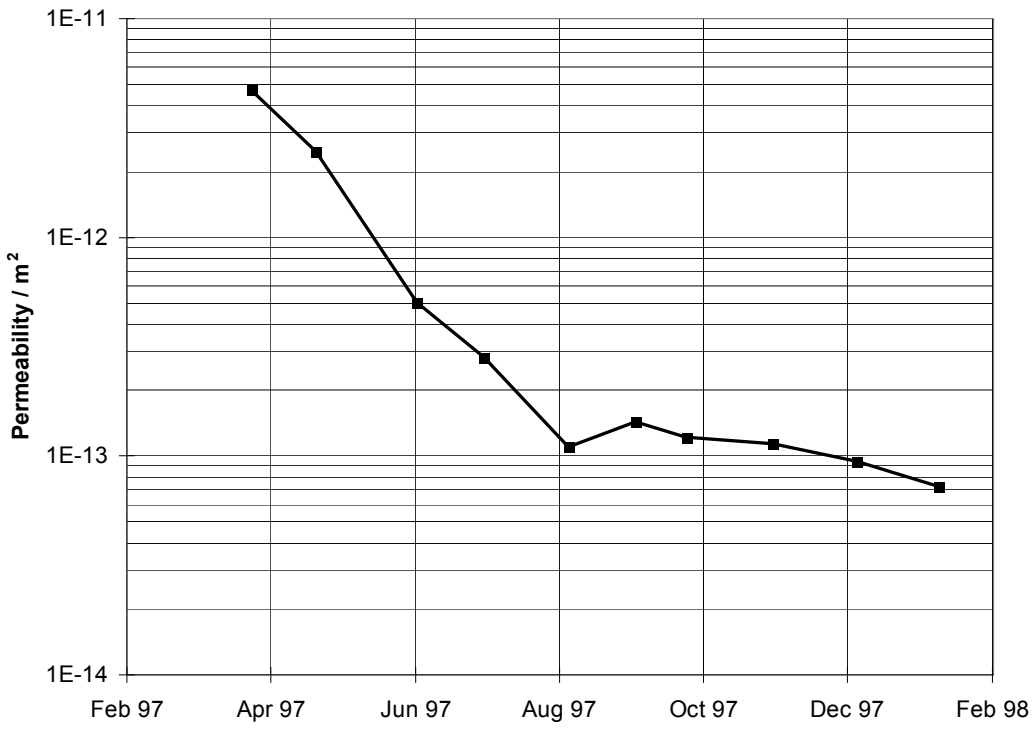

Figure 2-15 Development of backfill permeability in DEBORA 1.

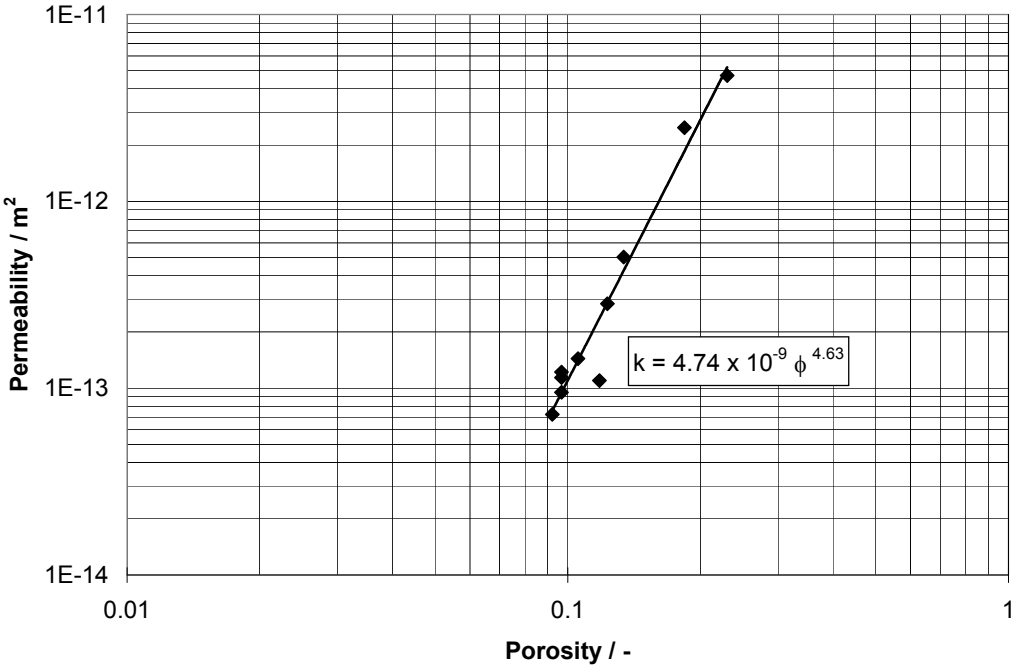

Figure 2-16 Relationship between permeability and porosity in DEBORA 1.

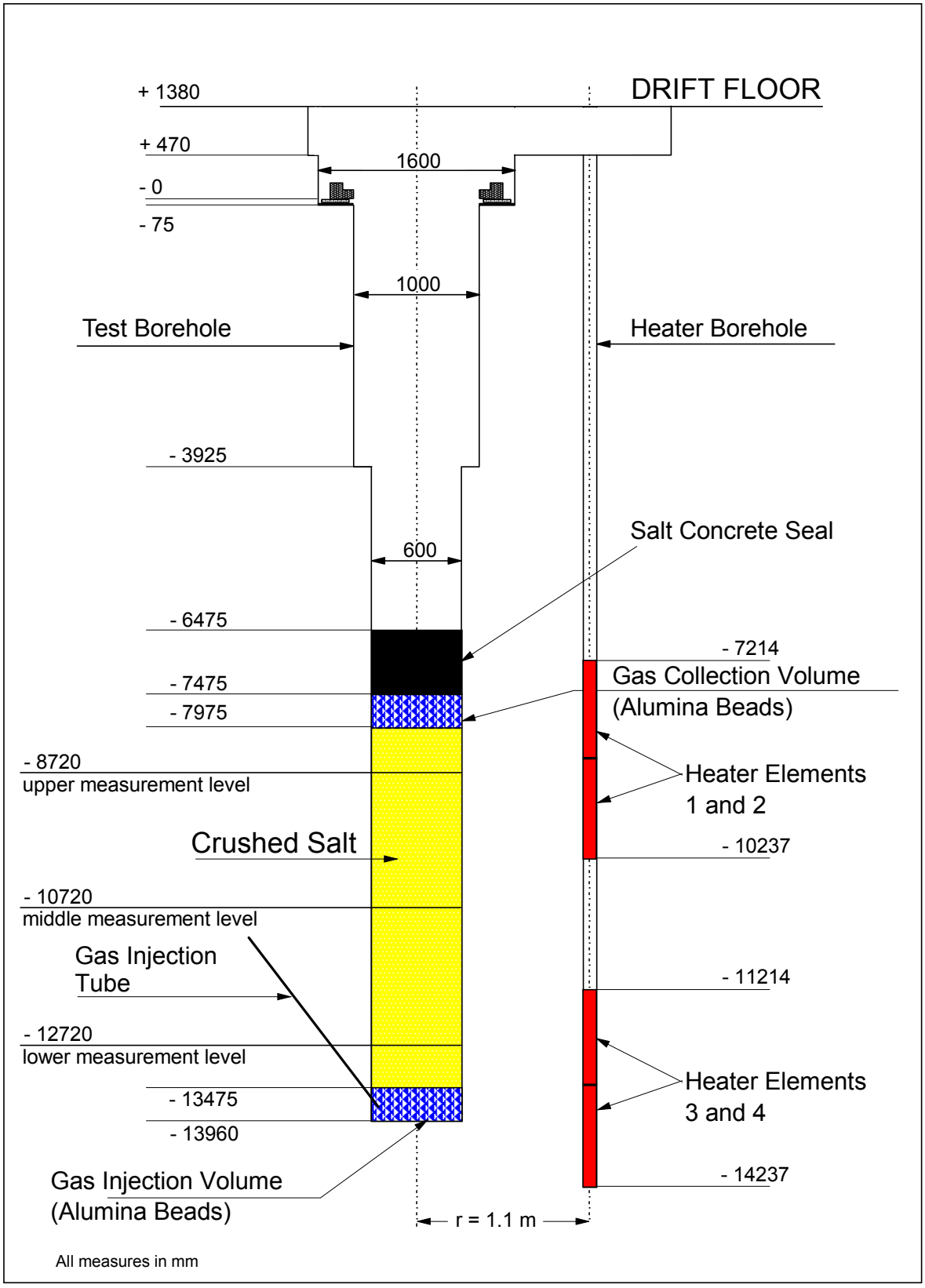

Figure 2-17 Layout of the experiment DEBORA 2 for the investigation of crushed salt compaction in borehole seals.

The flow tests for the determination of the backfill permeability were performed with the same gas measuring station that also had been used in DEBORA 1.

Temperatures, stresses, and displacements were measured at three levels 10.1 m, 12.1 m, and 14.1 m below the floor. The gauges were mounted at different azimuthal directions on a hollow frame located in the centre of the borehole. The diameter of the frame was 0.114 m and all cables were guided inside the frame to avoid preferential pathways for the nitrogen gas during the flow tests.

The pressure/temperature sensors had the same technical specifications as the sensors used in DEBORA 1 (see Section 2.1.1). The only difference was that at each measuring level in DEBORA 2 one pressure sensor was facing in axial direction and one in radial direction. Temperature measurements were performed with all the sensors.

The displacement gauges for DEBORA 2 were very similar to the gauges used in DEBORA 1 (see Section 2.1.1). They could measure a displacement range of 193 to 253 mm with an accuracy of $\pm$ 0.2 mm for the switching moments and a resolution of 1.875 mm. The maximum design temperature was 200 °C and the maximum design pressure was 200 bar.

2.2.2 Performance

DEBORA 2 became operational in September 1997 and was terminated on 4 December 1998. In contrast to DEBORA 1, the heater operation continued over the experimental period without major disturbances.

Based on the experiences gained with the transducers in DEBORA 1, in order to reduce the influence of intruding salt, the dimensions of the pressure release holes in the displacement gauges were reduced, and the signal voltage differences over the five-signal sliding contacts were increased.

In addition, with the purpose of maintaining a low water vapour content of the backfill and of reducing the amount of water and salt dust which could enter the displacement gauges, the test interval containing the crushed salt was continuously flushed with dry nitrogen. Since obviously strengthening of the protective silicon layers of the pressure

sensors would lead to an unacceptable reduction of the sensibility of the pressure sensors, the pressure membranes were protected against penetration of sharp-edged salt grains (as observed in DEBORA 1) by strapping small bags filled with fine grained salt in front of the pressure sensors.

During the experiment it turned out that the measures mentioned above were sufficient. All displacement gauges and temperature sensors performed very well. A malfunction of the axial pressure sensor at 10.1 m below the floor must be attributed to a short-circuit of one of the signal cables during installation.

2.2.3 Results

The temperature development is shown in Figure 2-18. The initial temperature rise is slower than in DEBORA 1, because in DEBORA 2 the heaters were located outside the central borehole at a radial distance of 1.1 m. Compared with the DEBORA-1 experiment, a better agreement was achieved between predicted and measured temperatures.

The development of the observed radial stress is shown in Figure 2-19. Like in DEBORA 1, the measured stresses are lower than predicted. As already explained in Section 2.3.1.3, stress concentrations at the protruding sensor surface around the measurement membrane could have caused the measurement of reduced stress values. According to the post-test laboratory calibrations of the stress sensors, also in case of DEBORA 2 the stress values shown in Section 5.3 have been multiplied by a factor of 2.

The pressure decrease since March 1998 may have various reasons. In early March 1998, an unintended temporary power increase resulted in an increase in temperature and stress. After the heater power had been corrected, both temperature and stress decreased again. The resulting contraction of the salt may have caused a separation of the backfill material from the sensor membrane. It is assumed that the contact between backfill and sensor membrane was never fully established again. This effect may have been assisted by the increasing rigidity of the compacting backfill. Another reason for this deviating radial stress behaviour could be that due to deformation of the initially circular borehole, caused by non-equal thermal expansion of

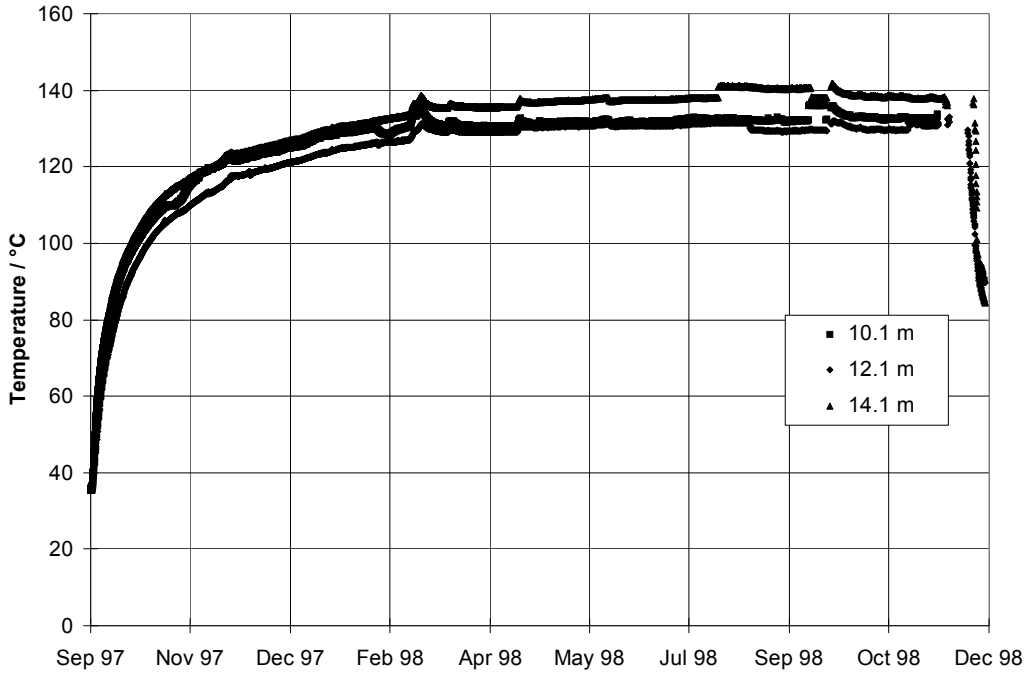

Figure 2-18 Development of backfill temperature in DEBORA 2.

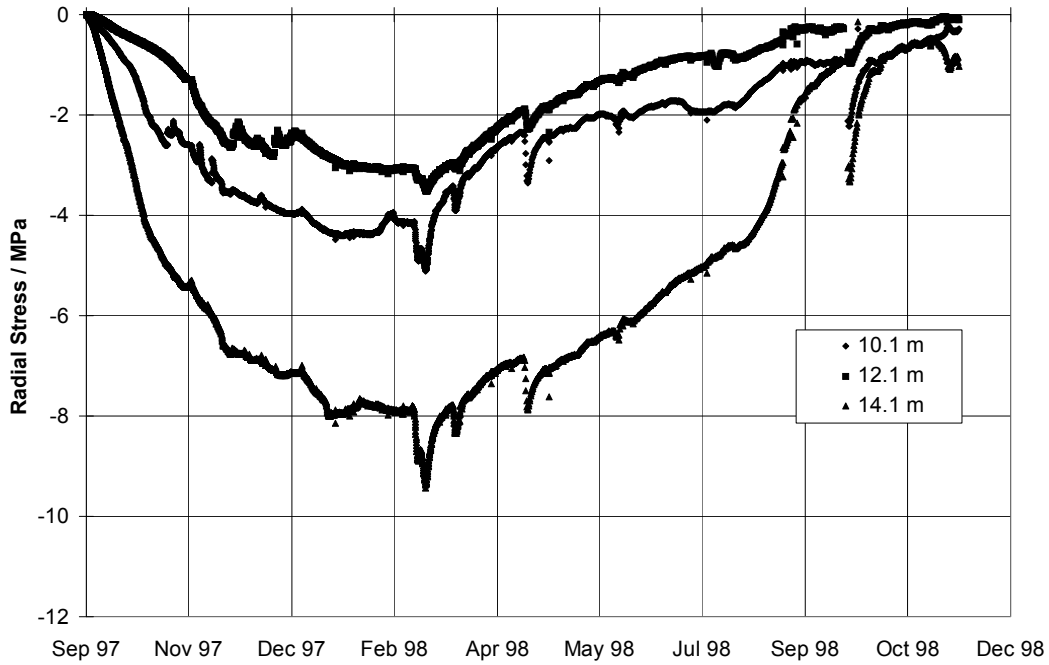

Figure 2-19 Development of radial stress in the backfill of DEBORA 2.

the rock around the borehole, the circumferential stress became relevantly higher than the radial stress. In that case, the effective stress deviates from radial direction and the three radially directed pressure sensors monitor decreasing stresses.

In fact, one of the axially directed stress sensors showed a similar behaviour (Figure 2-20). However, the point of time at which the stress started to decrease is somewhat earlier compared to the radial stress sensors. The low (later positive) stresses monitored with this axial stress sensor are probably due to its position at the non-heated mid-height of the test interval. Generally, the axial stresses observed were much lower than the radial ones. Possibly, the backfill material was not adequately confined in the axial direction.

The compaction of the crushed salt was determined, like in DEBORA 1, by evaluating the borehole wall displacement measurements. In order to obtain a homogeneous compaction of the crushed salt backfill over the whole length of the test interval, the peripheral heaters had been manufactured with an unheated central part (see Figure 2-17). The development of the borehole radius at the three measurement levels is shown in Figure 2-21. In fact, an almost uniform reduction of the borehole radius can be seen at the upper and the lower measurement level, whereas a slightly smaller reduction was recorded at the central level. The corresponding backfill porosity (assuming full axial confinement) is shown in Figure 2-22.

The displacement rates decreased to below 0.05 mm/day after more than one year of heating (Figure 2-23). Since no further significant compaction of the backfill material was expected in this situation, the heaters were switched off on 4 December 1998.

The corresponding decrease of backfill permeability over almost three orders of magnitude from $1.4 \cdot 10^{-10}$ m^2 to $4.6 \cdot 10^{-13}$ m^2 is shown in Figure 2-24. Figure 2-25 presents the relationship between porosity and permeability as observed for this coarse grained backfill material. This relationship differs slightly from that obtained in the experiment DEBORA 1 (see Figure 2-16). The data of both experiments, however, are within the 95 % confidence interval around the regression curve of the data evaluated by Müller-Lyda et al. (1999).

Similar as in case of DEBORA 1 the test borehole was uncovered after termination of the heating period in order to get access to the compacted crushed salt for post test

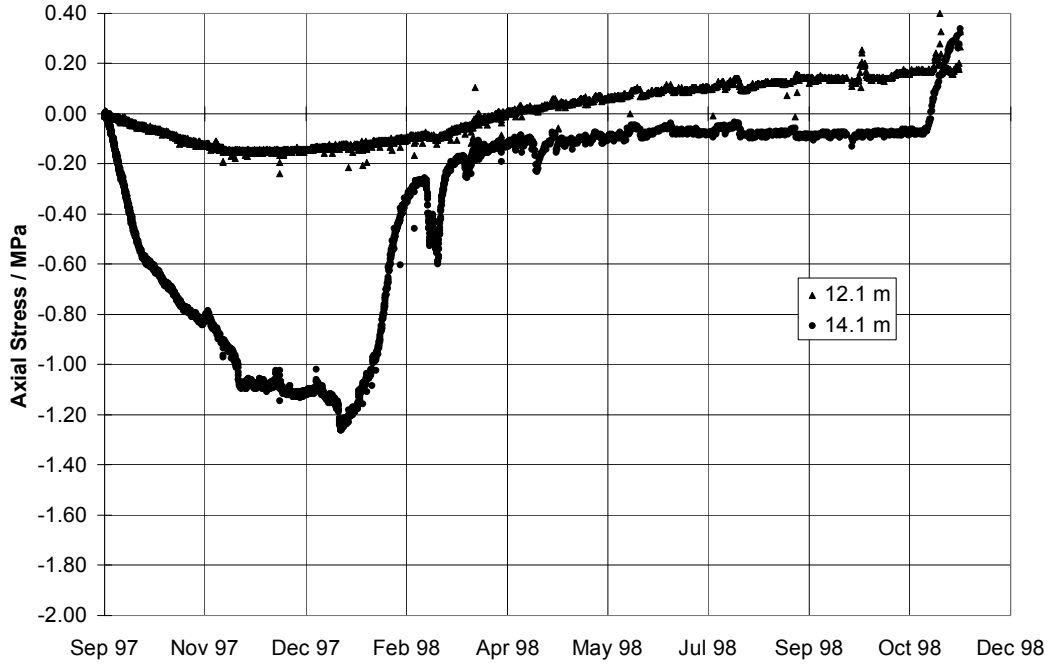

Figure 2-20 Development of axial stress in the backfill of DEBORA 2.

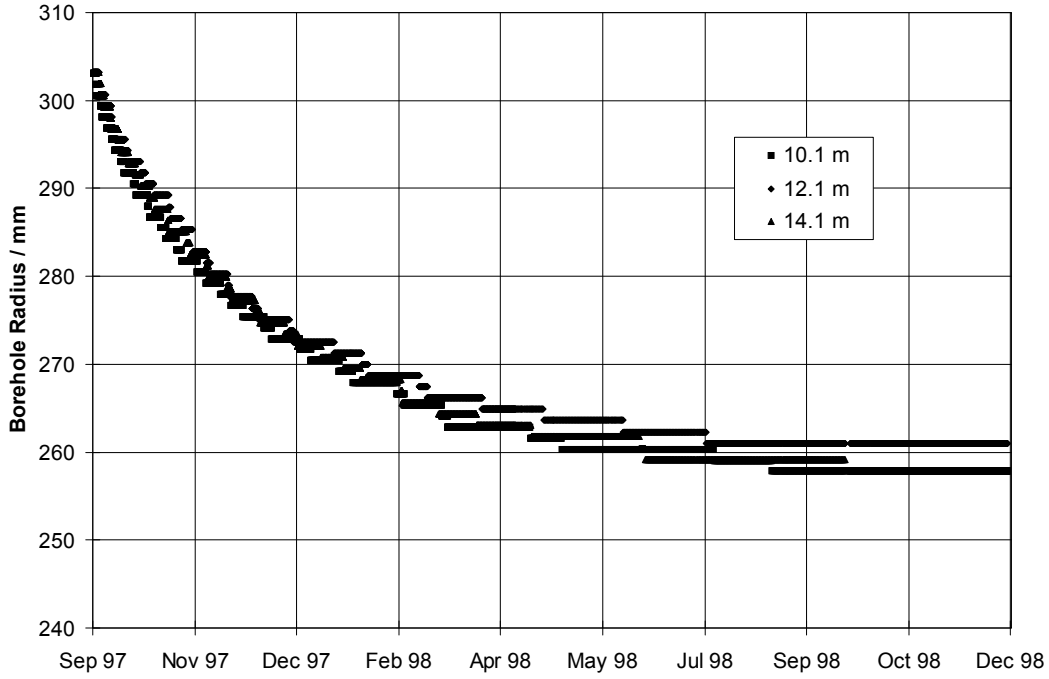

Figure 2-21 Development of borehole radius in DEBORA 2.

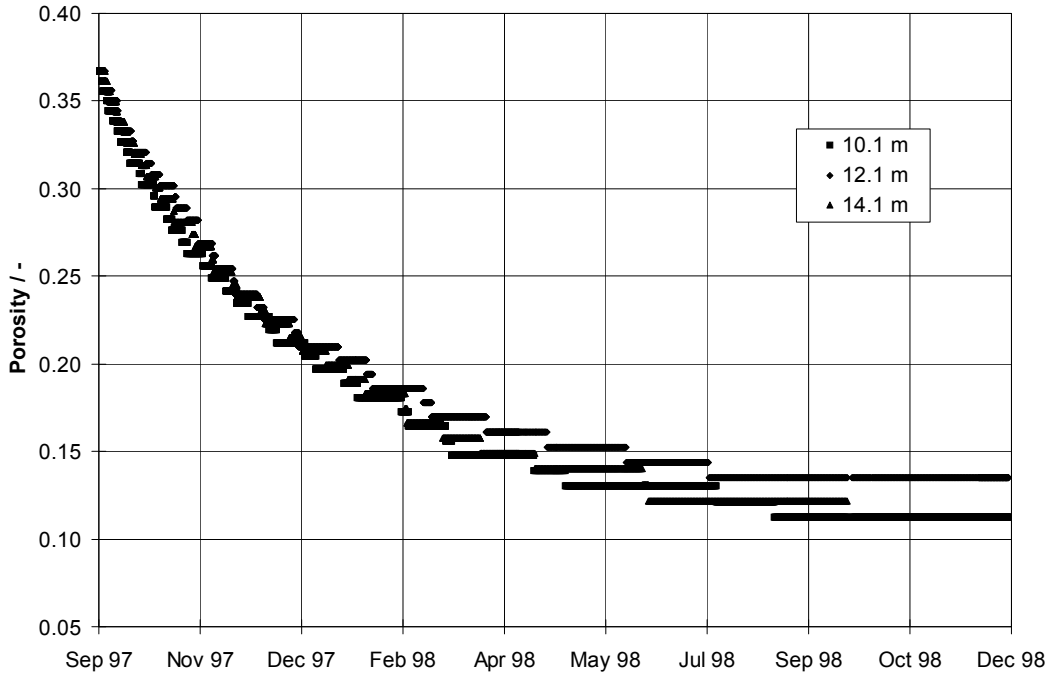

Figure 2-22 Development of backfill porosity in DEBORA 2.

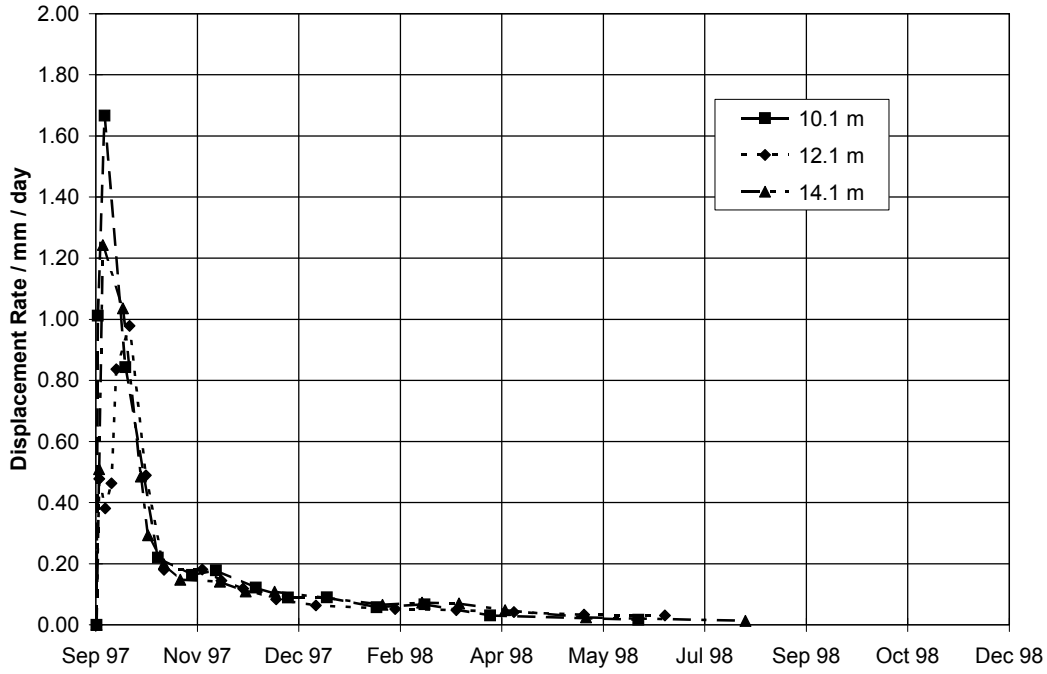

Figure 2-23 Development of displacement rates in DEBORA 2.

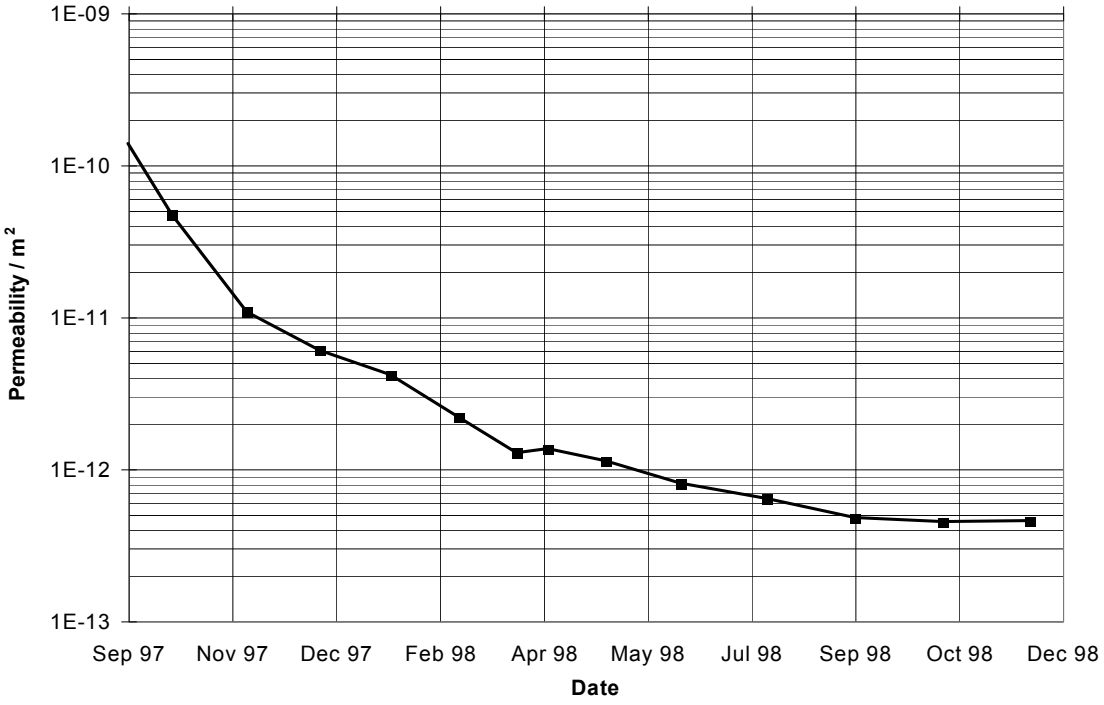

Figure 2-24 Development of backfill permeability in DEBORA 2.

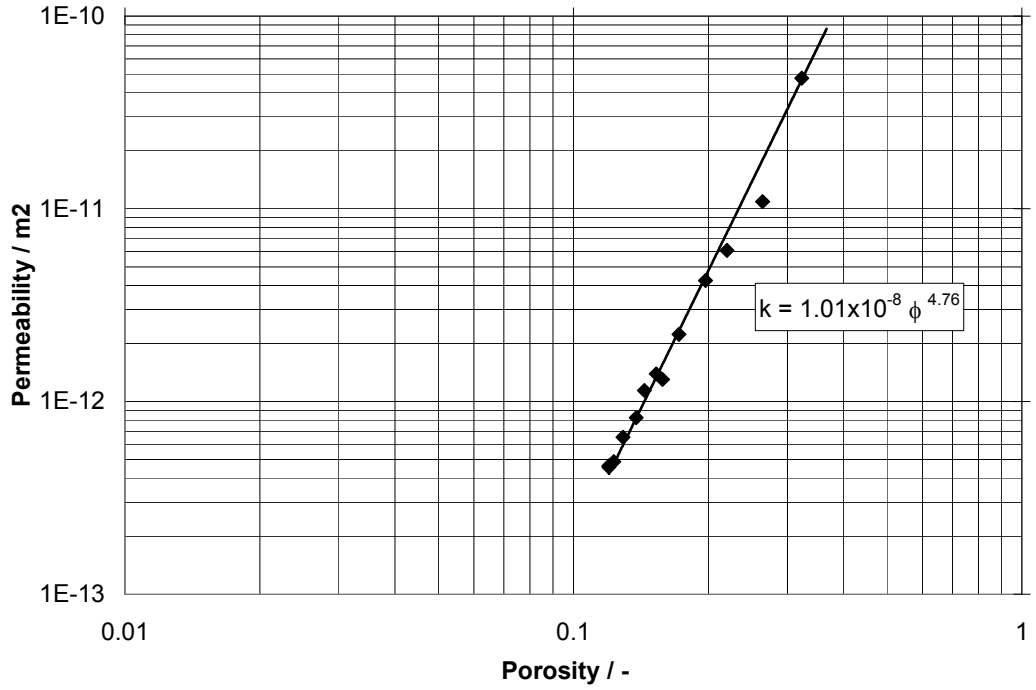

Figure 2-25 Relationship between permeability and porosity in DEBORA 2.

sampling and analysis. An access gallery was mined from the location of the already uncovered DEBORA-1 borehole into the direction of the DEBORA-2 borehole. As far as possible and acceptable, the rock salt around the backfilled borehole was removed by a continuous miner. Subsequently, specimens were cut with an electric saw from the compacted material (Figure 2-26) at several levels below the floor. Two samples at radial positions of 0.08 m and 0.16 m distance from the borehole axis were prepared from each specimen.

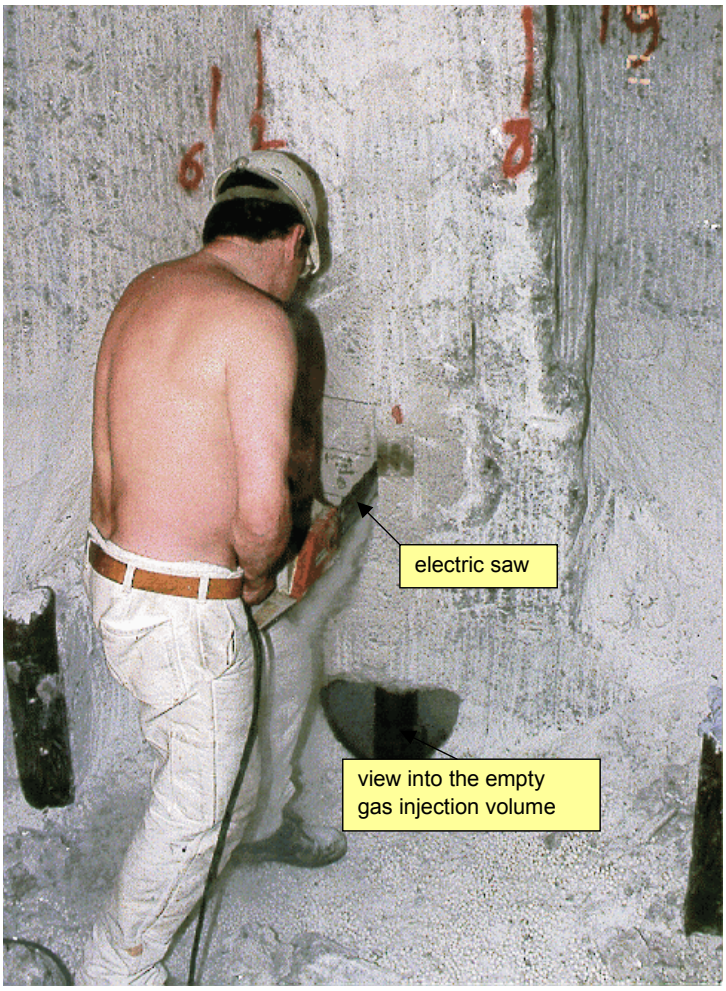

Figure 2-26 Specimen sampling at DEBORA-2 test site.

The distribution of porosity and permeability of the samples representing the situation in the backfill at the end of the compaction period is shown in Figure 2-27. Comparing the results with the data displayed in Figure 2-24 and Figure 2-25 it can be stated that

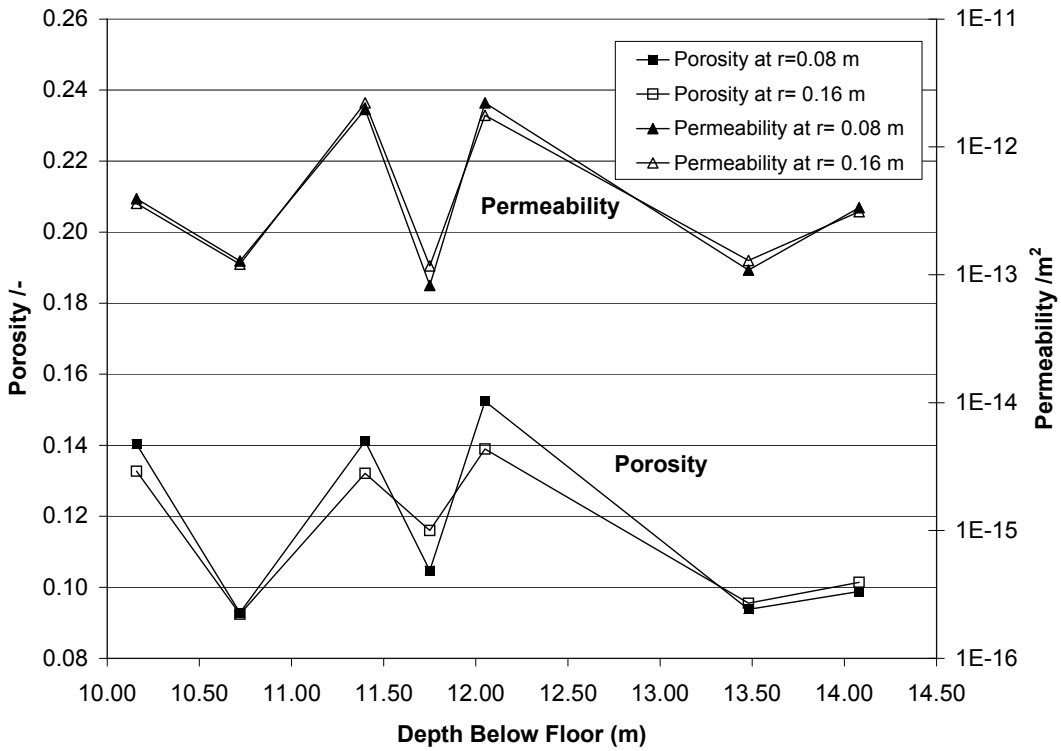

Figure 2-27 Distribution of porosity and permeability in the DEBORA-2 backfill material at termination of the heating period.

the porosity values determined by the in-situ convergence measurements are pretty well confirmed by the results of the post test analysis. All in-situ determined values lie within the bandwidth of the laboratory values. The results of the post test analysis also indicate that the backfill was compacted rather homogeneously in radial direction since a dependence of the data on the radius is hardly to be seen.

2.3 Conclusions

In the performance of the DEBORA experiments a satisfactory reliability of the measurements could be observed. This can be attributed to the relatively short experiment duration and, to a large extent, to the preceding “DEBORA Phase I” from 1991 to 1995 (Rothfuchs et al., 1996) in which a detailed test plan had been prepared. Only a comparatively small number of measuring sensors failed or showed erroneous measuring signals. A detailed discussion on the instrument performance can be found in Section 6.2.

In DEBORA 1, a maximum crushed salt temperature of about 185 °C was achieved while the maximum temperature in DEBORA 2 amounted to about 135 °C. These temperatures were more or less consistent with the concept for disposal of vitrified high-level waste canisters in salt formations which allows a maximum temperature of 200 °C at the interface between the canister surface and the salt formation.

Caused by heating, an accelerated borehole closure and backfill compaction was observed. In both experiments, the decrease of the borehole radius was measured at three levels and azimuths. In DEBORA 1, the borehole radius decreased from initially 300 mm to 275 mm and in DEBORA 2 from initially 303 mm to 259 mm. The backfill porosities were reduced from 38 % to 9 % and from 37 % to 12 %, respectively. The backfill permeability was measured monthly. In DEBORA 1, the permeability decreased from $5 \cdot 10^{-12}$ m^2 to $7 \cdot 10^{-14}$ m^2 and in DEBORA 2 from $1 \cdot 10^{-10}$ m^2 to $4 \cdot 10^{-13}$ m^2. The corresponding relationships between permeability k and porosity ϕ were determined to $k = 4.74 \cdot 10^{-9}\ \phi^{4.63}$ and $k = 1.0 \cdot 10^{-8}\ \phi^{4.76}$, respectively. Comprising all project data, those of the two in-situ experiments, of the post-test analyses, and of the parallel performed laboratory investigations (see Section 3) the relationship was determined to $k = 1.9 \cdot 10^{-8}\ \phi^{5.27}$ (see Figure 2-28).

The achieved final permeabilities in both experiments were still rather high in comparison to the very low permeabilities of less than 10^{-21} m^2 measured by Wieczorek et al. (1998) in situ in undisturbed rock salt in the Asse mine. It is questionable, whether such permeabilities are achievable by simple mechanical compaction of dry crushed salt. However, the relationship between permeability and porosity obtained from DEBORA 1 seems to satisfy not only the observed upper permeability/porosity range of interest, but also its lower part. Using the porosity of 0.004 given by Jockwer et al. (1995) as a minimum value for Asse salt, the relationship yields a permeability of $5 \cdot 10^{-22}$ m^2 which is in good agreement with the in-situ data measured in undisturbed rock salt.

The differences between the results obtained in DEBORA 1 and DEBORA 2 were small. Despite of the different grain size distribution of the backfill used in the experiments, the compaction behaviour seemed to be rather similar. The permeability/porosity data of both experiments, for instance, are lying within the 95 % confidence interval of the regression line determined by Müller-Lyda et al. (1996) on the basis of respective data published earlier by several other investigators.

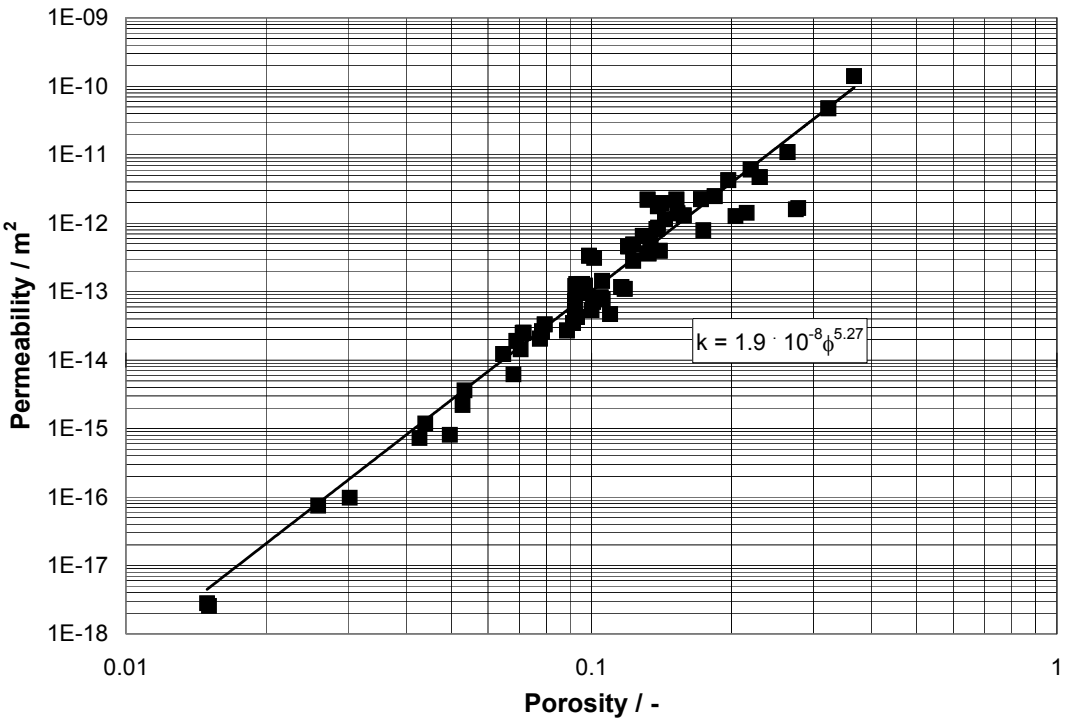

Figure 2-28 Relationship between permeability and porosity obtained from all in-situ and laboratory data of the DEBORA project.

The DEBORA experiments showed that much more time is required to achieve the high degrees of compaction or the low permeability values which would be representative for the long-term behaviour of crushed salt. For the assessment of the long-term effectiveness of drift and borehole seals made of crushed salt it is therefore indispensable to rely on model calculations. By the in-situ investigations a large amount of representative in-situ measuring data were made available for model development and model confirmation.

3 Laboratory Investigations

The major objective of the laboratory experiments was to investigate the compaction behaviour of fine- and coarse-grained crushed salt backfill. In addition to this, the sealing capability of the backfill was to be determined by the investigation of the gas permeability in dependence of the degree of compaction.

3.1 Backfill Compaction

For predicting the compaction behaviour of the crushed salt in the DEBORA experiments the constitutive law given by Hein (1991) was applied.

$$\dot{\varepsilon}_{ij} = \frac{A}{2} \cdot \left[\exp\left(-\frac{Q}{RT} \right) \right] \cdot \left(h_1 \cdot p^2 + h_2 \cdot q^2 \right)^2 \cdot \left(\frac{1}{3} h_1 \cdot p \cdot \delta_{ij} + h_2 \cdot S_{ij} \right) \qquad (3\text{-}1)$$

with

$\dot{\varepsilon}_{ij}$ = strain rate tensor in s^{-1}

A = constant factor in MPa . s^{-1}

Q = activation energy in J . mol^{-1}

R = universal gas constant: 8.314 J . $mole^{-1}$ K^{-1}

T = absolute temperature in K

p = hydrostatic pressure in MPa

q = invariant of stress tensor in MPa; $q = \sqrt{S_{ij} \cdot S_{ji}}$

δ_{ij} = Kronecker-Symbol; δ_{ij} = 1 if i = j, otherwise 0

S_{ij} = deviator of stress tensor in MPa

h_1, h_2 = material parameter (dependent on porosity) in MPa^{-2}

The parameters h_1 and h_2 are dependent on the porosity ϕ as follows:

$$h_1(\phi) = \frac{1 - d(\phi) \cdot c_3^2}{\left(\frac{c_4}{c_5} \left(\left(\frac{1-\phi}{1-\phi_0} \right)^{c_5} - 1 \right) \right)^2}, \qquad h_2(\phi) = c_6 + c_7 \cdot h_1(\phi) \tag{3-2}$$

with $d(\phi) = c_1 \cdot \exp(c_2 \cdot \phi)$ being a further porosity dependent material parameter, c_3 being $\tan\varphi$ the coefficient of internal friction (φ=angle of internal friction) and ϕ_0 being the initial porosity of the crushed salt.

The flow condition for crushed salt as given by Hein is presented in equation (3-3).

$$d\left(\frac{p}{q} - n\right)^2 + h_1 \cdot p^2 + h_2 \cdot q^2 = 1 \tag{3-3}$$

In order to determine the porosity dependent parameters h_1, h_2 and d, pairs of the p, q-values and the dilatancy factor n are determined by compaction tests in which the transition from the elastic to the irreversible plastic behaviour is reached. By performing three independent tests three linearly independent equations are obtained which permits to solve equation (3-3) for a defined porosity. The coefficient of internal friction which is explicitly contained in the factor of dilatancy must be determined in a separate test.

For the experimental determination of the material parameters several crushed salt compaction tests in two triaxial cells and in an oedometer were conducted.

3.1.1 Experimental Design

Fine-grained crushed salt

The parameters h_1, h_2, d were determined at ambient temperature in a small triaxial pressure cell (Karman type), which is designed for accepting samples with a diameter up to 100 mm and a height up to 200 mm. Because of the dimensions of the load pistons, the investigations were restricted to fine-grained Asse crushed salt with a grain size less than 8 mm. The grain size distribution is plotted in Figure 3-1 and summarized in Table 3-1.

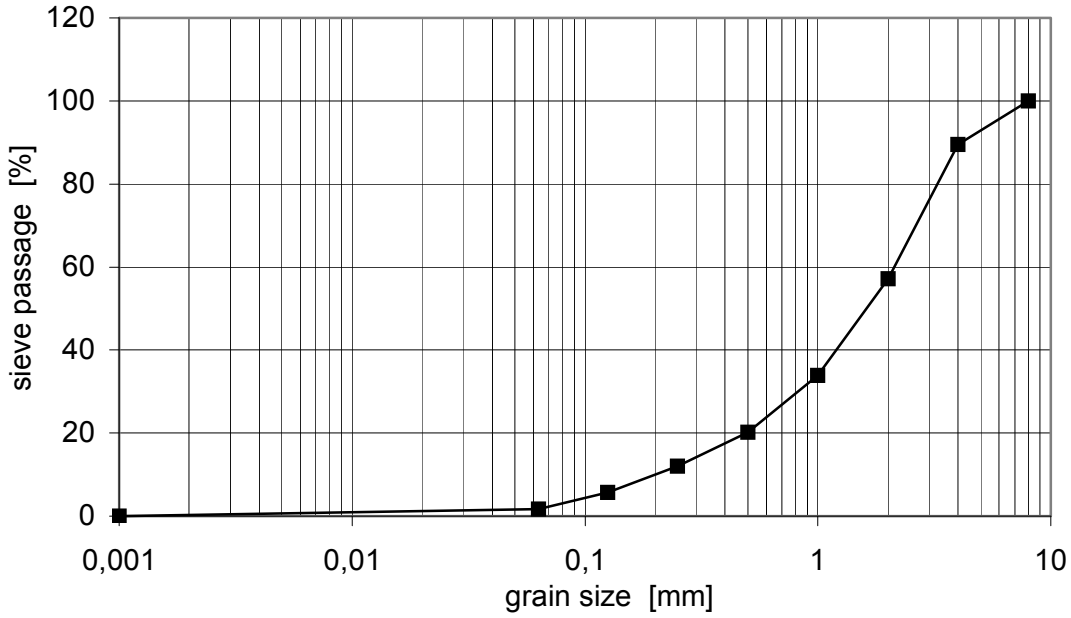

Figure 3-1 Characteristic screening curve for the fine-grained Asse crushed salt employed for the compaction tests.

Table 3-1 Summary of results from the sieve analysis of the fine-grained crushed salt.

Grain size	Sieve passage
mm	%
8	100
4	89.441
2	57.13
1	33.895
0.5	20.209
0.25	11.98
0.125	5.655
0.063	1.649
0.001	0

For determining the porosity, the grain density was always measured following the specifications in DIN 18124 with the use of a Beckman air pycnometer. An important requirement for all of these tests is the determination of the water content in the material supplied. This measurement was performed by furnace drying following the DIN 18121. For this purpose, a partial sample is dried at 105 °C for about 72 hours, and the water content is determined by weighing. Furthermore, characteristic screening curves are determined for the loose material. The axial deformation of the test specimen is measured with the use of a displacement gauge. The volumetric compressive strain can likewise be determined very accurately by means of an installed volume controller. Short-term compaction tests were conducted on the backfill material with constraint lateral expansion in an oedometer (Figure 3-2) as well as under hydrostatic pressure in the triaxial testing machine. The parameters c_4 and c_5 were determined in the oedometer; to a certain extent, these parameters are a measure of the volumetric stiffness of the material under investigation.

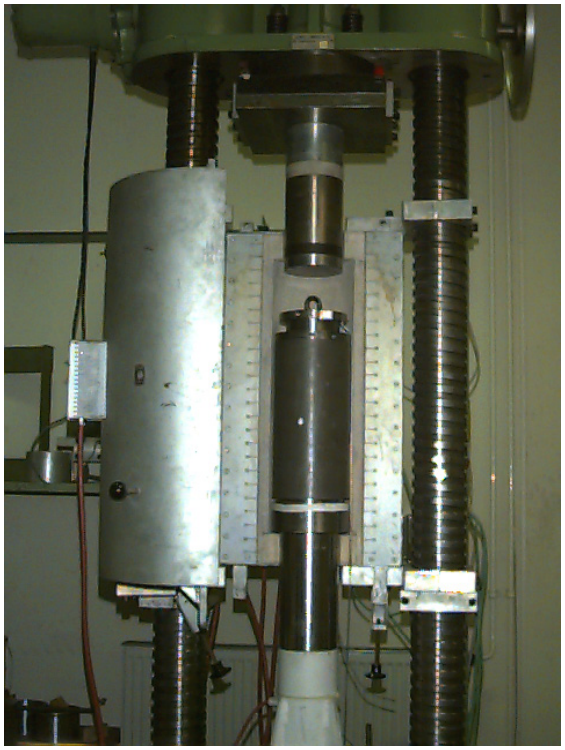

Figure 3-2 Amsler uniaxial test machine with installed oedometer between the upper and the lower platen.

Also the coefficient of internal friction was determined by tests in the small triaxial testing machine.

Coarse-grained crushed salt

The grain size distribution of the coarse-grained crushed salt is shown in Figure 3-3 and in Table 3-2. The laboratory tests were performed on granular material in a large triaxial testing machine (Figure 3-4). The load piston has a diameter of 280 mm, and the maximum installed height of the backfill sample is 700 mm. Thus, the ratio of the load piston diameter to the largest grain size is about 10. This ratio should be sufficient for minimizing interfering effects of cell limitations on the sample material under investigation. Otherwise, these tests were similar to those performed with the smaller apparatus just described. The volumetric compressive strain was determined with the use of a measuring device which permits a measurement of the sample diameter during the test; in this case, a gauge ring is installed in the annulus of the cell (in-vessel measurement).

3.1.2 Performance

Fine-grained crushed salt

For determining the material parameters of the Hein constitutive law for fine-grained backfill material, a large number of cylindrical test specimens were prepared. The grain size was less than 8 mm. For the investigations with the small triaxial testing machine, loose rock salt was compacted at a rate of 1 MPa/min under hydrostatic pressure. Subsequently, the crushed salt specimen was allowed to stand for about 17 hours under the given compaction pressure. The envisaged porosity values were 18 %, 15 %, 11 %, and 4 %; the corresponding pressures required for preparation (compaction pressures) were 10 MPa, 15 MPa, 30 MPa, and 60 MPa, respectively. After the consolidation time, the compacted crushed salt test specimens were deformed at a strain-controlled rate of 0.5 mm/min, from an initial hydrostatic stress in the axial direction. For this purpose, the confining pressure on the sample was maintained at the initial hydrostatic stress level with values of 10 MPa, 5 MPa, and 1 MPa. The transition from elastically reversible to plastically irreversible deformation is recognisable from the variation in deviatoric stress with increasing axial compressive strain. It has already

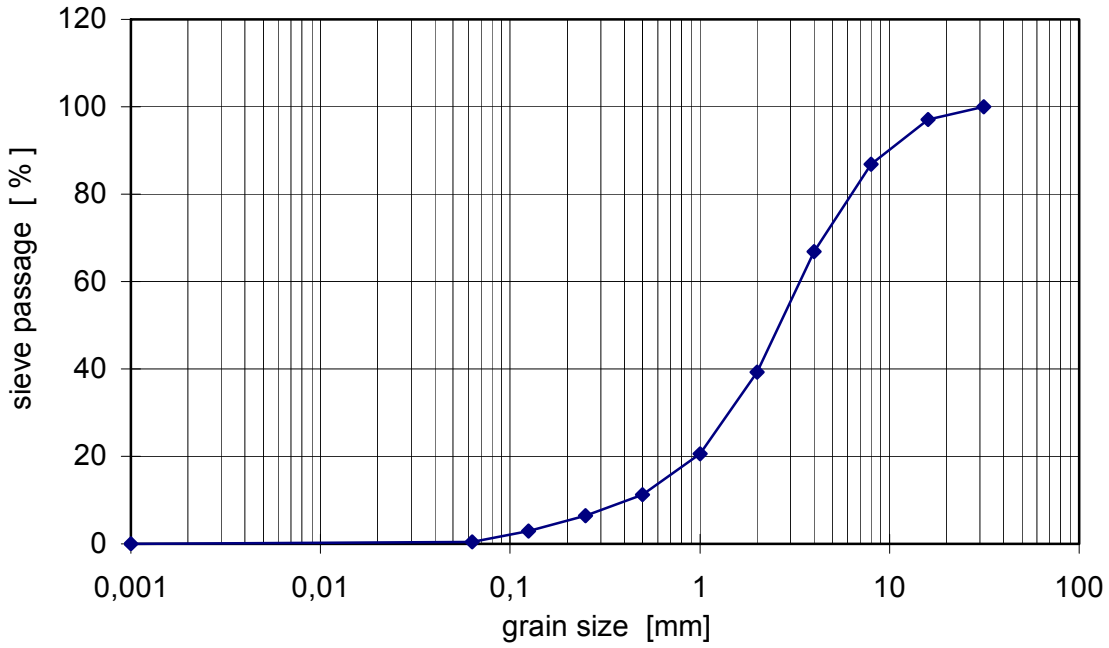

Figure 3-3 Characteristic screening curve of the coarse crushed salt employed for the compaction tests.

Table 3-2 Summary of results from sieve analysis of the coarse crushed salt.

Grain size	Sieve passage
mm	%
31.5	100
16	97.1
8	86.89
4	66.79
2	39.29
1	20.53
0.5	11.26
0.25	6.49
0.125	2.97
0.063	0.49
0.001	0.07

Figure 3-4 MTS triaxial test machine with inserted jacketed cylindrical crushed salt sample, the vessel is uplifted. In the mid-height of the sample a device for diameter measuring is shown.

been pointed out elsewhere that three identical test specimens are also necessary for determining the three parameters h_1, h_2, d for the respective porosity. In the Hein flow condition, the material-specific coefficient of internal friction is explicitly included in the dilatancy factor.

The coefficient of internal friction for crushed salt with a grain size less than 8 mm was determined under triaxial test conditions at room temperature. For this purpose, the backfill samples were subjected to an initial hydrostatic pressure of 1 MPa or 5 MPa and subsequently to axial deformation at a rate of 0.5 mm/min. The respective confining pressure was thereby held constant at 1 MPa or 5 MPa. After attainment of maximum compaction, further axial loading results in deconsolidation of the sample material. The transition between these two states determines zero dilatancy, at which no volume change occurs. By means of the two Mohr circles, the angle of internal

friction or the coefficient of internal friction can be determined in the well-known τ,σ-plot after Mohr-Coulomb (Leibholz 1968).

For the compaction of backfill samples with defined porosity, certain preparation pressures are necessary for short-term compacting. A functional relationship exists between the irreversible volumetric compressive strain and the applied pressure; this relationship depends on the initial porosity. The material parameters c_4 and c_5 which describe this relationship have been determined in the laboratory. For the backfill material of grain size less than 8 mm, the results have been obtained from oedometer or triaxial tests (hydrostatic). In the oedometer, tests were performed at ambient temperature and at 150 °C; the axial rate was 0.1 mm / min. The values for the heated samples were lower by 30 % or 15 %.

Coarse-grained crushed salt

The tests conducted with the large triaxial test machine for determining the material parameters, such as the angle of internal friction φ as well as c_4 and c_5, were always performed in the same manner as those with the smaller triaxial testing machine. The dimensions allow testing of backfill samples with grain sizes of the order of 30 mm. First tests for determining the parameters for the flow condition given by the Hein flow rule have revealed that the samples with porosities of 17 % and 14 % under a supporting confining pressure of 5 MPa have already lost their internal coherence at an axial pressure of 6 MPa and 7 MPa, respectively.

A consideration of the results in the p,q-plane indicates highly inhomogeneous compaction of the sample material. For the repetition of the test six specimens with precompacted porosities of 18 % and 13 % were additionally investigated in the laboratory. Experimental results are shown in Figure 3-5.

3.1.3 Results

Fine-grained crushed salt

The values compiled in Table 3-3 for the parameters of the flow condition have been determined from the results of tests on 12 samples.

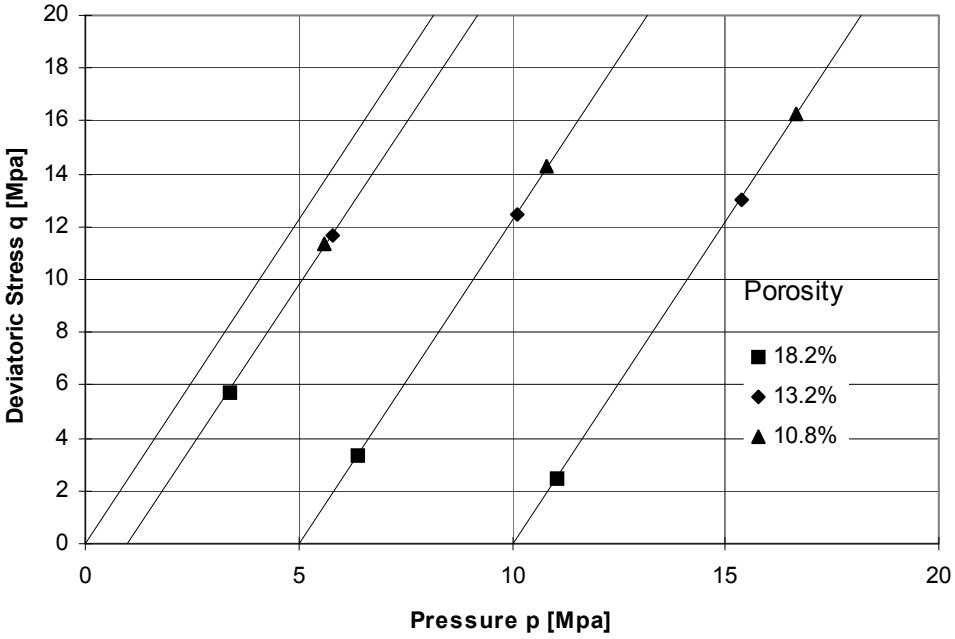

Figure 3-5 p, q-values indicating the transition from the elastic to the plastic irreversible material behaviour of coarse-grained salt samples.

Table 3-3 Numerical values of parameters h_1, h_2 and d for describing the flow condition in accordance with the flow condition equation for fine-grained crushed salt. The p,q-values were obtained from confined compression tests using a tan φ of 1.3.

Porosity	h_1	h_2	d
-	MPa^{-2}	MPa^{-2}	-
0.176	0.00513	0.00822	0.19178
0.160	0.00477	0.00569	0.15739
0.114	0.00152	0.00279	0.07870
0.044	0.00048	0.00079	0.08061

For parameter determination a tan φ of 1.3 was used

From the data presented in the table, functional relationships between the parameter h_1 and the parameter h_2 were determined. This relationship is plotted in Figure 3-6 by means of a linear trend curve.

The straight line is expressed by the following equation

$$h_2 = 1.3506 \cdot h_1 + 0.0004 \qquad (3\text{-}4)$$

With appropriate matching of the data, the following relationship is obtained for the parameter d and the porosity ϕ:

$$d = 0.0515 \cdot \exp(6.682\phi) \qquad (3\text{-}5)$$

This relationship is illustrated in Figure 3-7.

A further result of the investigations for determining relevant parameters is the coefficient of internal friction. For the fine-grained crushed salt the coefficient of internal friction was c_3 = 1.3; the corresponding angle of internal friction was φ = 52.4°, and the cohesion was 0 MPa.

In the laboratory tests for determining the material-specific parameters c_4 and c_5, the short-term compaction of salt granulate was performed in the oedometer, that is, quasihydrostatically, as well as under hydrostatic conditions in the triaxial testing machines. The results are summarised in Table 3-4. The values presented here have been determined on the basis of the effective volumetric compressive strain $\varepsilon_{vol,I}$.

Coarse-grained crushed salt

The tests performed on the coarse-grained crushed salt with the size of < 30 mm in the large triaxial testing machine have revealed that the samples with porosities of 17 % and 14 % have already lost internal integrity at an axial pressure of 6 MPa and 7 MPa. The determination of the material parameters h_1 and h_2 was therefore not possible. The results of the additional measurements with porosities of 13 % and 18 % together with

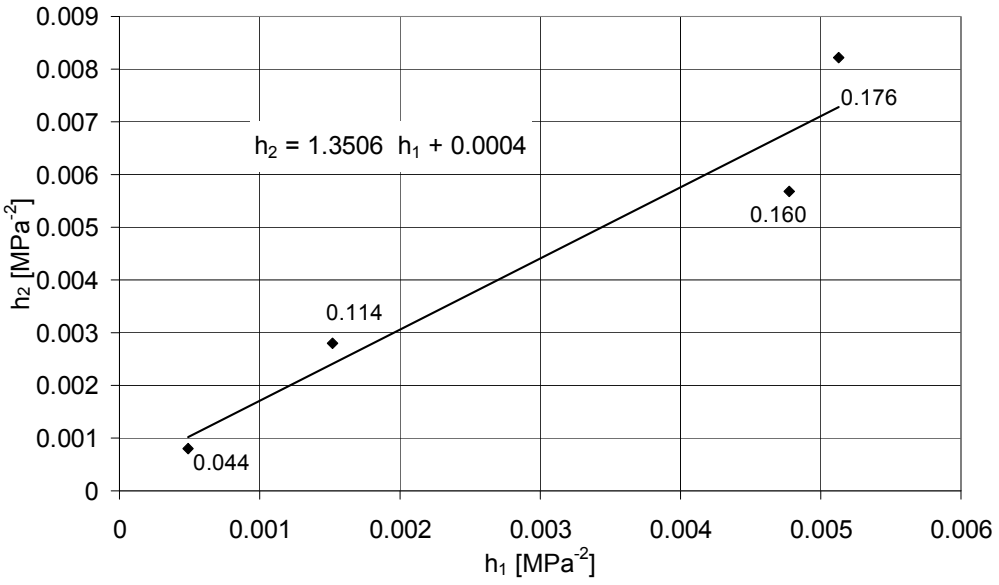

Figure 3-6 Parameter h_2 as a function of the material parameter h_1. The functional relationship was obtained from least-squares regression.

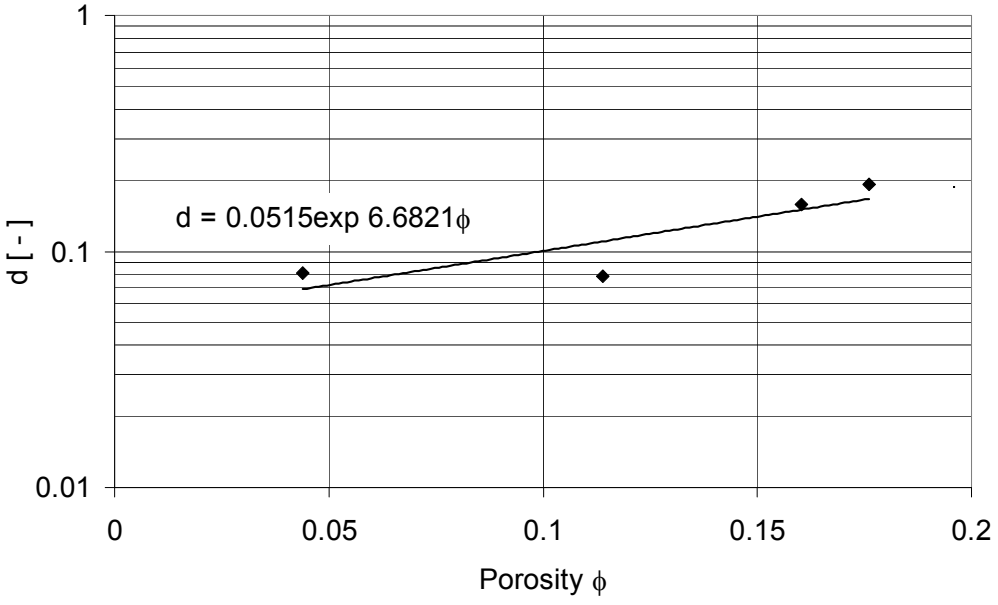

Figure 3-7 d as a function of the porosity ϕ. The functional relationship was obtained from least-squares regression.

Table 3-4 Determination of material parameters from short-term compaction tests on crushed salt at ambient temperature. The parameters were determined on the basis of natural (logarithmic) volume strain.

Experiment	Specification	Grain size	C_4	C_5	Initial porosity
		mm	MPa	-	
7	Oedomet.	< 8	36.032	7.209	~0.3
8	Oedomet.	< 8	38.950	6.878	~0.3
9	Oedomet.	< 8	39.300	6.632	~0.3
10	Oedomet.	< 8	38.444	6.526	~0.3
11	triaxial/hydrost.	<8	34.962	7.078	0.37

the results of the samples with 11 % from the first test are shown in Figure 3-5 (compare Section 3.1.2). The measurements for the 18 % porosity specimens at confining pressures of 5 MPa and 10 MPa exhibit an anomalous behaviour in the p-q plane. Generally, the solutions of the flow condition equation (3-3) are for the present case unrealistic. It is conceivable that the results are strongly influenced by inhomogenities caused by segregation of the granular fractions when pouring the specimen material into the rubber jacket.

The material parameters c_4 and c_5 for that specific crushed salt were determined to 62.471 MPa and 11.105, respectively. The initial porosity was 0.27. The coefficient of internal friction for this crushed salt was determined to $c_3 = 0.87$, and the corresponding angle to $\varphi = 41°$. The cohesion was 1.1 MPa.

3.2 Backfill Permeability

A further objective of the laboratory analyses was to determine the dependence of the permeability on the degree of compaction and thus on the porosity. Also these analyses were performed on fine-grained as well as coarse-grained crushed salt.

3.2.1 Experimental Design

Fine-grained crushed salt

These measurements were also performed in the small triaxial testing machine which accommodates test samples of dimensions up to 100 mm in diameter and 200 mm in height. The radial and axial stresses could be controlled independently of one another. The permeability measurements were performed with axial flow of nitrogen through the test specimens. The gas injection pressure was determined with the use of pressure transducers, and the gas flow rate was measured with thermal mass flow sensors. At very low permeabilities, the volume flow rate of the gas was measurable only from the displacement of water in a burette.

Coarse-grained crushed salt

The permeability determinations were performed in combination with the measurements for determining the angle of internal friction and the parameters h_1 and h_2 of the Hein's constitutive law. In order to avoid unnecessary interferences with these measurements, the permeability was determined at the initial hydrostatic stresses intended for these experiments or at the associated initial porosities.

The measurements were performed in the triaxial testing machine which accommodates test samples of dimensions up to 280 mm in diameter and 700 mm in height. Also here, the radial and axial stresses could be controlled independently of one another. The permeability measurements were performed with axial flow of nitrogen through the test specimens. Again, the gas injection pressure was determined by use of pressure transducers, and the gas flow rate was measured with thermal mass flow sensors.

3.2.2 Performance

Fine-grained crushed salt

The same fine-grained Asse crushed salt with a grain size less than 8 mm which was used in the compaction tests (see Section 3.1.1) was employed for preparing the test specimens.

The moisture content was determined by drying to 0.02 % at 105 °C for 72 h. The grain density was determined with the use of an Beckman air comparison pycnometer; the value thus obtained was 2195 kg/m^3.

For preparing the samples, the crushed rock salt was compacted under hydrostatic conditions in a triaxial testing machine (Karman type). The compacting pressure was applied at a rate of 1 MPa/min. Subsequently, the samples were maintained at the respective, preset compacting pressure for a period of 17 h to 20 h. Compacting pressures of 30 MPa, 45 MPa, and 60 MPa were applied for the purpose; one test specimen was prepared for each pressure stage. For attaining lower porosities, a further test specimen was prepared at elevated temperature. The material was hydrostatically compacted at 30 MPa and subsequently heated to 107 °C. The sample thus prepared had an initial porosity of 28.3 % and a final porosity of 6.18 %. The porosities of these samples are compiled together with the associated initial porosities in Table 3-5.

For the test specimens prepared at ambient temperature, the gas permeability was determined with nitrogen under respective constant hydrostatic pressure conditions (30 MPa, 45 MPa, and 60 MPa). For the evaluation, the generalized Darcy's law for compressible media for steady-state flow was applied:

$$k_g = \frac{2 \cdot q_g \cdot \mu_g \cdot l \cdot p_0}{A \cdot \left(p_1^2 - p_0^2\right)} \tag{3-6}$$

with:

k_g	Permeability measured to gas	m^2
q_g	Flow rate of the gas	m^3/s
p_1	Injection pressure	Pa
p_0	Atmospheric pressure	Pa
μ_g	Viscosity of the gas	Pa·s
l	Sample length	m
A	Cross-sectional area of the sample	m^2

Subsequently, the samples were deformed deviatorically by increasing the axial stress

Table 3-5 Summary of the porosities for the test specimens prepared.

Sample	Temperature	Preparation pressure	Initial porosity	Porosity after preparation
	°C	MPa	%	%
Perm V1	ambient	30	28.9	10.01
Perm V2	ambient	45	28.9	6.80
Perm V4	ambient	60	27.7	4.97
Perm V6	107	30	28.3	6.18

at a rate of 0.5 mm/min, and the gas permeability was redetermined at different individual stages of compaction and thus at different porosities. This method permitted the attainment of maximum compaction without exceeding the dilatancy point. The final values of the porosity were 2.59 % (30 MPa), 1.51 % (45 MPa), and 1.49 % (60 MPa); these values depend on the conditions of preparation at ambient temperature indicated in parentheses.

In the case of the sample Perm V6 prepared by heating to 107° C, a porosity of 1.24 % was attained by deviatoric compaction from the initial hydrostatic pressure of 30 MPa under these boundary conditions. However, the gas permeability was measured on this sample at ambient temperature.

Coarse-grained crushed salt

Coarse-grained crushed salt with a grain size less than 32 mm as already described in Section 3.2.1 was employed for preparing the test samples.

The moisture content was again determined by drying to 0.02 % at 105 °C for 72 h. The grain density was determined with the use of an air comparison pycnometer; the value thus obtained was 2199.5 kg/m^3.

The crushed salt was poured into the rubber jacket of the large triaxial testing machine and subsequently compacted at various hydrostatic confining pressures for attaining

different porosities. The sample preparation as well as the tests for determining the permeability were performed exclusively at ambient temperature.

In the case of the tests for determining the angle of internal friction, samples were prepared under defined initial hydrostatic conditions. For determining the parameters h_1 and h_2, however, the corresponding experiments were performed in porosity ranges specified in advance.

After pouring of the crushed salt into the cell, the permeabilities were determined at the corresponding installation porosities. Subsequently, the material was compacted under hydrostatic conditions. After attainment of the respective degree of compaction, the permeabilities associated with the resulting porosities were determined with nitrogen. For the evaluation, Darcy's law for compressible media was applied for steady-state flow (see preceding).

3.2.3 Results

Fine-grained crushed salt

In the case of the samples prepared at ambient temperature, the porosity values ranged between 10.01 % and 1.49 %. The associated permeabilities corrected in accordance with Klinkenberg ranged between $5.36 \cdot 10^{-14}$ m^2 and $2.81 \cdot 10^{-18}$ m^2; the permeability value for the lowest porosity is somewhat higher than that for the next higher porosity (ϕ = 1.51 %; k = $2.56 \cdot 10^{-18}$ m^2). The dependence of the permeability on the porosity is indicated in the double-logarithmic plot in Figure 3-8 for the samples prepared at ambient temperature.

The porosity of the sample which had been heated to 107 °C and deviatorically compacted was 1.235 %. A Klinkenberg correction of the measured permeability values was not possible, presumably because of the very low permeability, since even very small variations in the boundary conditions during the experiments affect the measurements. Consequently, the permeability varied from $1.08 \cdot 10^{-21}$ m^2 to $4.24 \cdot 10^{-22}$ m^2 as the injection pressure and thus the confining pressure varied between 2.37 MPa and 4.95 MPa.

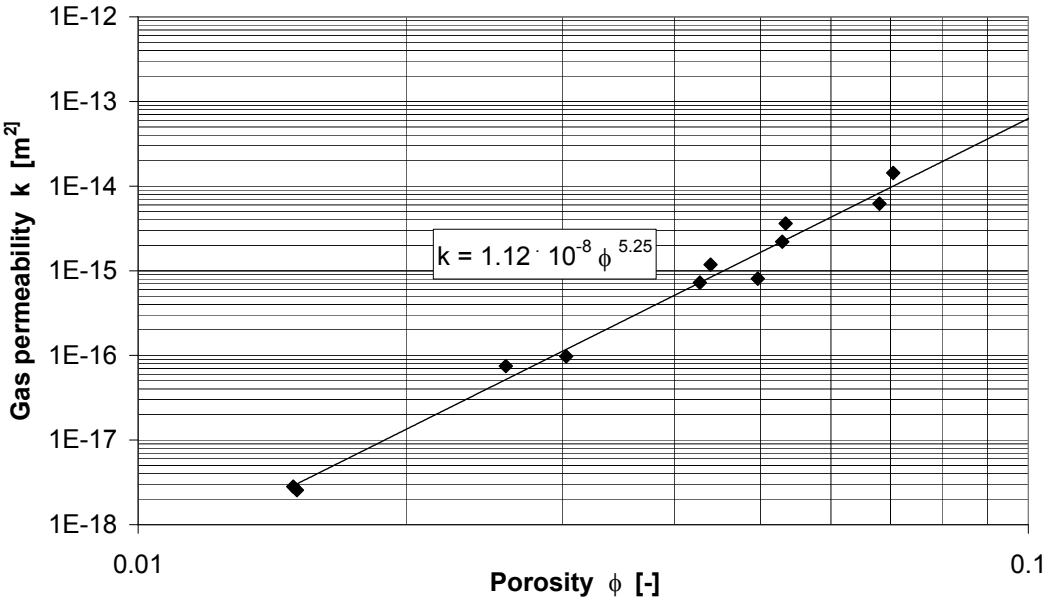

Figure 3-8 Dependence of the permeability on the porosity of the Asse crushed salt samples with maximum grain size of 8 mm compacted at ambient temperature.

The results of the tests are presented in Table 3-6, the permeability value for the Perm V6 sample is thereby referred to the measurement at the lowest injection pressure.

A comparison of the results obtained with the samples prepared at ambient temperature with those for the sample prepared by heating indicates that the permeability of $1.08 \cdot 10^{-21}$ m^2 is decidedly lower, although the corresponding porosity attains a value of only 1.235 %, and thus the decrease is by no means so overproportionate.

After attainment of porosities less than about 1.5 % - this applies to the final values for samples Perm V2 and Perm V4 as well as Perm V6 - it was no longer possible to perform the permeability measurements under the confining conditions indicated in Table 3-6. This is due to the long measuring times associated with the very low permeabilities, during which the samples had altered under the high confining pressures, and the permeability measurements were affected accordingly. These samples were investigated at low hydrostatic pressure; in this case, the injection pressures were equal to the confining pressures.

Table 3-6 Summary of results from the compaction tests on Asse fine-grained crushed salt; grain density: ρ_g = 2195 kg/m^3.

ρ	σ_1	$\sigma_2 = \sigma_3$	$\sigma_1 - \sigma_3$	ϕ	ϕ	k
kg/m^3	**MPa**	**MPa**	**MPa**	**%**	**-**	**m^2**
Ambient temperature						
1975.00	29.64	29.92	-0.28	10.01	0.1001	$5.36 \cdot 10^{-14}$
2040.00	64.11	29.92	34.19	7.05	0.0705	$1.43 \cdot 10^{-14}$
2078.00	75.94	29.91	46.03	5.34	0.0534	$3.63 \cdot 10^{-15}$
2099.00	82.86	29.92	52.94	4.40	0.0440	$1.18 \cdot 10^{-15}$
2138.00	97.06	29.92	67.14	2.59	0.0259	$7.48 \cdot 10^{-17}$
2046.00	44.37	45.04	-0.67	6.80	0.0680	$6.19 \cdot 10^{-15}$
2079.00	78.58	44.88	33.70	5.29	0.0529	$2.20 \cdot 10^{-15}$
2101.00	88.05	45.00	43.05	4.28	0.0428	$7.25 \cdot 10^{-16}$
2129.00	100.13	45.08	55.05	3.03	0.0303	$9.75 \cdot 10^{-17}$
2162.00	116.42	44.85	71.57	1.51	0.0151	$2.56 \cdot 10^{-18}$
2086.00	60.00	59.98	0.02	4.97	0.0497	$8.07 \cdot 10^{-16}$
2162.00	132.42	59.87	72.55	1.49	0.0149	$2.81 \cdot 10^{-18}$
T=107 °C						
2168	73.34	29.95	43.39	1.24	0.0124	$1.08 \cdot 10^{-21}$ *)

*) The permeability value has been determined at ambient temperature, and not under the confining conditions indicated in the table. The confining conditions as well as the indicated temperature refer only to the sample preparation.

k	Permeability	m^2
T	Temperature	°C
σ_1	Axial stress	MPa
$\sigma_2 = \sigma_3$	Confining stress	MPa
ϕ	Porosity	-
ρ	Bulk density	kg/m^3

A closer consideration of the porosities generated under the individual differential stresses reveals that only a kind of "limiting porosity", in this case about 1.5 %, is evidently approached during short-term tests (duration: about 1 week) (Figure 3-9). With this type of salt, this behaviour is observed under different confining conditions and under the boundary conditions with respect to moisture, ambient temperature, and test period.

Coarse-grained crushed salt

Since three individual measurements were performed for determining h_1 and h_2 in each porosity range, the permeability was also determined for each of these individual measurements. The values were averaged for all porosities and permeabilities in the installation condition as well as for the individual porosity ranges. The results of the permeability measurements performed in conjunction with the determination of the angle of internal friction were also taken into account in calculating these averages.

A Klinkenberg correction was not possible for experimental reasons, since turbulent flow effects presumably occurred at the very high permeabilities. Consequently, only the permeabilities determined at the lowest injection pressure are considered.

The values of the installation porosity ranged between 30.8 % and 23.2 %. The corresponding permeability values in the installation condition were $1.32 \cdot 10^{-12}$ m^2 and $3.29 \cdot 10^{-12}$ m^2. The porosities after hydrostatic compaction ranged from 10.58 % to 27.49 %. The associated permeabilities ranged between $7.77 \cdot 10^{-14}$ m^2 and $1.59 \cdot 10^{-12}$ m^2. The results are compiled in Figure 3-10.

A consideration of the results reveals that an appreciable decrease in permeability occurs only at a porosity less than 20 %. Furthermore, slight variations in porosity apparently do not decidedly affect the permeability. Thus, the permeability value at a porosity of 13.91 %, for instance, was measured to be even somewhat higher than the permeability at a porosity of 17.41 %, although this is higher by about 3.5 %-points.

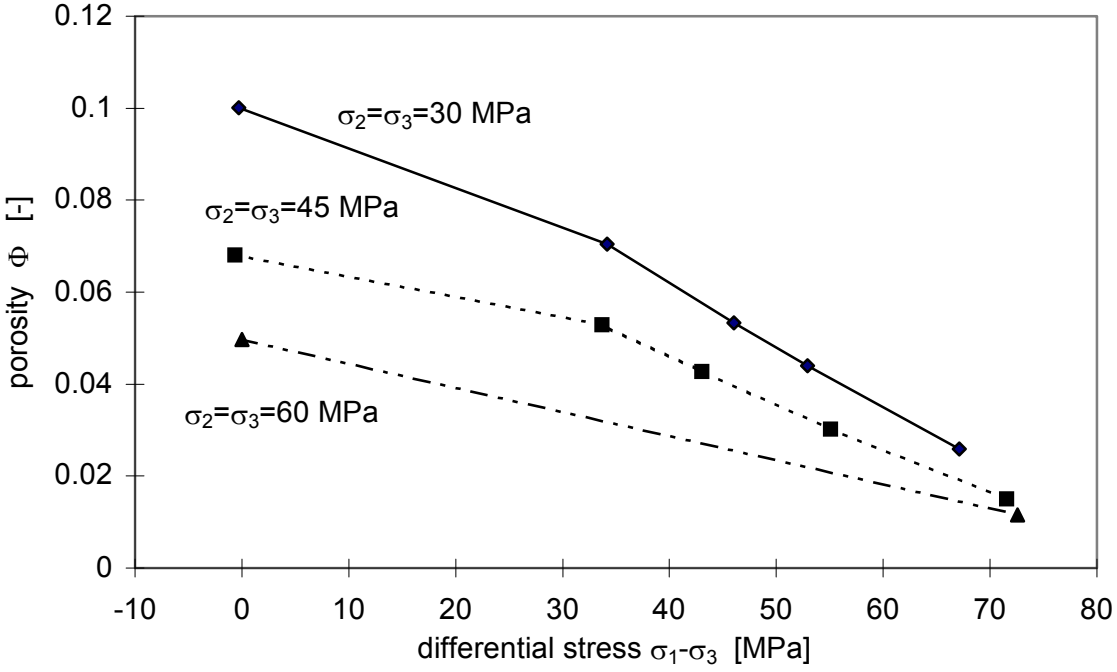

Figure 3-9 Porosity as a function of the differential pressure for various confining stresses in the samples prepared at ambient temperature.

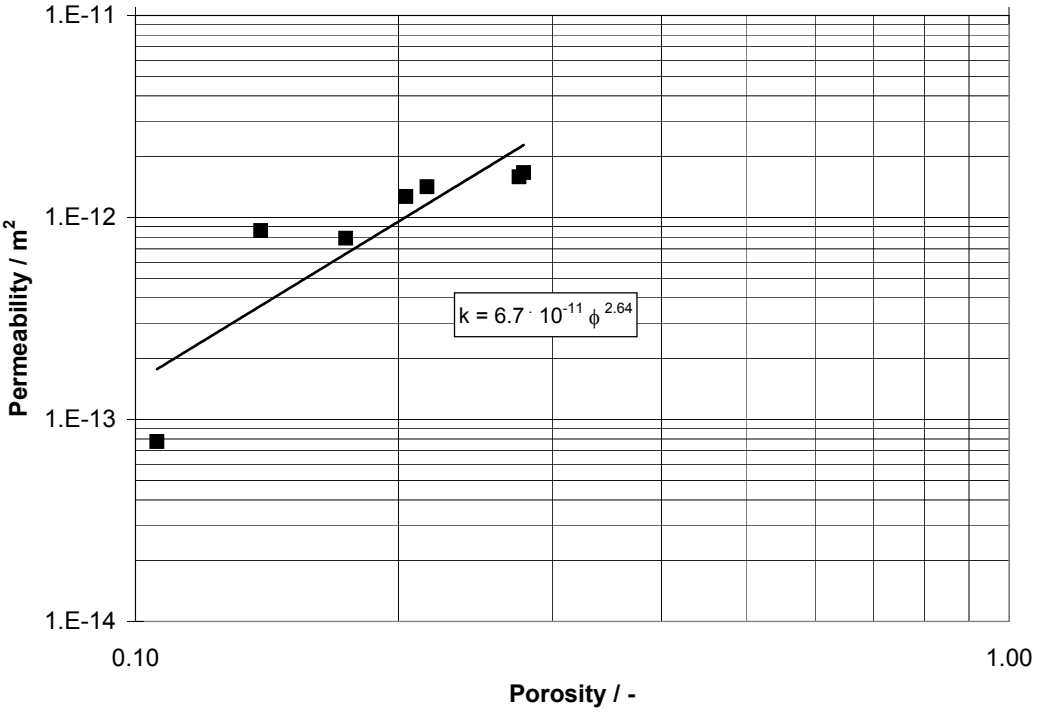

Figure 3-10 Dependence of the permeability on the porosity of the Asse crushed salt samples with maximum grain size of 30 mm compacted at ambient temperature.

3.3 Conclusions

The crushed salt laboratory experiments were performed in order to determine the material-specific parameters of Hein's constitutive law for granular backfill material.

The laboratory triaxial experiments were conducted using conventional triaxial cells (Karman type) of different sizes and loading capacities and one oedometer cell. In some cases, the experiments were performed at higher temperature.

For crushed salt with grain size less than 8 mm and an initial porosity of ~0,3 the parameters c_4 and c_5 that determine the pressure dependent volumetric moduli of compression (c_4 is the initial compression modulus) was determined at ambient temperature and at 150° C in an oedometer. From these experiments it is concluded that for the granular salt used the temperature influences essentially the parameter c_4 resulting in a reduction of about 30 % when the temperature rises to 125 °C. As a consequence of this, the material behaves softer.

The experiments were repeated for coarse grained salt less than 31 mm in a large triaxial testing machine under hydrostatic stress conditions and at ambient temperature. The results gathered indicate a higher stiffness of the parameters in comparison to the fine-grained material by a factor of about two.

The coefficient of internal friction c_3 was determined at ambient temperature for fine-grained salt, at ambient temperature in an oedometer, and for coarse-grained salt again in the large triaxial cell. From these experiments it was concluded that the parameter is largely influenced by grain size distribution and the shape of the granular material.

The mentioned material parameters are involved in a more or less complex manner in the determination of the parameters d, h_1, h_2 in the flow condition equation. For the fine-granular salt the determined numerical values of these parameters satisfy the equation for the given porosities but it could not be solved in case of the coarse-grained salt, obviously because of local material inhomogeneities leading to mechanical instabilities of the samples at higher porosities.

The major conclusion is that there is a need for more experimental work using carefully controlled starting material to investigate the mechanisms that control the compaction process.

The gas permeability has been successfully determined in dependence of the porosity at increasing degree of compaction. In the case of fine-grained crushed salt, however, sample preparation from dry material at ambient temperature was possible only for porosities over 1 %. Especially during the tests on fine-grained crushed salt, it was observed that a kind of "limiting porosity" is attained under the given boundary conditions (ambient temperature, moisture) as the stress difference is increased. Even with a sample prepared at elevated temperature, an appreciably lower porosity is not attained. The regression analysis of the data obtained for the fine-grained material resulted in the relationship $k = 1.12 \cdot 10^{-8} \phi^{5.25}$ between the permeability k and the porosity ϕ.

The investigations on coarse-grained crushed salt were coupled with measurements for determining the above mentioned material parameters. In order to avoid unnecessary interference with these measurements, tests were performed under the respective hydrostatic conditions for preparing the test specimens for these measurements. For this reason, preparation was possible only at pressures up to about 30 MPa which corresponds to a porosity of about 10.58 %. The relationship between permeability and porosity obtained for this material is $k = 6.7 \cdot 10^{-11} \phi^{2.64}$.

A comparison of the relationships obtained for both types of crushed salt is shown in Figure 3-11. The relationship for the fine grained material agrees rather well with the data obtained from the in-situ measurements (compare Figure 2-16 and Figure 2-25) and also with the relationship for naturally moist crushed salt presented by Müller-Lyda et al. (1999) after an evaluation of data of various investigators. According to Müller-Lyda et al. (1999), the coarse grained material behaves obviously more like a very dry material.

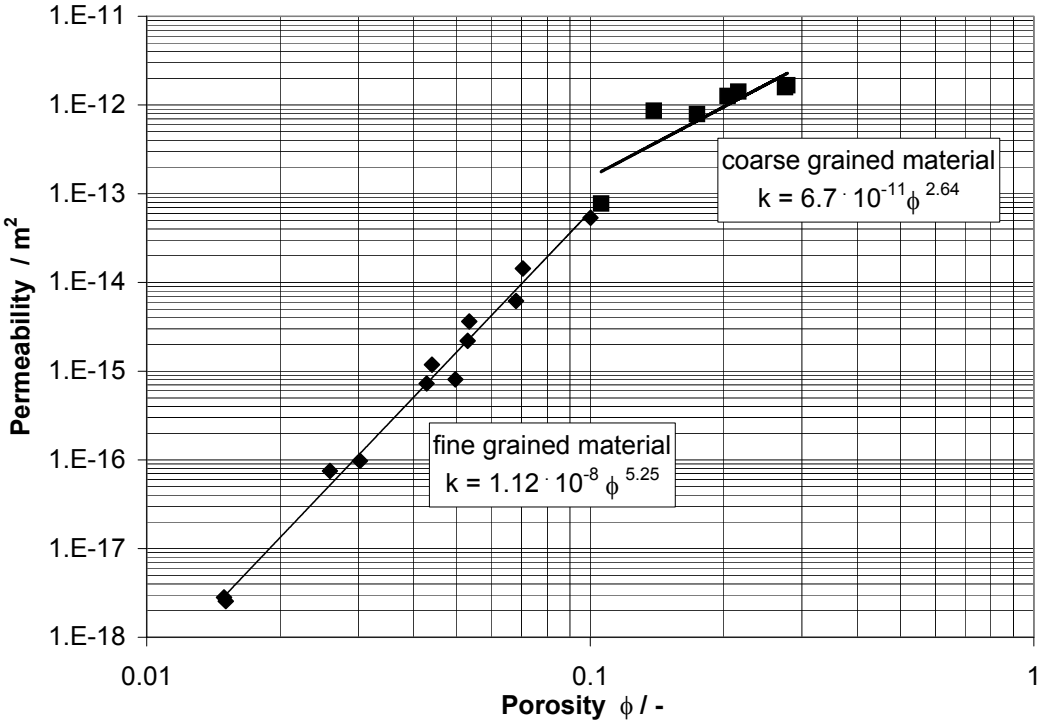

Figure 3-11 Comparison of the relationships between permeability k and porosity ϕ for fine and coarse grained crushed Asse salt.

4 Modelling

4.1 Thermomechanical Analyses

Most of the thermomechanical modelling was performed on basis of Hein's constitutive model (see Section 3.1) implemented in the SUPERMAUS code (Breidenich, 1993). This code had been especially developed for the coupled thermomechanical analysis of problems arising with the disposal of heat generating HLW in rock salt. Some additional analyses were performed by use of the constitutive model developed by Zhang et al. (1993). In the latter case the ANSYS code (Swanson, 1992) was used.

4.1.1 Analyses on Basis of Hein's Constitutive Model

4.1.1.1 Features of Analysis

The thermomechanical calculations were performed with the SUPERMAUS code in which an axisymmetric finite element model (Figure 4-1) consisting of 752 8-node elements with 2345 nodes was adopted. In the DEBORA-2 calculations, the peripheral heaters were modelled as heater rings consisting of rock salt with uniform thermal power distribution.

For rock salt, the classical elastic-creep constitutive law described in Wallner et al. (1979), Albrecht and Hunsche (1980), and Hunsche (1984) was used, whereas for crushed salt backfill Hein's material model (Hein, 1991) was employed. The thermal and mechanical properties for rock salt and crushed salt are summarized in Table 4-1 and Table 4-2 with $\dot{\varepsilon}_c$ being the steady-state creep rate, A the structural parameter, Q the activation energy, R the gas constant, T the temperature, and σ_{eff} the effective stress. In the laboratory studies performed by GRS, new parameter values were derived (see Section 3.1.3), and the calculations were repeated with these new parameter values.

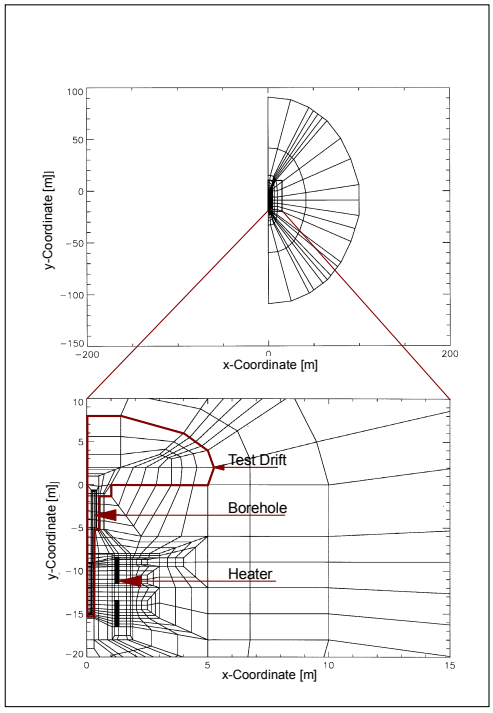

Figure 4-1 Schematic representation of the finite element mesh used for calculations of DEBORA 1 and DEBORA 2.

In the modelling, the actual history of the test field was taken into account (i. e., excavation and drilling of the boreholes). The initial stress was assumed 12.5 MPa at the heater mid-height with a vertical gradient corresponding to the rock-salt density of 2180 kg/m^3. In DEBORA 1, heating started 11.2 years after test field excavation with a total heat power of 9 kW. The initial porosity of the backfill material was 38 %. Heating lasted for 450 days. In the DEBORA-2 calculation, heating started 12.42 years after test field excavation and lasted for 547 days, with a thermal power of 14 kW and an initial porosity of 36.6 %. During the time period between excavation and experiment performance, in-situ stresses in the borehole area had reduced to about 9 MPa.

4.1.1.2 Results

Figure 4-2 to Figure 4-9 show the calculation results for two crushed-salt parameter

Table 4-1 Thermal properties of rock salt and crushed salt used for SUPERMAUS modelling.

	ROCK SALT	**CRUSHED SALT (ϕ = porosity)**
THERMAL CONDUCTIVITY (W/mK)	$\lambda_r(T)$: 5.51at 25 °C 5.1 at 50 °C 4.26 at 100 °C 3.33 at 180 °C 2.51 at 200 °C	$\lambda_c(T,\phi) = \frac{\lambda_r(T)(1-\phi)}{(h_o(1-(1-\phi)^b)+(1-\phi)^b)}$ h_o = 4.56 $b = \ln(2/3)/\ln(-\phi_o)$
HEAT CAPACITY (J/kgK)	$c_r(T)$: 862 at 25 °C 867 at 50 °C 876 at 100 °C 890 at 180 °C 911 at 200 °C	$c(T,\phi) = c_r(T)\times(1-\phi)$

Table 4-2 Mechanical properties of rock salt and crushed salt used for SUPERMAUS modelling.

MECHANICAL CONSTITUTIVE MODEL FOR ROCK SALT	**MECHANICAL CONSTITUTIVE MODEL FOR CRUSHED SALT (Hein, 1991)**
$E = 24000\,\text{MPa}$ ν = 0.27 α = 4.2×10^{-5} K^{-1} $\dot{\varepsilon}_c = A\sigma_{eff}^n \exp(-\frac{Q}{RT})$ $n = 5$ $A = 2\times10^{-6}\,s^{-1}MPa^{-n}$ $Q = 54.21\,kJ/mol$	$E = E_r\ \exp(-c_k\phi((1-\phi_o)/(1-\phi)))$ ν = 0.27 $c_k = 12.27$ $\dot{\varepsilon}_{ij} = \frac{A}{2}\exp(-\frac{Q}{RT})(h_1p^2+h_2q^2)^2(\frac{1}{3}h_1p\delta_{ij}+h_2S_{ij})$ (see Section 3.1 for description of Hein's constitutive model)

sets for temperature, borehole closure, porosity, and backfill stress as function of time (in days) since start of heating.

For DEBORA 1, the calculated temperature development on the liner at the three measuring levels 13.5 m, 12 m, and 10.5 m is shown in Figure 4-2. For both parameter sets, an almost uniform temperature along the liner can be seen. Therefore, a rather uniform borehole closure is expected. Also the temperature development over time is nearly the same for the two sets of backfill parameter values. The liner temperature rises to a maximum of about 220 °C.

Figure 4-3 shows the evolution of the width of the annulus between liner and borehole wall with time. It can be seen that with the crushed salt parameter values determined by GRS a slightly larger closure is obtained than with Hein's parameter values, although the difference is quite small. The resulting development of backfill porosity is shown in Figure 4-4. The porosity at the end of the heating phase varies between 9 and 12 % when Hein's parameter values are used, while GRS laboratory data yield a porosity ranging between 8.5 and 12 %.

Finally, Figure 4-5 shows the calculated radial stress in the backfill at the three depths considered. Stresses range from 14 to 20 MPa. Hein's parameter values give a somewhat higher stress, which is in accordance with the calculations presented in Figure 4-3 in which a more rigid backfill behaviour was observed when these values were used. After heater shutdown (on day 450), tensile stresses are computed with both models, implying that fracturing of the compacted backfill can not be excluded.

The calculated temperature development in the backfill of the DEBORA-2 borehole at the locations of the temperature sensors, 14.1 m, 12.1 m, and 10.1 m below the drift floor, are shown in Figure 4-6. It can be seen that there is no difference in the calculation with Hein's parameter values and with the GRS parameter values. The maximum backfill temperature at the end of heating varies between 138 °C (at 12.1 m depth) and 147 °C (at 14.1 m).

Figure 4-7 shows the closure of the DEBORA-2 borehole. In contrast to DEBORA-1 results, a higher closure is calculated with Hein's parameter values. The development of the backfill porosity derived from the borehole closure is shown in Figure 4-8.

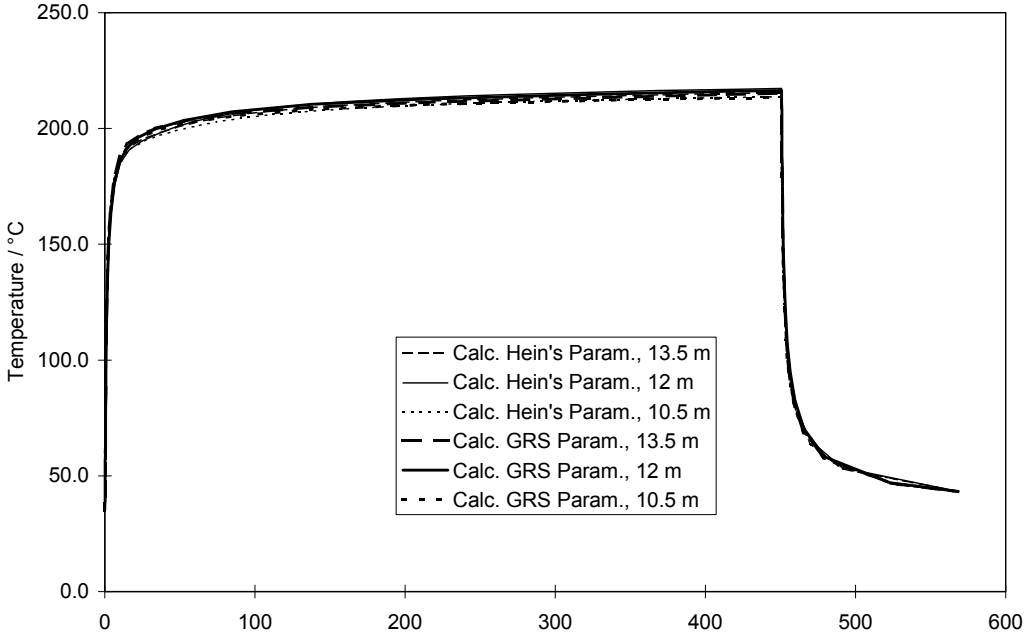

Figure 4-2 Temperature development on the DEBORA-1 liner at different depths.

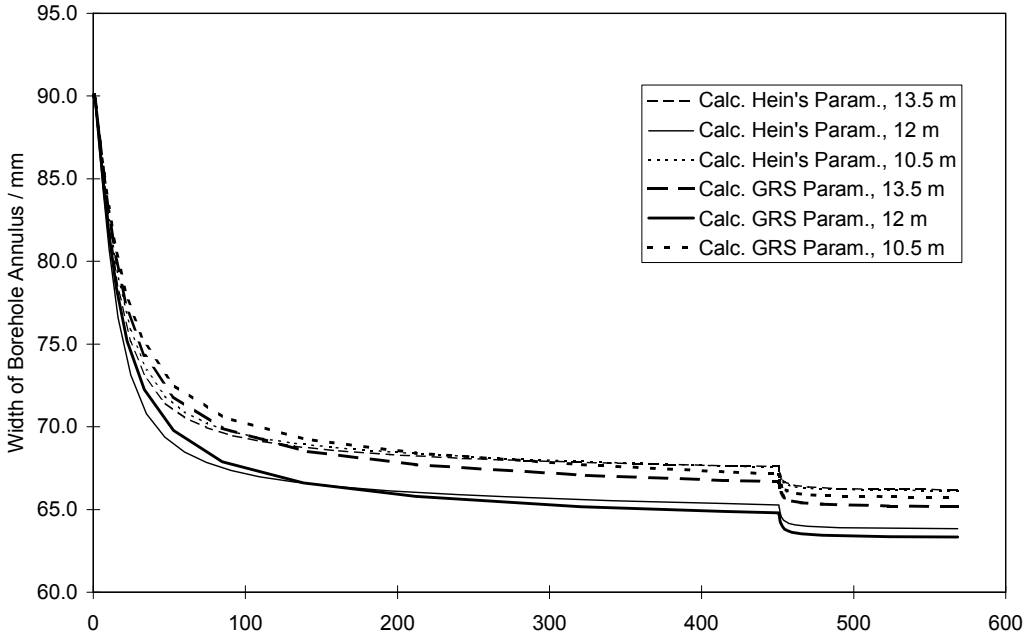

Figure 4-3 Development of the annulus width between liner and borehole wall - DEBORA 1.

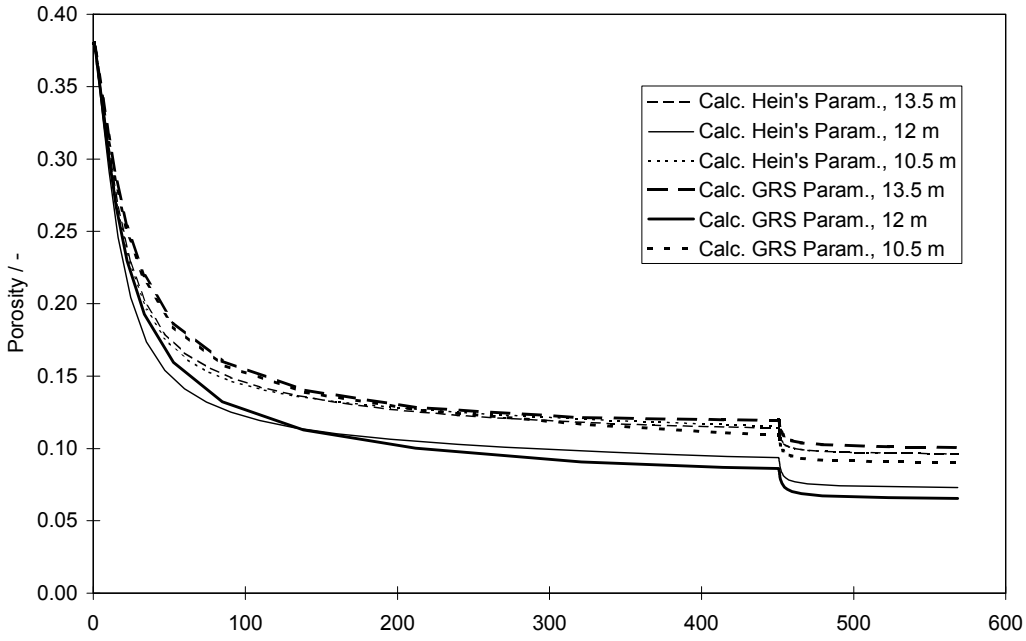

Figure 4-4 Porosity development in the backfilled annulus - DEBORA 1.

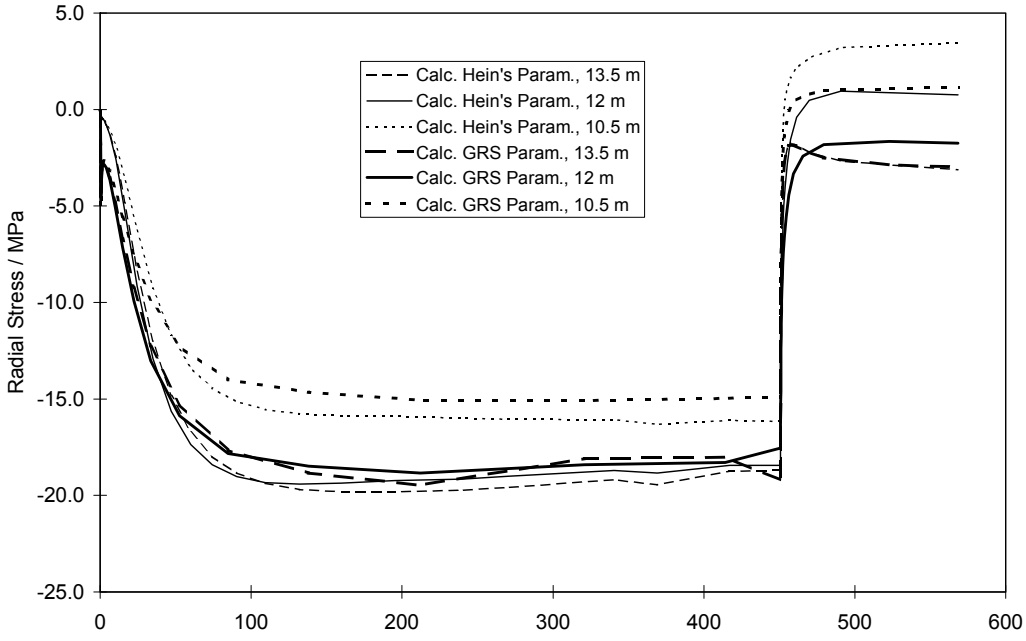

Figure 4-5 Development of radial stress in the backfilled annulus - DEBORA 1.

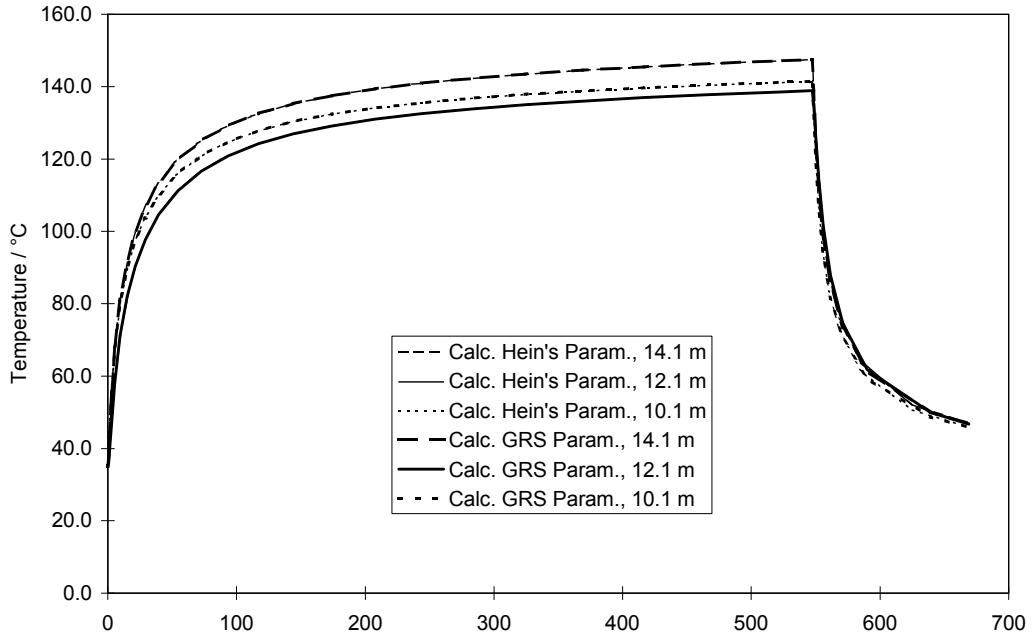

Figure 4-6 Temperature development in the backfill at three different depths - DEBORA 2.

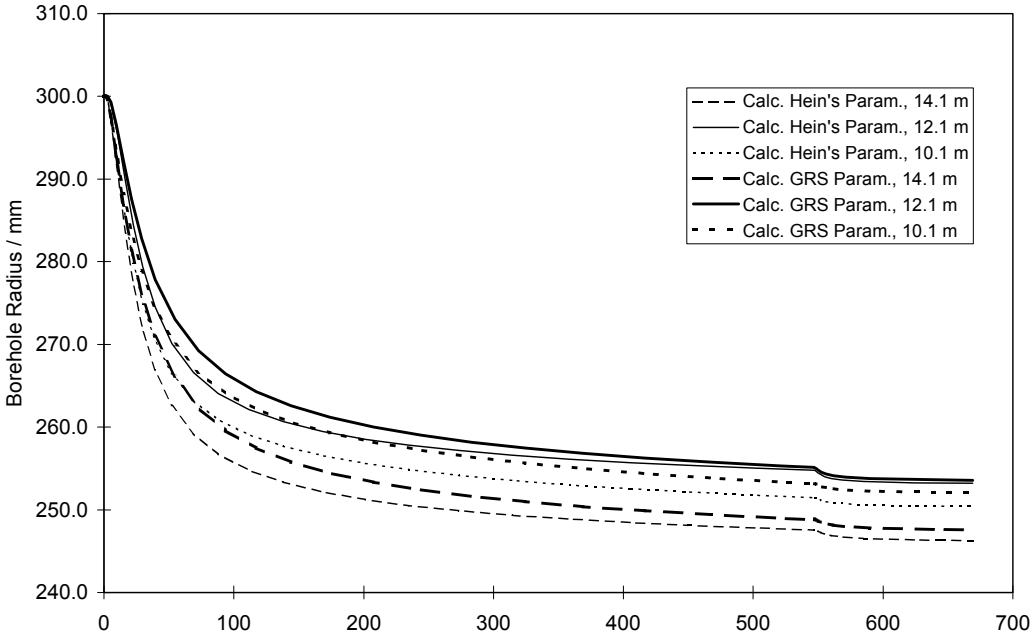

Figure 4-7 Closure of the backfilled borehole - DEBORA 2.

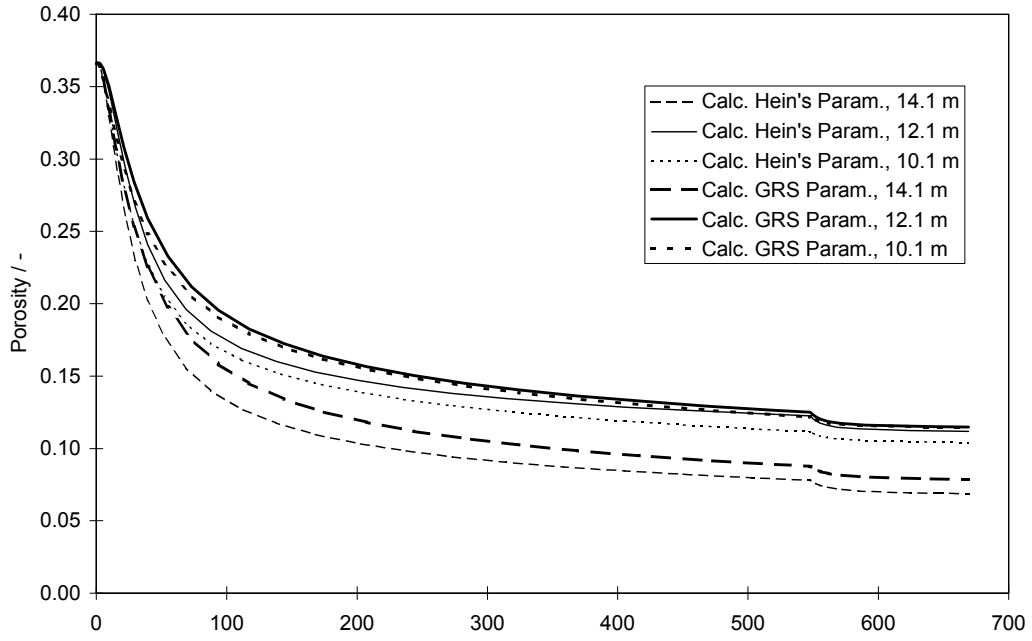

Figure 4-8 Porosity development in the backfilled borehole - DEBORA 2.

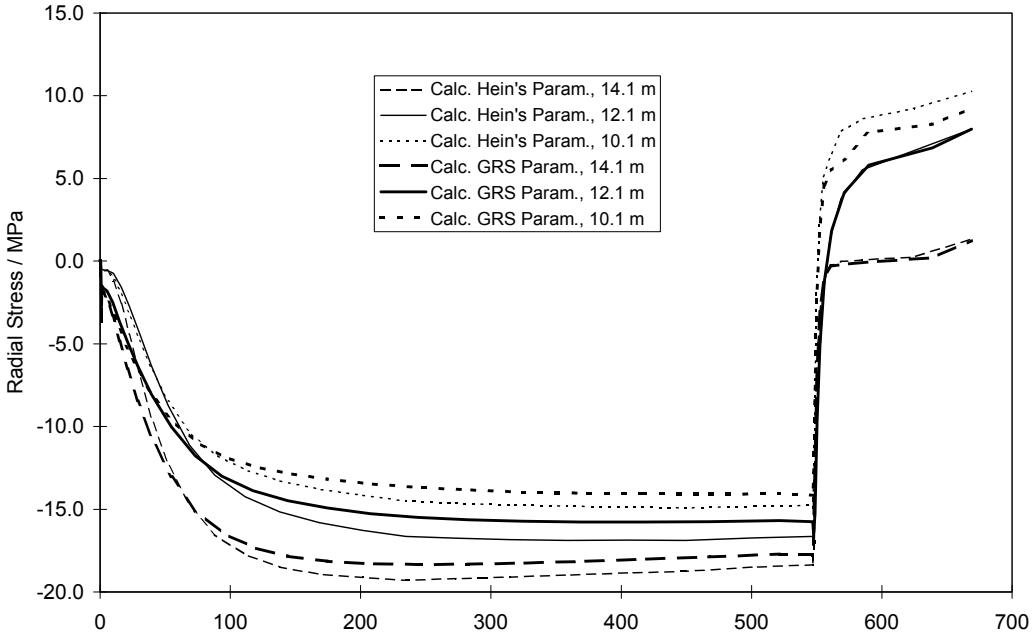

Figure 4-9 Development of radial stress in the backfill - DEBORA 2.

At the end of heating the porosity ranges between 7.8 and 12.3 % (Hein's parameter values) and between 8.8 and 12.5 % (GRS parameter values). From the development of radial stresses in the backfilled borehole (Figure 4-9) it can be seen that the backfill behaves somewhat softer when the GRS parameter values instead of Hein's values are adopted. The calculated radial stress is about 15 MPa.

4.1.1.3 Comparison Between Modelling Results and in-situ Measurements

This section presents the comparison between the calculation results shown above with the measurement results presented in Sections 2.1.3 and 2.2.3. Also, some additional calculations performed as a consequence of the comparison are discussed.

For DEBORA 1, the modelling results and the measured data are presented in Figure 4-10 to Figure 4-13. The most significant discrepancies between measurement and calculation are found in the temperature (about 25 °C) (Figure 4-10). This is surprising because, normally, thermal fields are well reproduced by modelling. Several possible reasons were considered. First, the temperature sensors were attached to the distance gauges that were made of metal and extended through the backfill to the borehole wall, possibly providing a thermal short-circuit. Calculations showed that this effect could account for a difference of some degrees C, but that it was not sufficient to explain the observed difference. A second possible cause is convection heat loss inside the liner that was not accounted for in the model. No definite explanation for the heat loss mechanism could be satisfactorily achieved, however.

During the first months of the heating period, rates of borehole closure (Figure 4-11) and backfill compaction (Figure 4-12) were lower than predicted, whereas towards the end of the heating phase the experimental results were higher than the calculation results. The parameter values determined in the GRS laboratory yielded a better prediction than Hein's parameter values. The difference in the development of the closure/compaction rates possibly could be related to a geometry effect. As the geometrical model was axisymmetric, the drift was modelled as much smaller than in reality. This may have influenced the mechanical behaviour even at a depth of more than 10 m below the floor. In order to assess the importance of this effect, the DEBORA model was changed by doubling the drift radius. It was found that the

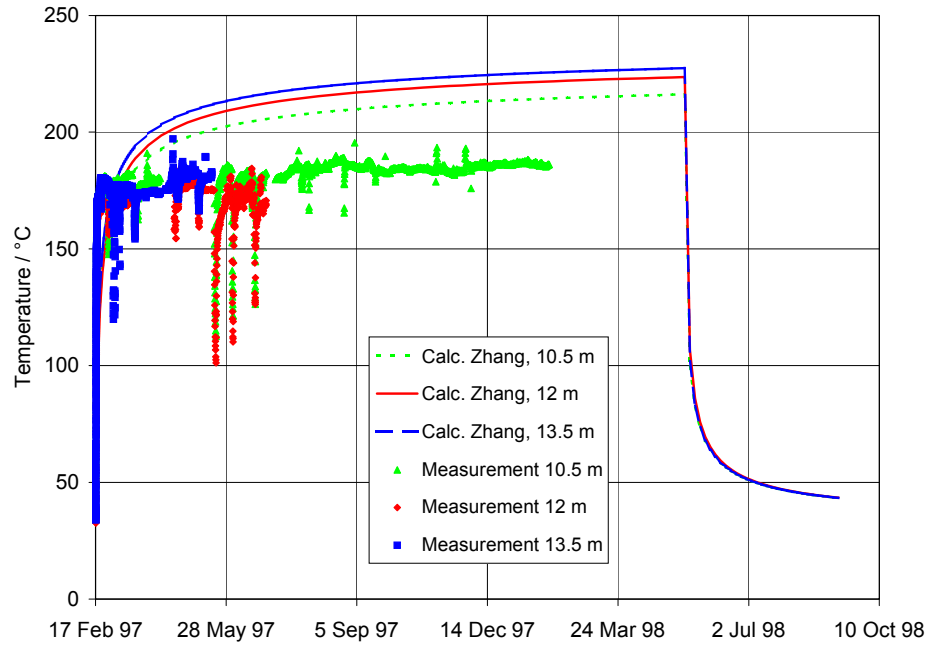

Figure 4-10 Temperature development on the DEBORA-1 liner; measurement and calculation.

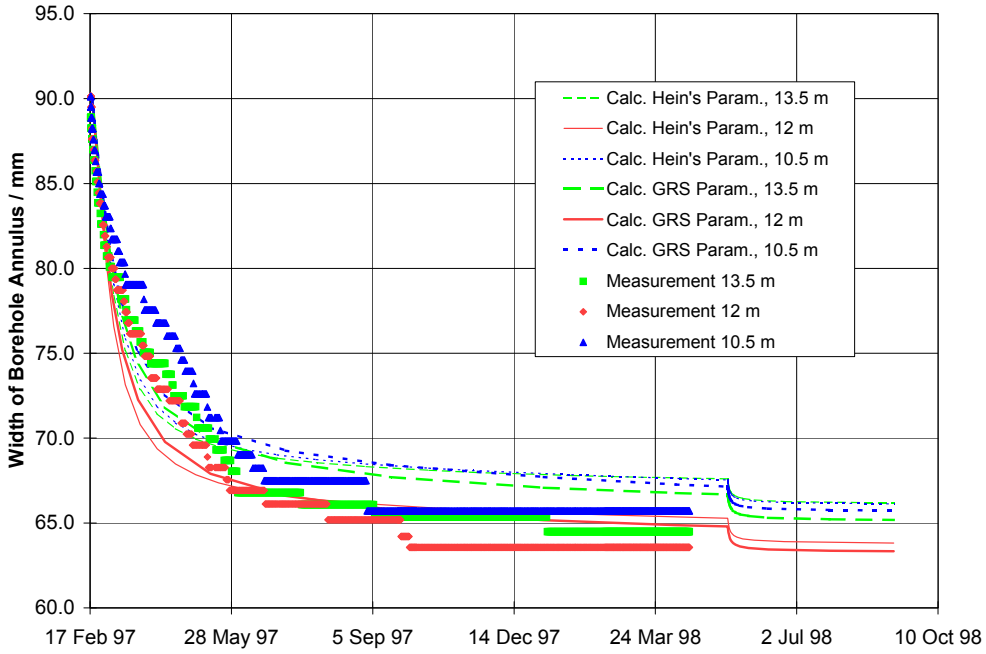

Figure 4-11 Development of the annulus width between liner and borehole wall of DEBORA 1; measurement and calculation.

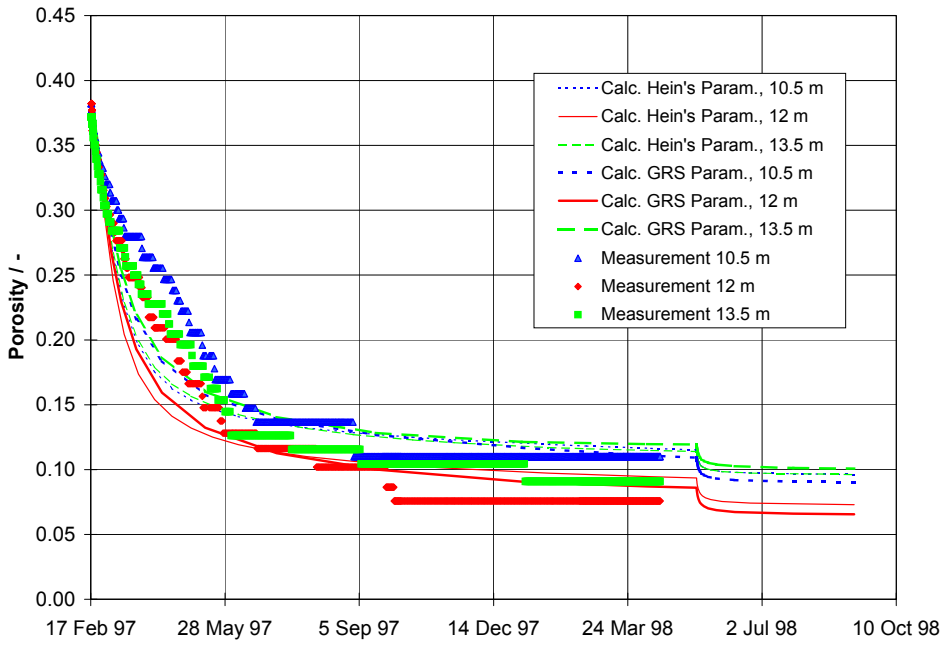

Figure 4-12 Porosity development in the backfilled annulus of DEBORA 1; measurement and calculation.

differences between experimental results and calculation results decreased. However, by this calculation only a rough estimate of the effect could be obtained. True three-dimensional modelling will be required to prove the precise significance of this effect.

Radial stress (Figure 4-13) develops slower than predicted, which is in agreement with borehole closure (Figure 4-11). In view of the difficulties in measuring stresses in viscoplastic media, the agreement between measured and calculated stress can be considered as being satisfactory. Again, better results were obtained from the prediction using the GRS parameter values. The modelling results of DEBORA 2 are shown in Figure 4-14 to Figure 4-17 together with the measured data. Here, a good agreement was achieved between the measured temperature development and the modelling results (Figure 4-14), supporting the assumption that some unaccounted heat loss occurred in the DEBORA-1 experiment. Borehole closure and, consequently, backfill compaction was somewhat lower than predicted (Figure 4-15 and Figure 4-16). In contrast, a good agreement is found in the radial backfill stresses (Figure 4-17). As in DEBORA 1, the calculation using the GRS parameter set for crushed salt

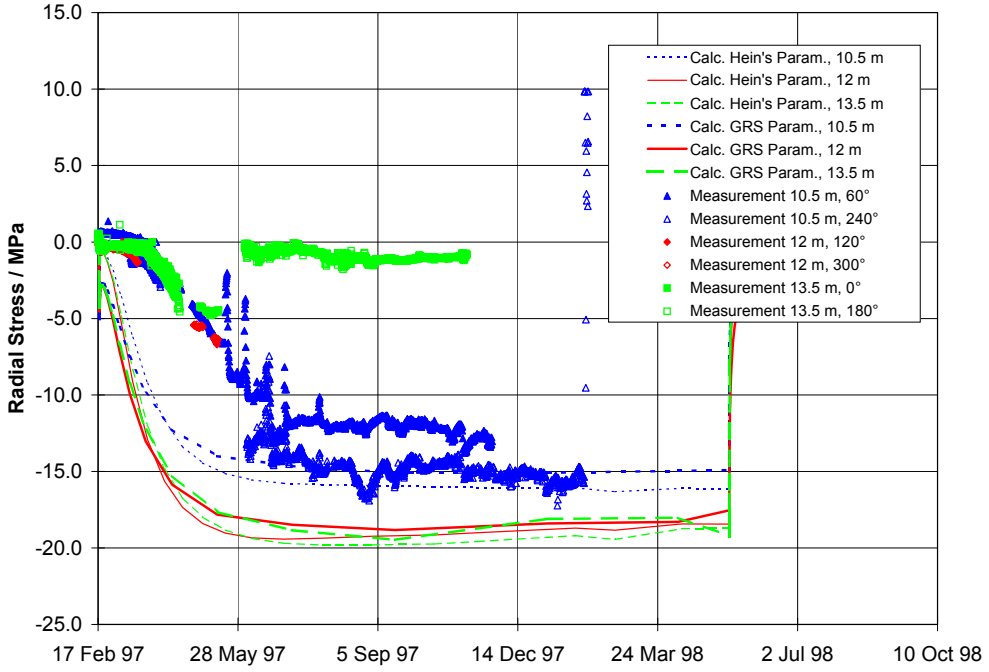

Figure 4-13 Development of radial stress in the backfill of DEBORA 1; measurement and calculation.

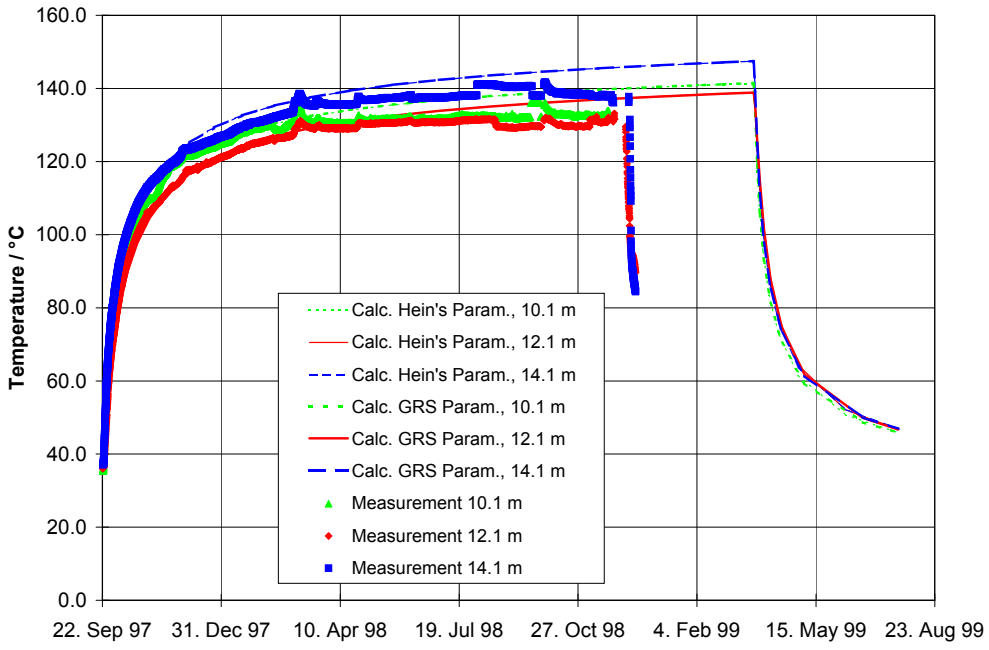

Figure 4-14 Temperature development in the backfilled borehole of DEBORA 2; measurement and calculation.

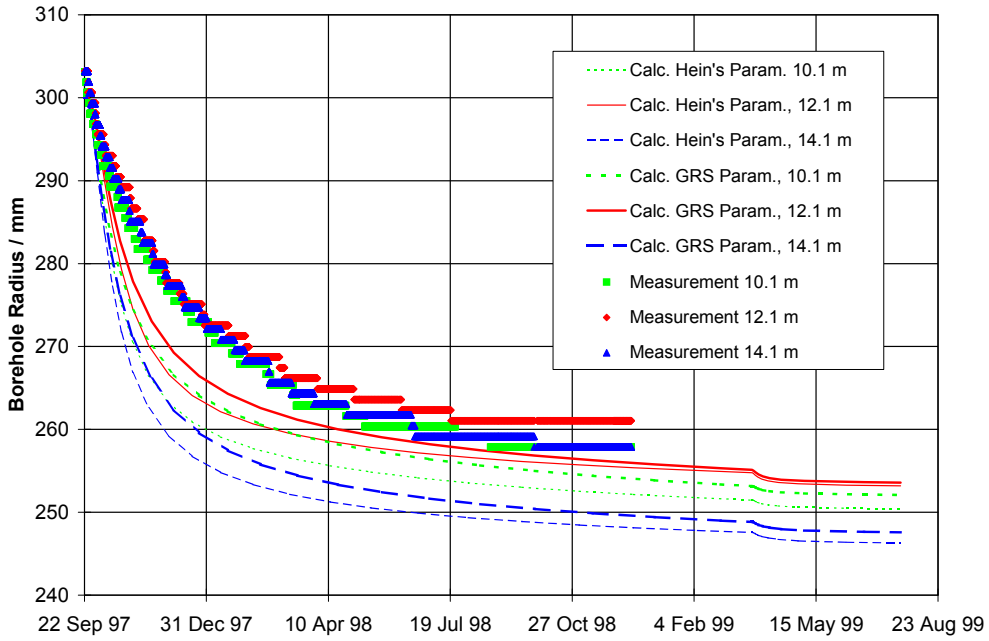

Figure 4-15 Closure of the backfilled borehole DEBORA 2; measurement and calculation.

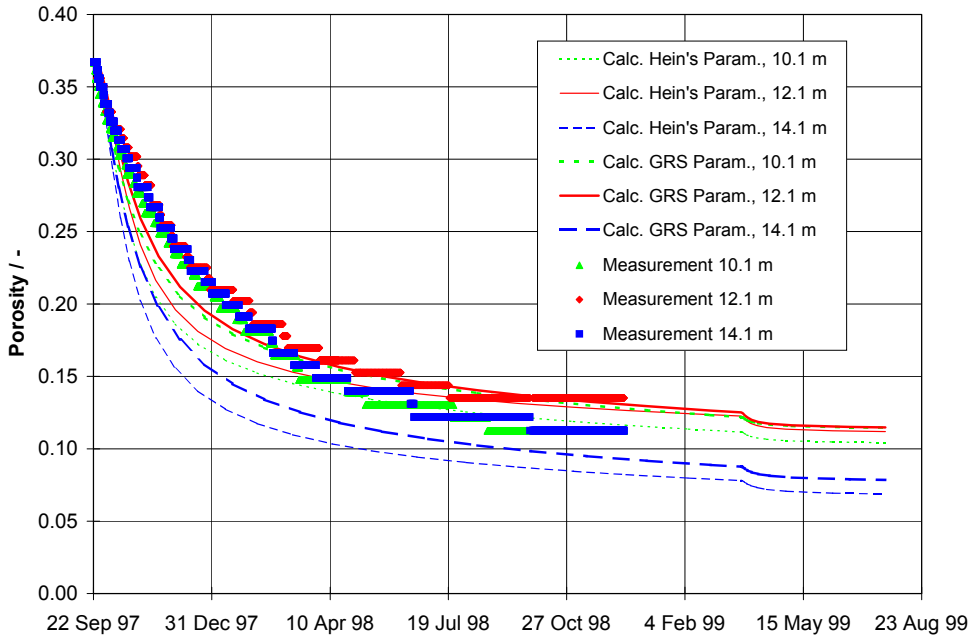

Figure 4-16 Porosity development in the backfilled borehole DEBORA 2; measurement and calculation.

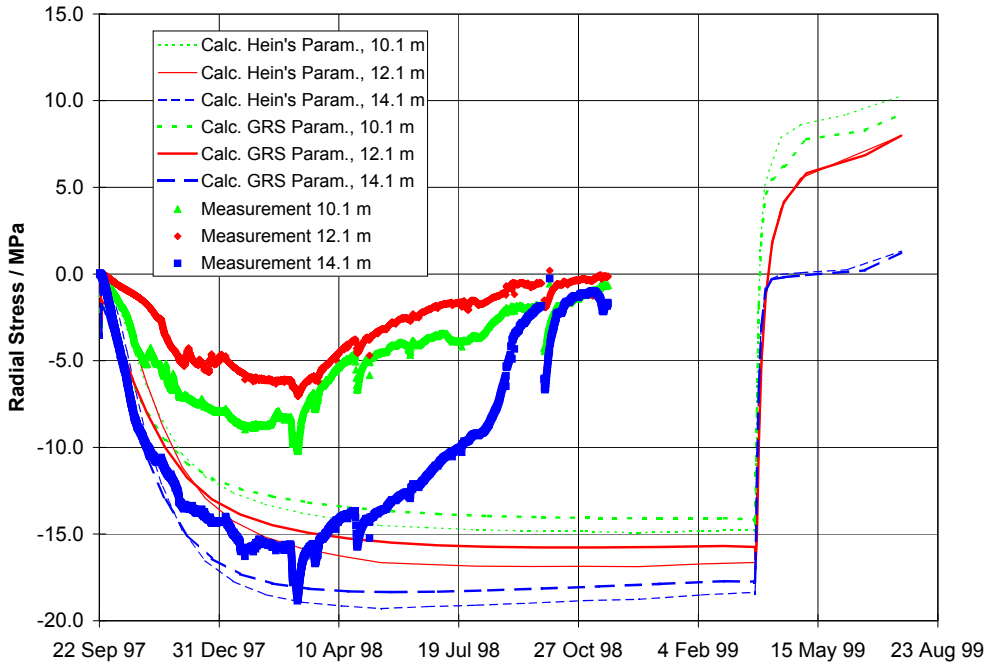

Figure 4-17 Development of radial stress in the backfill of DEBORA 2; measurement and calculation.

is closer to the measurements than the calculation using Hein's parameter values. Again, the use of a two-dimensional axisymmetric model may have contributed to the difference between modelling and measurement results.

4.1.2 Analyses on Basis of Zhang's Constitutive Model

In addition to the mechanical modelling performed with the SUPERMAUS code using Hein's constitutive model for crushed salt, calculations using an alternative material model were conducted for DEBORA-1. For these calculations the commercial code ANSYS (Swanson, 1992) was extended by an empirical creep law developed by Zhang et al. (1993), with the completion suggested by Duddeck and Guericke (1995).

4.1.2.1 Features of Analysis

Starting from the steady-state creep model for rock salt (see Table 4-2) Zhang et al. (1993) developed the following empirical constitutive model for crushed salt from numerous oedometer tests:

$$\dot{\varepsilon}^{V} = A \cdot \exp(-\frac{Q}{R \cdot T}) \cdot S^{n} \cdot (\ln(\frac{\varepsilon^{VE}}{\varepsilon^{VE} - \varepsilon^{V}}))^{-m}$$

with $\dot{\varepsilon}^{V}$ compression rate

S first stress invariant ($\sigma_{11} + \sigma_{22} + \sigma_{33}$) / 3, S = hydrostatic pressure

ε^{V} actual compression

ε^{VE} end compression at zero porosity

The term $\frac{\varepsilon^{VE}}{\varepsilon^{VE} - \varepsilon^{V}}$ can be replaced by $\frac{\phi_0 \cdot (1 - \phi)}{\phi \cdot (1 - \phi_0)}$, where ϕ_0 stands for the start porosity and ϕ for the actual porosity.

In order to extend Zhang's constitutive model, which can only be used for homogeneous stress states, to triaxial stress states, Duddeck and Guericke (1995) suggest the following extension:

$$\dot{\varepsilon}_{ii}^{V} = A \cdot \exp(-\frac{Q}{R \cdot T}) \cdot s^{n} \cdot (\ln(\frac{\varepsilon^{VE}}{\varepsilon^{VE} - \varepsilon^{V}}))^{-m} \cdot \frac{\sigma_{ii}}{s} \cdot K \qquad \text{(volumetric part)}$$

$$\dot{\varepsilon}_{ij}^{D} = A \cdot \exp(-\frac{Q}{R \cdot T}) \cdot \sigma_{eff}^{n} \cdot (\ln(\frac{\varepsilon^{VE}}{\varepsilon^{VE} - \varepsilon^{V}}))^{-m} \cdot F \cdot \frac{\partial F}{\partial \sigma_{ij}} \cdot K \quad \text{(deviatoric part)}$$

with K compaction condition (K = 1 for S < 0, else K = 0)

σ_{eff} effective stress; $\sigma_{eff} = \sqrt{3 \cdot J_2}$ with J_2 = second (deviatoric) stress invariant

F flow condition after von Mises; $F = \sqrt{J_2} - \sigma_0$ for $\sqrt{J_2} > \sigma_0$, else F = 0 (σ_0 is the uniaxial flow limit stress)

The above constitutive model was included in the finite element code ANSYS (Swanson, 1992), Release 5.4.

For the DEBORA-1 calculation, an axisymmetric finite element model of 926 8-node elements with 2863 nodes was used. Although ANSYS allows three-dimensional modelling, an axisymmetric model was chosen, since the DEBORA-1 experiment is appreciably axisymmetric, and also for better comparability with the SUPERMAUS calculations using Hein's material law for crushed salt.

Except for crushed salt, the material parameters were the same as in the SUPERMAUS calculations. The mechanical parameters for crushed salt were given by Zhang: n = 7.1, m = 10.9, A = 5.903 · 10^{-49} s^{-1} Pa^{-n} (equals 1.41 · 10^{-4} min^{-1} MPa^{-n}, see Zhang et al., 1993). Actually, these parameters would have had to be determined in laboratory tests on the DEBORA backfill; for this first orientating calculation, however, Zhang's parameters were thought to be sufficient.

There is no direct coupling between thermal parameters and porosity in the extended ANSYS code. Therefore, averaged thermal parameters for crushed salt had to be used. The chosen values are exact for a porosity of 10 %.

4.1.2.2 Results

Figure 4-18 to Figure 4-21 show the calculation results using Zhang's constitutive model for crushed salt together with the measured data for temperature, deformation, porosity, and stress, respectively.

The temperature of the backfill close to the borehole liner is shown in Figure 4-18. As in the SUPERMAUS modelling, the calculated temperatures are considerably higher than the measured ones. The temperature at the end of the heating period ranges between 216 °C and 227 °C, which is in sufficient agreement with the SUPERMAUS results using Hein's material law. The temperature increase at early time is slower with the ANSYS calculation (compare Figure 4-2 or Figure 4-10). This is a result of the averaged thermal conductivity for crushed salt which is accurate for a porosity of 10 %.

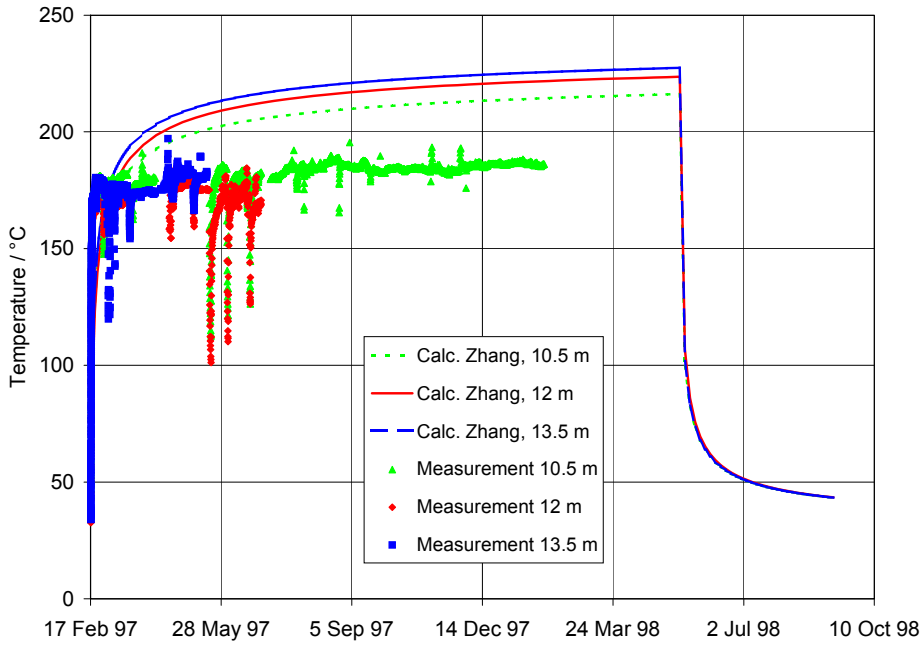

Figure 4-18 Temperature development on the DEBORA-1 liner; measurement and calculation using Zhang's constitutive model for crushed salt.

At higher porosities the thermal conductivity is lower, resulting in higher temperatures on the borehole liner. At later times, when the backfill has compacted, this difference disappears.

Figure 4-19 shows the decrease of the width of the backfilled borehole annulus with time. At early time the annulus width decreases at a lower rate than calculated, but the calculated end value is higher than measured. Consequently, the calculated end porosity of 10 to 12 % is somewhat higher than the measured 7.5 to 11 % (see Figure 4-20). Both the curve form and the end values are, however, very close to the results of the SUPERMAUS calculation. Apparently, the backfill compaction process is dominated by the rock salt behaviour. The constitutive model used for the backfill seems to play a minor roll, at least for DEBORA-1 where the dimensions of the backfilled annulus are rather small.

The measured and calculated radial stress development in the backfill is shown in Figure 4-21. It can be seen that the measured stress increase with time is much slower than predicted, which agrees with the porosity results. The calculated stress is even higher than with the SUPERMAUS modelling (see Figure 4-13).

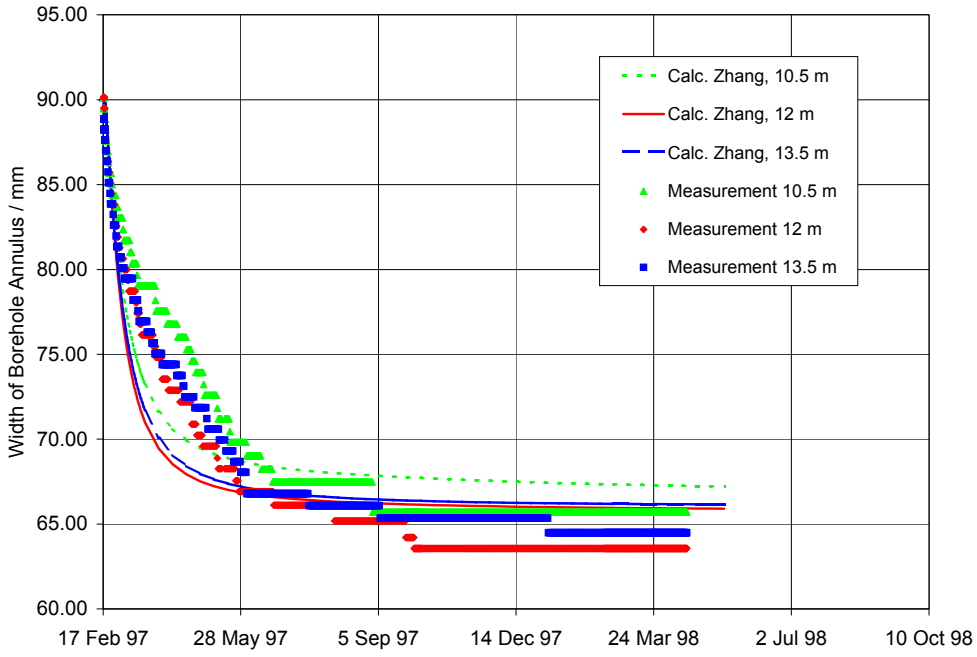

Figure 4-19 Development of the annulus width between liner and borehole wall of DEBORA-1; measurement and calculation using Zhang's constitutive model for crushed salt.

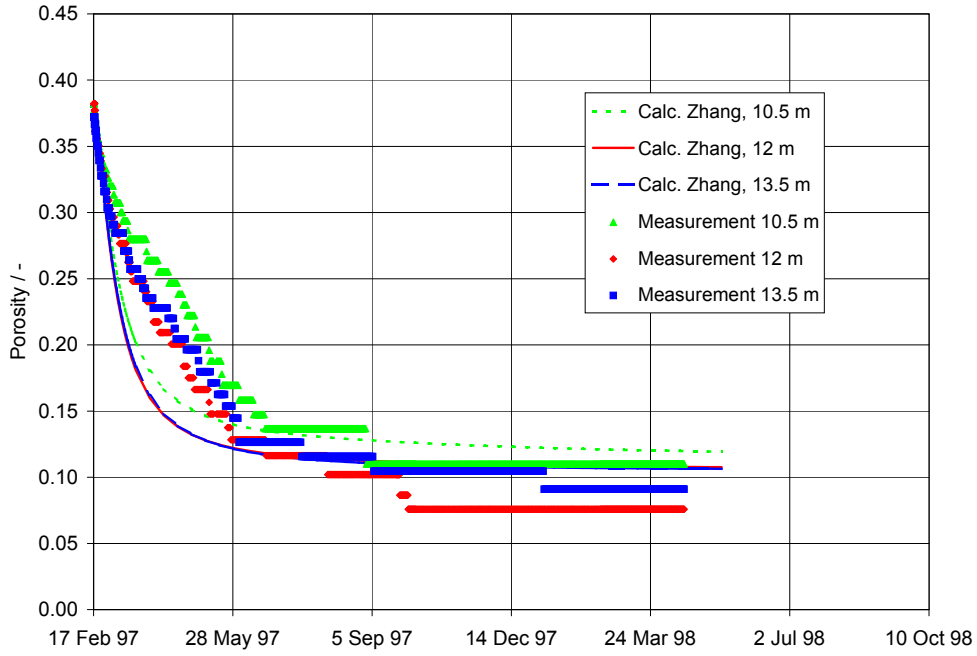

Figure 4-20 Porosity development in the annulus of DEBORA-1; measurement and calculation using Zhang's constitutive model for crushed salt.

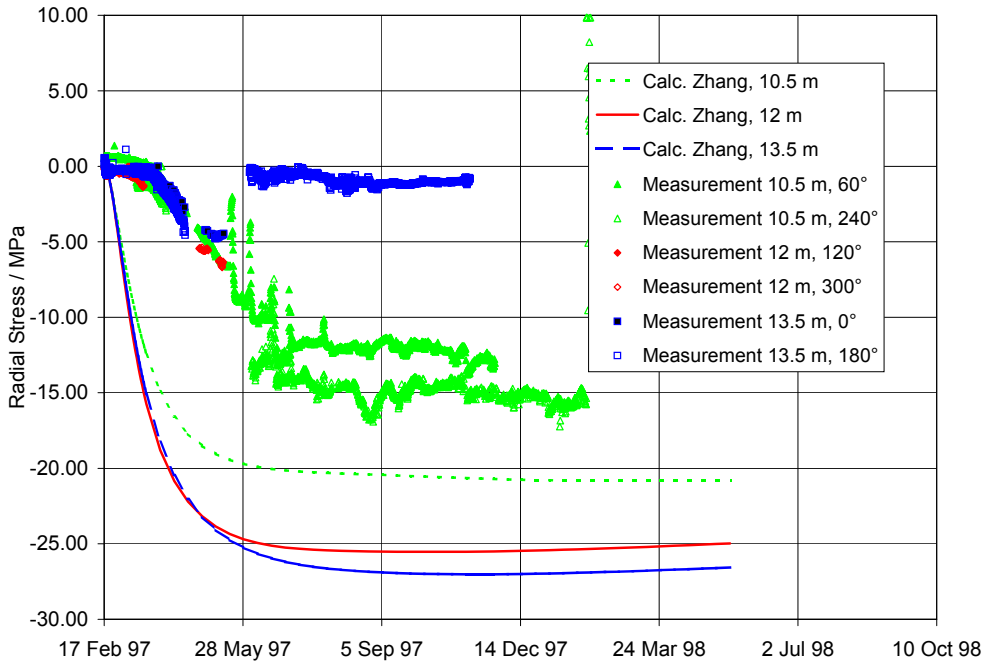

Figure 4-21 Development of radial stress in the backfill of DEBORA-1; measurement and calculation using Zhang's constitutive model for crushed salt.

On the whole, it can be stated that the results of the ANSYS modelling using Zhang's constitutive law for the backfill resemble closely of the SUPERMAUS results with Hein's material law. Although no effort was made to obtain accurate parameters for the crushed salt behaviour, the differences between the two models are negligible. Both models show the same deviations from the measured behaviour. As mentioned above, the behaviour of the surrounding salt rock seems to be more important than the constitutive model for crushed salt backfill.

4.1.3 Conclusions

The development of the porosity in both DEBORA experiments is somewhat different in comparison to the results of the numerical predictions. The material models used in the calculations indicate a softer material behaviour than observed in situ. This is especially true for porosities above 0.2. It is possible that the material parameter values used in the calculations are not valid for this porosity range because they were always derived from laboratory experiments on samples with porosities below 0.2.

The compaction rates observed in the later stage of the experiments at porosities below 0.2 agree much better, thereby confirming the aforementioned assumption.

The discrepancies between measurements and calculations might also be caused by restraints of the geometrical models of rotational symmetry. These models neglect the true extension of the test drift above the test boreholes which leads, especially in the early phase of the heating period, to an overestimation of thermally induced stresses and thus of deformations in the rock salt around the test boreholes.

A comparison of the results of the calculations performed with the models of Hein and Zhang shows a good agreement of the predicted deformations in contrast to an inadequate agreement of the stresses. This result indicates shortcomings in at least one of these material models or the respective material parameter values.

In conclusion it can be stated that the actual models seem to be suited to qualitatively predict the compaction behaviour of crushed salt. However, the observed quantitative deviations and the inconsistencies regarding the prediction of deformations and stresses indicate shortcomings in the material models that need to be clarified.

4.2 Hydraulical Analyses

4.2.1 Experiment Design Calculations

Design calculations for the gas flow tests during the two DEBORA experiments were carried out to develop appropriate test procedures for the evaluation of permeability and porosity and to determine the parameter range to be expected. For this purpose a simple one-dimensional model based on several idealising assumptions was used. Three types of test procedures were conceived considering different initial and boundary conditions. The characteristics of these procedures are listed in Table 4-3. Exemplarily, the characteristic mass flux curves at the boundaries and the time dependent gas pressure distribution over the test interval are plotted in Figure 4-22. Note, that the difference of the flux rates in Figure 4-22 account for the gas mass which is stored due to the increasing pressure in the test interval. Material data which were to be measured yet had to be assumed based on a compendium for laboratory data for crushed salt (PSE, 1985).

Table 4-3 Short description of the main characteristics of the three flow test variants.

	inflow boundary condition	outflow boundary condition	initial pressure
Variant A	constant excess pressure	atmospheric pressure	atmospheric pressure
Variant B	constant excess pressure	atmospheric pressure	constant excess pressure
Variant C	no flow	atmospheric pressure	constant excess pressure

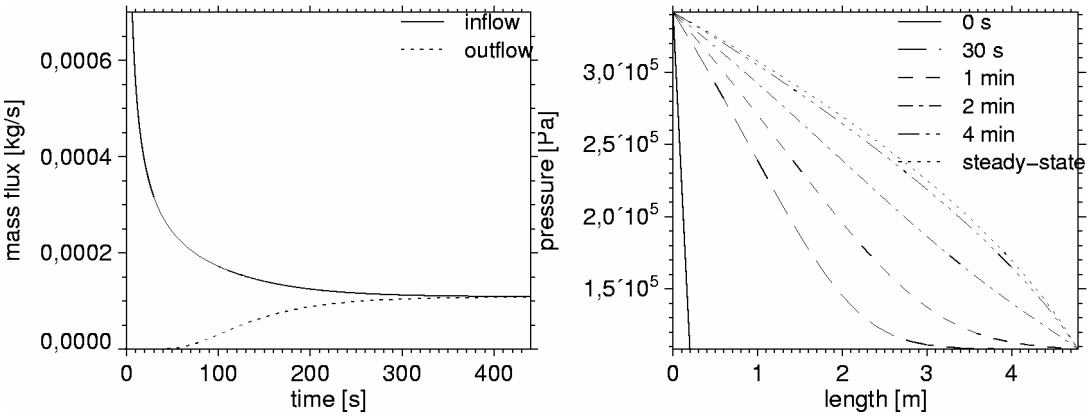

Figure 4-22 Characteristic mass flux and gas pressure curves for test variant A.

Influence of the Klinkenberg effect

The measured gas permeability is usually divided by a factor of (1 + b/ p') in order to take the effect of slip flow into account. This factor contains the mean absolute gas pressure p' and the Klinkenberg constant b which can be exactly determined by measurements only. However, in this case the constant was estimated from a comprehensive compilation of measurements (Rieckmann, 1970).

The greatest influence of slip flow is observed for a low mean pressure and low porosity values because the Klinkenberg constant b is inverse proportional to the free path length of the gas molecules (Karman, 1956). In order to estimate the maximum difference between apparent and absolute permeability it was assumed that a hypothetical measurement was performed at a mean gas pressure of one bar and at a permeability of 10^{-14} m^2. This leads to a maximum value of 0.5 bar for the constant b including uncertainties due to the natural data scattering in the compilation mentioned above. Under these conditions the increase of the absolute permeability amounted to 33 %. This stated an upper boundary for the deviations to be expected and proved to be a very good estimation for the data derived from the DEBORA experiments.

Comparison prediction-measurements

The predictions for the flow tests were not met precisely during the experiments. This is mainly due to the fact that the permeability-porosity function derived from data of the DEBORA experiments deviated from the function used for the design calculations. Minor differences concerning the test parameters arose as well. Yet the main conclusions from the design of the experiments proved to be valid in the actual tests:

- The porosity dependent steady-state mass flux rate changed over two orders of magnitude for the porosity range observed when the same excess pressure was used.

- The transient mass flux rate in a single flow test changed over about one order of magnitude.

- The flow test duration lay on the order of ten minutes except for high porosity values when it took considerable time to build up the pressure at the inflow boundary.

A comprehensive compilation of the differences between model predictions and measurements related to the experiment DEBORA 1 is given in Table 4-4.

4.2.2 Estimation of Measuring Errors

In order to estimate the confidence level for the experimentally gained permeability and porosity values, an error analysis has been performed for DEBORA 1. With regard to the permeability the analytical solution of the continuity equation for gas flow was used to derive a formula for the total error using the measurement error margins as input data. Based on geometric considerations the porosity can be expressed as a function of the borehole wall displacement and be treated in the same way.

Porosity evaluation using inverse modelling was based on a one dimensional idealized model with constant cross-section area and homogeneous material. In this case the

Table 4-4 Differences of test parameters between model predictions and measurements for the experiment DEBORA 1.

	Prediction	**Measurement**
temperature [K]	433	445-459
viscosity [Pa s]	$2.56 \cdot 10^{-5}$	$2.36 \cdot 10^{-5}$ - $2.41 \cdot 10^{-5}$
length of test interval [m]	4.77	4.875
cross-section area [m^2]	0.1452	0.109 - 0.0983
porosity-permeability-relation [m^2]	$k = 2 \cdot 10^{-8} \phi^{4.5}$	$k = 1.2 \cdot 10^{-8} \phi^{5.47}$

permeability has to be determined experimentally in advance and the concerning errors are introduced additionally. Some of the errors in question could be derived directly, some of them could be evaluated in terms of error bounds only (Kröhn and Fein, 1999).

Assuming validity of the ideal conceptual model the analysis yielded an error of little more than 5 % for the permeability. Since the displacement transducers worked with a constant error the total error in the porosity using the geometric approach grew exponentially during the DEBORA experiment (see Figure 4-23). The error amounted to approximately 2 % at the beginning and increased up to 5 % for a porosity of about 10 % to 15 %. The estimated error of about 5 % to 6 % using the inverse modelling method was more or less independent of the porosity itself - the porosity range investigated lay between 1 % and 20 %.

The results showed that the geometric approach delivered more accurate data in the early test phase than the inverse modelling technique. In the range of 10 % to 15 % porosity both methods were of comparable precision.

In order to achieve significant new data with each measurement campaign, it is necessary to ensure that a new data point lies outside the error margins of its predecessor. For this reason the predictions of the thermomechanical model calculations concerning the time-dependent porosity (see Section 4.1) were correlated with the analytically derived measurement errors, which were expressed as porosity-dependent values. The constructed confidence range around the predicted permeability-porosity-curve showed that a monthly performed measurement campaign provided significantly new values for the time-dependent permeability as well as the porosity even if the compaction rate is very low (see Figure 4-24).

Most parameters required for the hydraulic design calculations and error estimations were equal or quite similar for both experiments. Differences existed in temperature (180 °C/130 °C), viscosity ($2.4 \cdot 10^{-5}$ Pa·s/$2.2 \cdot 10^{-5}$·Pa·s), cross-section area (0.1 m^2/0.21 m^2) and the height of the test interval (4.77 m/5.50 m). However, these differences had only little influence on the total error and hence the same conclusions could be drawn for both experiments. Most relevant for the performance of the flow tests was the difference in the cross-section area which was doubled in DEBORA 2 compared to DEBORA 1. Mass flow was therefore doubled as well under comparable conditions thus expanding the range to be covered by the mass flux measurements.

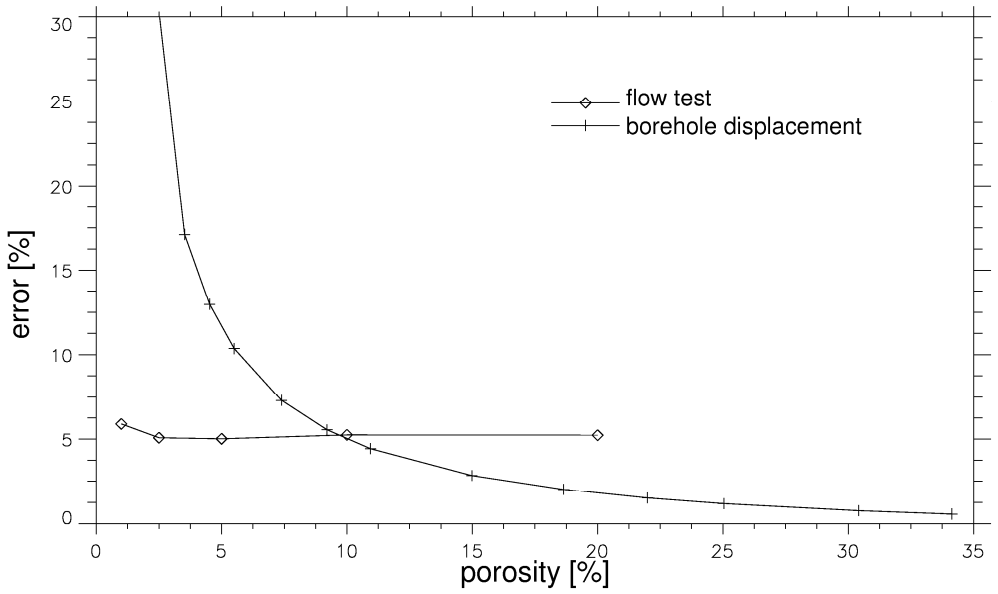

Figure 4-23 Relative error of the porosity using the inverse flow test modelling method (rhombus) and using displacement transducer measurements (plus).

4.2.3 Determination of Backfill Porosity

Data of the borehole wall displacement provided by six displacement transducers was used to determine the crushed salt porosity. The porosity values at the six locations were calculated based on geometric considerations and then averaged out. An alternative method which evaluates an integral porosity value is given by means of inverse modelling of the transient gas flow tests.

The analytically derived permeability value and the monitored pressure are used as input data for a gas flow model which provides transient mass fluxes at the boundaries of the crushed salt column. The calculated mass flux curves are then to be matched with the measured mass fluxes by varying the only unknown parameter in the continuity equation - the porosity.

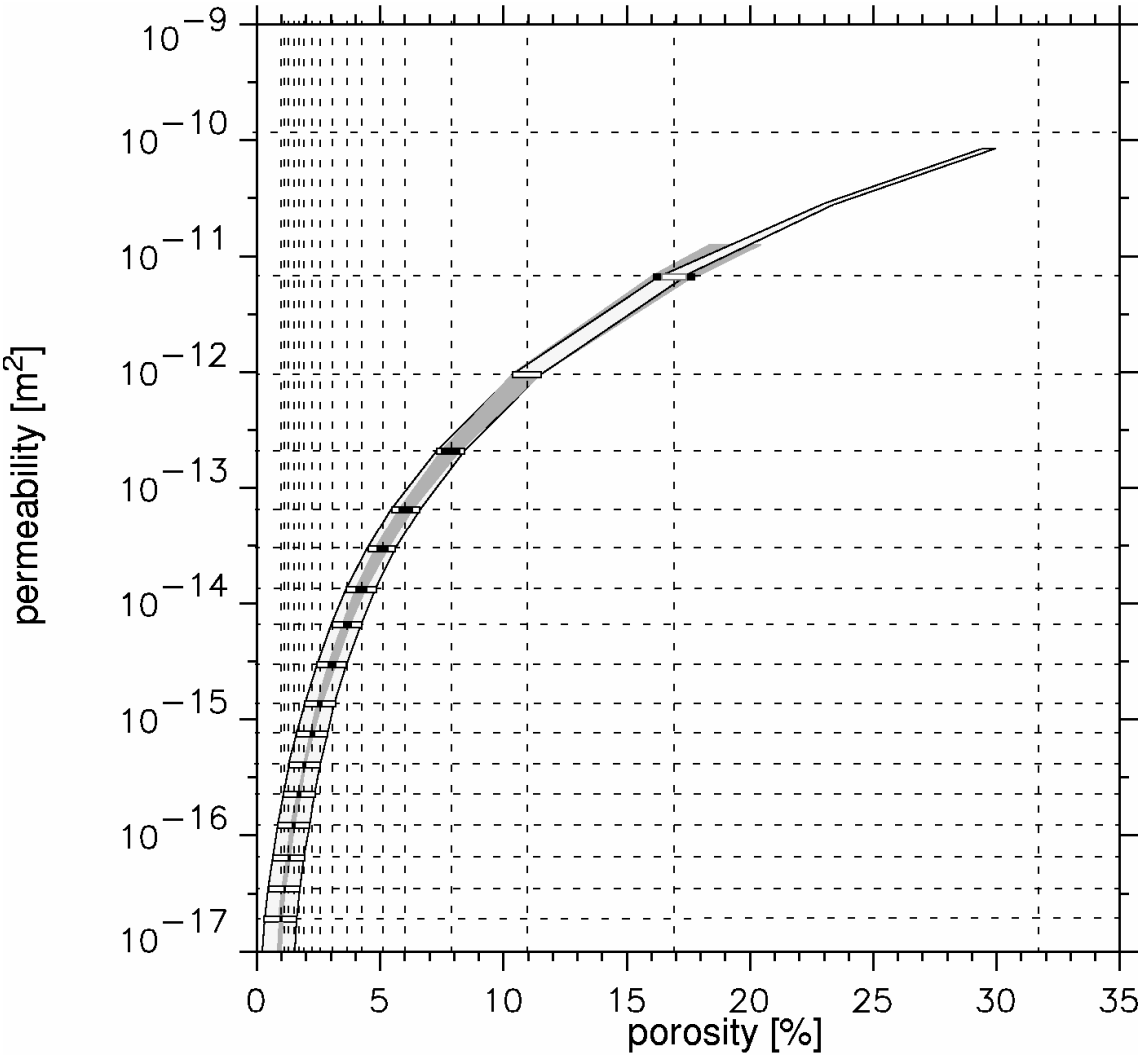

Figure 4-24 Theoretically derived error range for permeability and porosity for monthly measurements using a pressure difference of 0.1 MPa; - displacement measurements: light areas; - flow tests: dark areas.

Considerably more care and effort to the test performance is necessary if the flow tests are supposed to provide not only the permeability but data for inverse modelling, too. Several problems made the interpretation of the data difficult. Some of these problems were test immanent:

- A jump in the gas pressure at the boundary cannot be realised in reality.

- The mass flux meters cannot follow very quick changes in mass flow.

- An inhomogeneous material distribution could not be considered.

Some others could be fixed when recognised:

- Temporarily the inflow pressure could not be kept constant due to equipment failures.

- Humidity in the salt attacked the outflow mass flux meters making the measured data unusable for porosity evaluation (especially DEBORA 2).

Despite of these difficulties it was possible to interpret the data from DEBORA 1 flow tests measured in May, June, July and December 1997. All these tests followed a test procedure according to variant A (see Table 4-3).

Model calculations based on the complete set of idealising assumptions and measurements could not be matched, though. In order to determine the reason for the discrepancy, several input parameters for the numerical model were varied extensively within reasonable limits. It could be shown that inhomogeneity of the cross-section area and therefore the porosity as well as inhomogeneity of the permeability and variable temperature are of secondary importance to this problem. A sufficient match was not possible until the gas injection volume was added to the model and the measured time dependent input pressure was used as a boundary condition.

The porosity values determined by inverse modelling show a faster compaction rate for the first five months than the geometrically derived data (see Figure 2-11 in Section 2.1.3). The changes after that time are minimal and could not be demonstrated by this method. The same two phases of compaction can be recognised in the displacement data but the change into slow compaction is observed some three months later. The final porosity value at the end of DEBORA 1 determined by inverse modelling lies slightly below the displacement derived value.

However, the final porosity distribution along the crushed salt column was determined by post-test laboratory investigations. This distribution shows noticeable peaks at the location of the displacement transducers (see Figure 2-14 in Section 2.1.3). The average porosity appears to be about two percent lower than the peak value which is consistent with the results of the inverse modelling.

4.2.4 Conclusions

The design calculations proved to be a valuable tool in order to get a first impression on the hydraulic conditions during the flow tests. The system behaviour was qualitatively well described and the measured data deviated within reasonable tolerances from the predictions. Based on the resulting conclusions the design of the experiments could be successfully optimized.

The analysis of the errors introduced by tolerances of the measuring devices was of great value, too. It demonstrated a high accuracy of the hydraulic parameters which were derived from the in-situ measurements. Additionally, it showed that in order to evaluate the porosity, the flow tests were an equally adequate alternative to the geometric approach by measuring the annulus width.

The gas flow tests provided integral values of porosity as well as permeability. But the evaluation of the porosity requires more care and effort concerning test performance and data interpretation than determining the permeability. The permeability can be calculated directly using an analytical solution for steady-state flow at any pressure difference or mass flux rate, respectively. In order to evaluate the porosity, inverse modelling of the transient gas flow using a numerical model is necessary. Well defined initial conditions have to be established before starting the flow test and additionally, the transient pressure and mass flux rates at the inflow and the outflow boundary have to be monitored. However, the necessary instrumentation for the flow test is practically the same for both needs.

Inverse modelling of the flow tests was very sensitive to certain violations of the idealizing assumptions for the numerical model. But it proved to be a valuable addition to the geometric approach which uses displacement measurements. It set the results of the geometric method into perspective and gave reason for further investigations. With respect to the final porosity in DEBORA 1 the discrepancies between the results of the geometric method and inverse modelling were explained by the results of the post-test investigations. The porosity value coming from the inverse modelling was thereby confirmed.

5 Analysis of Altered Evolution Scenarios

5.1 Introduction

In addition to the experimental investigations, model calculations were performed within the framework of the project in order to analyze brine intrusion and two-phase flow of brine and gas in sealed HLW disposal boreholes. The calculations were done with the help of the two-phase flow code MUFTE (Helmig et al., 1994). The main objective of this work was to investigate the two-phase flow processes in view of the high material parameter contrasts at discontinuities like for instance shaft-drift interface or seal-drift-interface. The dynamics of the processes were to be analysed, in order to improve the understanding of the principal mechanisms and the significance of the two-phase flow in a sealed disposal boreholes. Specific problems with the numerical models for a realistic repository in rock salt were anticipated. The behaviour of the code and the reliability of the results were therefore to be identified and analyzed as well.

The considered system consisted of a short horizontal drift and a vertical borehole which contains the waste canister stack and a seal (see Figure 5-1). Drift, seal, and annulus around the canister stack were discretized using one-dimensional elements. Each of the three parts of the model is assumed to be filled with crushed salt in a different state of compaction. The material data used are based on laboratory investigations of two-phase flow in compacted crushed salt samples (Cinar et al., 1998). They are summarized in Table 5-1 together with the system geometry and the initial and boundary conditions for the three models. Homogeneity and isothermal conditions as well as constant porosity in the crushed salt were assumed in the model while these properties are actually time dependent in reality.

Three altered evolution scenarios were investigated:

- brine inflow into the drift and subsequently into the borehole from an instantaneously flooded 500-m-high shaft
- hydrogen production in a flooded borehole due to corrosion of the HLW steel canisters
- spontaneous connection of an unexplored brine pocket with the bottom of the borehole.

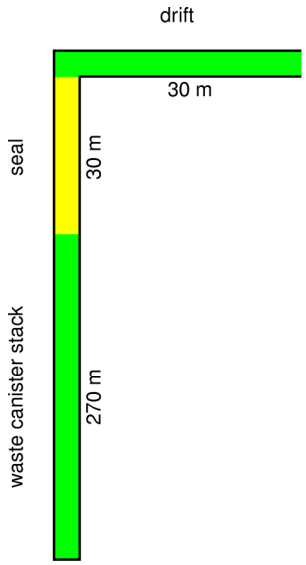

Figure 5-1 Sketch of the disposal borehole and connected drift.

Of special interest were processes like transient saturation/desaturation and gas pressure distribution in different repository regions as a function of time.

5.2 Numerical modelling

The first scenario investigated is numerically demanding due to big jumps in the variables (pressure and saturation) and changes in the material properties (permeability and equations of state for relative permeability and capillary pressure) at the interfaces between the different sealing components.

For the parameter set discussed here, the drift is flooded within one day. In the drift, the saturation of the backfill pore space with brine (see Figure 5-2) during this time is high enough to make the gas phase immobile except in the vicinity of the seal. The resulting gas pressure increase is shown in Figure 5-3.

Table 5-1 Material data, geometry, and initial and boundary conditions for the two-phase flow models.

	Annulus	**Seal**	**Drift**
height/length [m]	270	30	30
cross-section area [m^2]	0.1385	0.2827	10.50
permeability [m^2]	10^{-15}	10^{-14}	10^{-13}
porosity [-]	0.02	0.06	0.10
relative permeability after Brooks-Corey	λ=1.8095 S_{wr}=0.12 S_{nwr}=0.03	λ=1.8095 S_{wr}=0.10/014*) S_{nwr}=0.03	λ=1.8095 S_{wr}=0.10 S_{nwr}=0.03
capillary pressure after Van-Genuchten	α=4.0 n=0.0005 S_{wr}=0.08 S_{nwr}=0.02	α=4.0 n=0.000158 S_{wr}=0.08 S_{nwr}=0.02	α=4.0 n=0.0005 S_{wr}=0.08 S_{nwr}=0.02
initial brine pressure	scenario 1: 0.085 MPa scenario 2: 5 MPa in the drift and a hydrostatically increasing pressure in the borehole scenario 3: 0.085 MPa		
initial brine saturation	scenario 1: 0.14 everywhere except an exponential increase up to 1.0 at the inflow boundary (in the drift) scenario 2: 0.97 everywhere scenario 3: same as in scenario 1 with the exponential increase at the bottom of the borehole		
boundary conditions (scenario 1)	no flow		p_w = 5 MPa S_w = 100 %
boundary conditions (scenario 2)	$\dot{m}_{nw} = 9.8 \cdot 10^{-10} \frac{kg}{s\,m}$		p_w = 5 MPa S_w = 100 %
boundary conditions (scenario 3)	p_w = 8 MPa S_w = 98 %	p_w = 0.85 MPa S_w = 14 %	(not included in the model)

*) in the third model for numerical reasons (see end of this section)

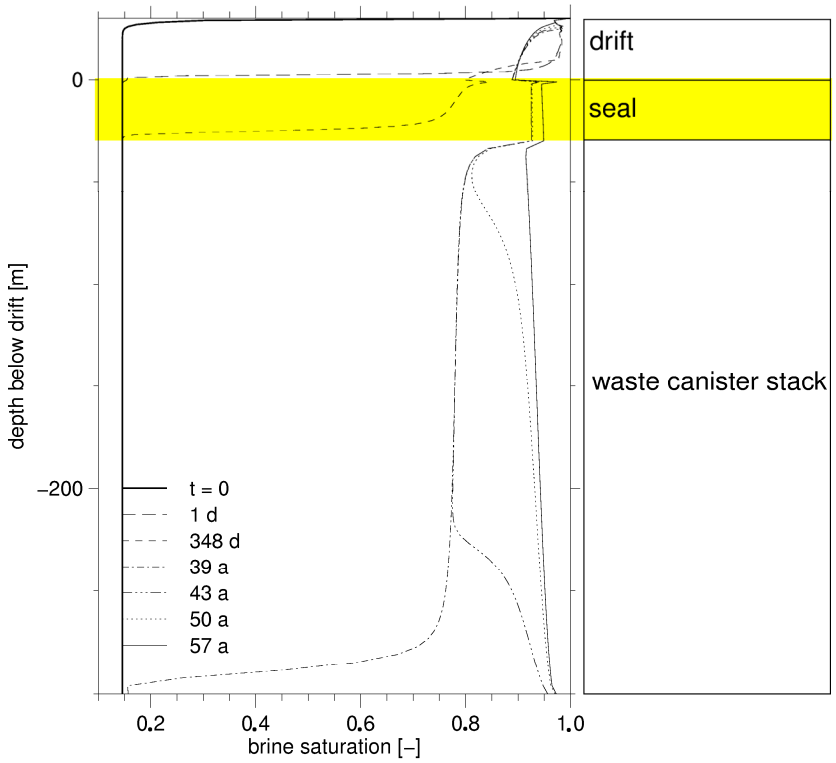

Figure 5-2 Time dependent brine saturation distribution for scenario 1.

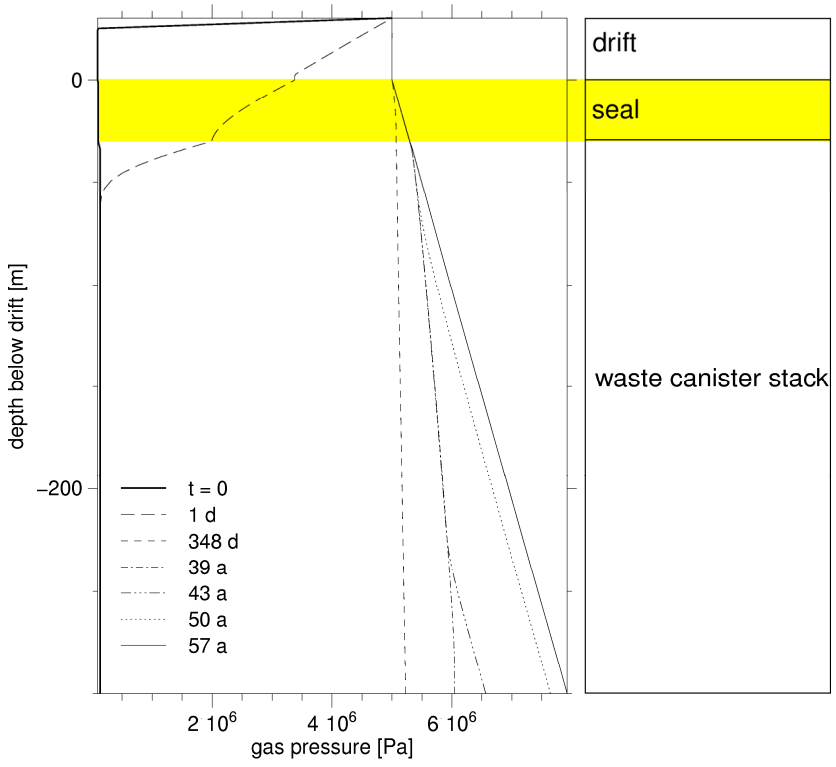

Figure 5-3 Time dependent gas pressure saturation distribution for scenario 1.

It takes about a year for the brine front to cross the seal and reach the canister stack. Gas and brine pressure are almost constant throughout the entire model at that time so that gravity and capillary pressure are the only remaining driving forces. The brine saturation in the borehole is significantly lower than in the drift allowing the gas to move upward. This is the beginning of a counter flow system in which water moves downward and pushes the gas upward and out of the system.

Brine reaches the bottom of the borehole after 40 years and afterwards the borehole becomes completely saturated from bottom to top. The velocity of this process depends on the gas mobility which in turn is inversely proportional to the brine saturation. The further the pores are filled with brine, the slower the gas flows in the remaining pore space. Most of the pore space is filled with brine within about another 20 years.

The considered gas production rate in the second scenario amounts to 9.263 kg/a for about 830 years. The figures correspond to the measured maximum corrosion rate of 60 μm /a (Smailos et al., 1992) for a material used for pollux canisters and a canister wall thickness of 5 cm.

In the second model hydrogen generation builds up gas pressure and pushes brine out of the annulus for the first few months. During this period gas flow into the seal remains insignificant due to the low mobility (compare Figure 5-4). Just before the gas finally intrudes into the seal, the gas pressure exceeds the hydrostatic pressure by almost 3 MPa at the bottom of the borehole (see Figure 5-5). Hydrogen reaches the drift after little more than one year. When this happens, the gas pressure begins to decrease again because the resistance to flow is much lower in the drift (higher permeability, porosity, and cross-section area values) than in the seal. A dynamic equilibrium in the backfilled borehole and the seal is reached after 10 years so that any gas produced after that time is stored in the drift or leaves the system, respectively.

It should be noted that during the period of dynamic equilibrium a considerable amount of hydrogen is stored in the backfilled borehole beneath the seal despite the fact that the intrinsic permeability increases from the borehole over the seal to the open boundary in the drift. But the high gas saturation at the borehole/seal-interface is needed in order to maintain the necessary gas mobility. Moreover, surprisingly high gas pressures are required in the preceding transient flow phase.

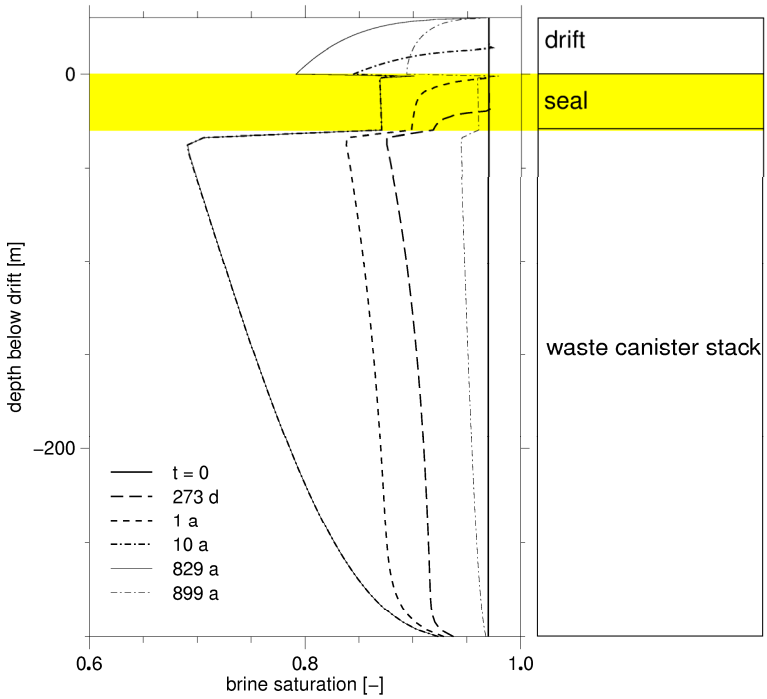

Figure 5-4 Time dependent brine saturation distribution for scenario 2.

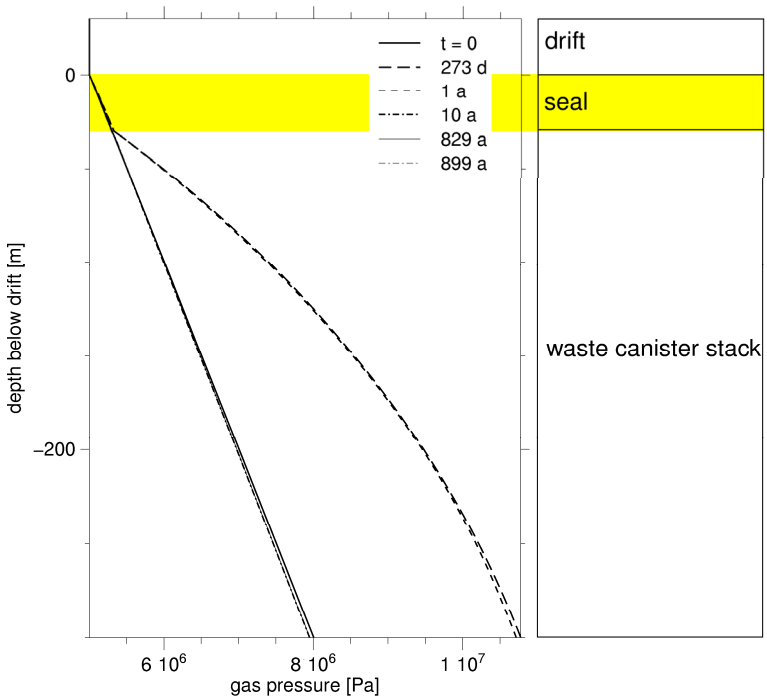

Figure 5-5 Time dependent gas pressure saturation distribution for scenario 2.

When the hydrogen production stops after 830 years, brine returns replacing the gas again. It takes about 70 years to fill most of the system.

In the third scenario the brine pocket is assumed to be large enough to keep the brine pressure of 8 MPa constant. The assumption provides an inflow rate which is consistent with a brine pocket of 200 m^3. A brine pocket of this size would be sufficient to maintain this rate until the borehole is completely filled with brine since the free pore volume in the model amounts to little more than one cubic meter.

Modelling this scenario is even more difficult than the first scenario despite the fact that the model results are quite simple. A saturation front moves upwards and leaves the system (see Figure 5-6). The front moves so slowly that the gas pressure does not rise significantly (see Figure 5-7). But the front is steeper than in scenario 1 and large oscillations (at the lower end of the front) appear and disappear during the simulation. This particular numerical behaviour is caused by the physical set-up. Flow in the upward direction means that gravity opposes the capillary forces and thereby sharpens the saturation front. The big jump in the saturation which was difficult to handle in scenario 1 is therefore maintained during the whole simulation.

5.3 Conclusions

The first two models show clearly that two-phase flow plays a vital role during brine intrusion and gas production in a repository. Both models demonstrate complex displacement processes of one phase by the other which cannot be captured by a single-phase flow model. This seems not to be the case in the third model because brine simply fills up the borehole from bottom to top. It has to be mentioned, though, that this behaviour is due to the fact that the permeability increases along the flow path. In a system where gas flow is significantly opposed by the seal the results would look rather different.

The complicated evolution of the saturation distribution could be explained satisfactorily by the principal mechanisms of the two-phase flow in all three models. However, the unusual hydraulic properties of compacted crushed salt in comparison with common soils introduce a considerable sensitivity of the results to the material parameters, initial and boundary conditions, and the structure of the repository in general.

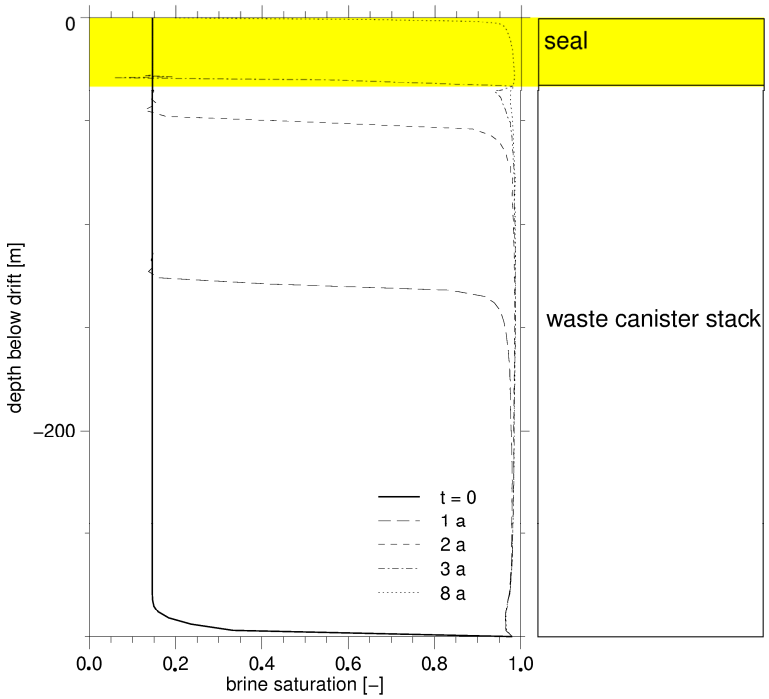

Figure 5-6 Time dependent brine saturation distribution for scenario 3.

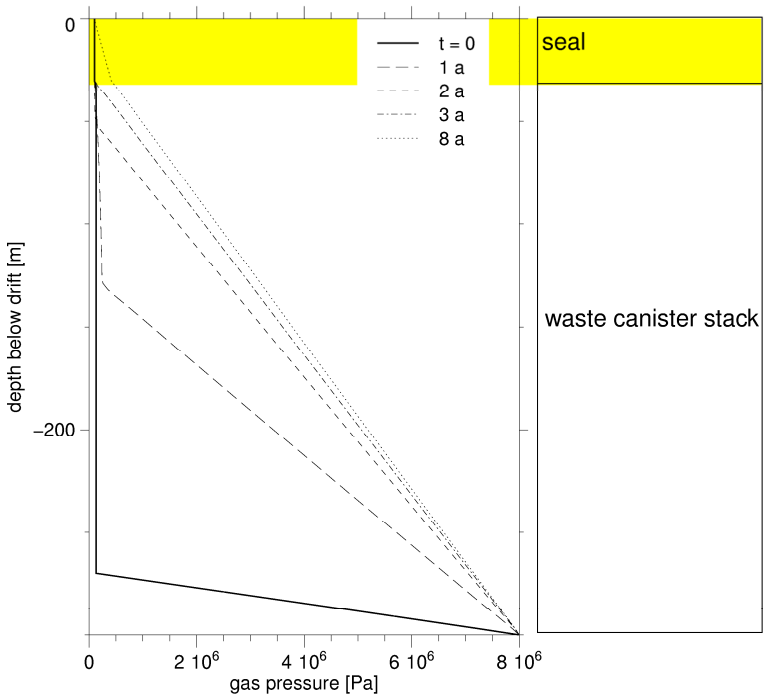

Figure 5-7 Time dependent gas pressure saturation distribution for scenario 3.

In comparison to common soil the compacted crushed salt shows very low permeability and porosity values. High contrasts exist between the materials in borehole seals and backfilled drifts. Additionally, two of the three scenarios considered require big jumps and high values of the primary and secondary two-phase flow variables. The modelling of altered evolution scenarios implies therefore demanding conditions for the numerical simulator. In this situation, it is not surprising that the results are sensitive to almost all parameters. Actual predictions need therefore a profound understanding of the material laws of compacting crushed salt and an adequate description of the repository layout.

6 Problems Encountered and Lessons Learned

6.1 Experiment Execution

An important issue in the in-situ experiments was to study the processes relevant to backfill compaction and sealing of potential flow paths in the repository. However, the lowest porosity values obtained in the in-situ experiments were 9 % in the borehole annulus, 12 % in the borehole seal.

The DEBORA experiments showed that a non-realistic experiment duration would have been required to achieve the high degrees of compaction or the low permeabilities which would be representative for long-term compacted crushed salt in a repository. For the assessment of the long-term effectiveness of borehole seals of crushed salt it is therefore indispensable to rely on model calculations. The material models used in these calculations are to be based on both, on in-situ data and on laboratory data representing the lower range of porosity and permeability missed in situ.

In the in-situ experiments, in order not to disturb the compaction process by “foreign bodies” in the backfill, instrumentation within the backfill was strongly restricted. Therefore, backfill porosities mainly were determined from borehole closure measurements by calculating the ratio between pore volume and total volume. In addition, successful attempts were made to determine the porosity by inverse modelling the gas-flow through the backfill. By these procedures, porosities were derived that were averaged over the whole test intervals.

Regarding instrument performance, it can be stated that the greatest part of the experimental equipment performed well throughout the duration of the in-situ experiments. However, malfunction of some distance gauges and pressure gauges was experienced. Instrument performance is discussed comprehensively in Section 6.2.

6.2 Instrument Performance

The overall performance of the DEBORA experiments was satisfactory with regard to their operating reliability. This can certainly be attributed to the preceding DEBORA phase I in the years 1991 – 1995 in which a detailed test plan including predictive

calculations had been set up (Rothfuchs et al., 1996). Based on these pre-investigations the measuring sensors were selected under consideration of the relevant measuring ranges and under consideration of the environmental conditions partly predicted by preceding model calculations.

The permeability measurements in the compacted crushed salt were, therefore, excellently reproducible and provided in-situ data on the relationship between permeability and porosity for the first time. This is important because this relationship is being used in long-term safety analyses considering the radionuclide transport in salt repositories.

Concerning the general applicability of the selected measuring sensors, it was found, that problems may occur if the gauges are used under severe environmental conditions as observed in DEBORA 1. Here, the underestimated corrosive atmosphere in the pore space of the backfill as well as the high stresses in the crushed salt led to a failure of some of the temperature/stress sensors and to a decrease of the signal quality of the displacement gauges during the testing period. Especially the measuring membranes of the stress sensors were damaged by the sharp edges of the salt grains pressed against the membranes. In addition, laboratory calibrations of the stress sensors, which were originally designed for measuring the pressure of fluids, showed that the sensor readings are to be corrected by about a factor of 2 when being used in crushed salt.

The uncovering of the DEBORA-1 liner enabled post-test investigations on the compacted crushed salt. These investigations revealed that the range of the displacement gauges was not large enough to evaluate the finally achieved degree of compaction at the end of the experiment.

The results of the post-test investigations confirmed that it is extremely valuable, if not indispensable, to perform, as far as possible, a final quality check of the obtained measuring data at the termination of an in-situ experiment, either by recalibration of the used measuring equipment or by post-test analyses of the considered materials.

6.3 Modelling

In the THM modelling studies there were some difficulties in quantitatively simulating the backfill compaction process and the overall experiment performance. Generally, in-

situ backfill compaction and pressure build-up was slower than predicted. Several factors were identified that may have caused these problems:

One reason for the problems in quantitatively predicting backfill compaction rates was the 3D test set-up that was modelled with the existing two - dimensional computer codes that had to be used because of the extreme computer time required for three - dimensional thermomechanical calculations. The models used were models of rotational symmetry and for the borehole geometry they represented quasi 3D models. However, the 60 m long drift above the boreholes is being modelled as a mushroom-shaped round opening with a diameter of about 5 m. This limited extension of the room in the model might cause a certain overestimation of stresses and hence of deformation especially in the early phase of the heating period.

Measurement accuracy and reliability may be a factor for problems associated with comparisons of in-situ measurement results and calculations. During the execution of the in-situ experiments most of the measurement values were obtained remotely, and drifting of the readings could neither be measured nor excluded. From these direct measurements, other values related to, for example, backfill porosity and the volumetric backfill compaction process were derived. Therefore, the question needs to be answered of how reliable the measured values are. In DEBORA 1 an attempt was made to determine the backfill porosity by a second procedure in which the porosity was calculated from the results of gas-flow tests. The porosity determined by this procedure was slightly lower than the porosity calculated from the measurements of the annulus width. Post-test measurements of the compacted backfill and sensor calibration revealed a higher accuracy of the flow-test procedure. This finding underlines the need to perform post-test investigations aimed at re-evaluating the experiment and assessing the measurement accuracy (see above).

Regardless of these findings, the data obtained constitute a firm basis for extrapolations in space and time and for assessments of the repository performance, provided the relevant parameter values are used.

Inverse modelling of the gas flow tests was very sensitive to violations of the idealizing assumptions for the numerical model. But, it proved to be a valuable addition to the geometric method which uses displacement measurements. Discrepancies between the results of the geometric method and inverse modelling were observed which gave reason for further investigations. With respect to the final porosity achieved in

DEBORA 1, the differences were explained by the results of the post-test investigations. The porosity value coming from the inverse modelling was thereby confirmed.

Predictive two-phase flow calculations for repositories in rock salt are different from modelling conventional soil systems mainly due to the hydrologic parameters of the porous media involved. The salt grit is typically rather tight and shows relatively high capillary pressures. The contrast of the material properties between different sections in the repository - like borehole seal and gallery – can easily exceed the differences between layers of natural soil formations. The results are therefore sensitive to almost all relevant model parameters: the material parameters especially the equations of state, the model geometry and the initial and boundary conditions for the considered scenarios. This implies that it is very important to know the uncertainties of the quantities mentioned above, too. Due to the strong non-linearity of the differential equations it is not possible to anticipate the sensitivity of a two-phase flow system to changes of the input parameters. Additional parameter variations are therefore necessary for a reliable interpretation of predictive model calculations.

7 Comparison of Objectives and Results

7.1 Operational Objectives

From an operational point of view, the overall objectives of the project had been separated in three work packages. In work package 1, “In-situ investigations”, the tasks were to study the backfill performance in borehole seals and in the borehole annulus. Work package 2, “Laboratory Investigations”, comprised tasks addressing backfill compaction and permeability. In work package 3, “Modelling”, codes and material models for computing the thermomechanical and hydraulical behaviour of crushed salt being used as backfill in disposal boreholes including heat sources and of the surrounding rock mass were tested and improved. As will be shown in this section, the operational objectives were achieved, and as described in Chapters 2 to 5, the tasks were carried out in accordance with planning:

The two in-situ experiments DEBORA 1 and 2 were completed within the contract period. The experiment DEBORA 1 was carried out from 17 February 1997 to 13 March 1998 and DEBORA 2 from 22 September 1997 to 4 December 1998. Heating in both experiments was terminated when almost stable conditions had been reached and the measurements showed only very minor alterations.

In the laboratory investigations, important parameters in material models for crushed salt were quantified using two triaxial test devices. Additional test were carried out to measure the development of permeability in dependence of backfill compaction.

In the THM modelling studies, the thermomechanical codes SUPERMAUS, ANSYS and MUFTE were evaluated as to their capability to simulate the behaviour of backfill and host rock under repository conditions. Additionally, the codes were employed to support the experiments’ design and to support the interpretation of in-situ measurements. By numerical simulations of the in-situ experiments using the material parameter values determined in the laboratory and by comparing the calculation results with measurements the applied models were continuously improved.

7.2 Scientific Objectives and Knowledge Gained

The main objective of phase II of the DEBORA-project was to provide the necessary experimental data and experiences needed for the valuation and confirmation of the used models.

To achieve these objectives, in-situ experiments with accompanying laboratory investigations were carried out that were aimed at evaluating the impact of heat and stress on backfill behaviour, at quantifying important parameters describing the processes, and at characterizing and modelling the thermomechanical processes in and around disposal boreholes. So it was possible to significantly improve the understanding of the processes in backfilled emplacement cavities and to increase the capability to simulate these processes numerically.

In addition, measurements were conducted in the in-situ experiments on gas transport in backfilled boreholes. In the DEBORA experiments, for the first time permeability measurements in crushed salt backfill were performed under in-situ conditions. The results obtained show that the permeability decreases by two to three orders of magnitude when the porosity decreases from e.g. 35 % to 9 % (see Sections 2.1.3 and 2.2.3). The permeability values obtained were successfully fitted to the relationship between permeability and porosity achieved from a synthesis of data of several other investigators.

The majority of the permeability measurements was performed in laboratory tests. The lowest porosity was 1.24 % (Section 3.2.3). These measurements served to complete the existing data base and to generate a relationship which could be fitted to a significant number of results from tests carried out under a wide range of temperatures and pressures. In a double-logarithmic diagram (Figure 2-28), the relationship between permeability and porosity could be fitted to a straight line. The following general relationship between permeability k and porosity ϕ was derived:

$$k = 1.9 \cdot 10^{-8} \, \phi^{5.27} \, m^2$$

In addition, it was realized that at the lowest porosities achieved the permeability still is several orders of magnitude higher than that of compact rock salt. Therefore it is to be assumed that the final transition to rock salt takes place by solution-precipitation processes, or by long-term creep of the grains, or that extremely high pressures are required.

In addition to the experimental investigations, model calculations were performed within the framework of the project in order to analyze brine intrusion and two-phase flow of brine and gas in sealed HLW disposal boreholes. The calculations were done with the help of the two-phase flow code MUFTE (Helmig et al., 1994). The analyses show that complex displacement processes of the fluid phases are to be expected in the boreholes. These processes cannot be captured sufficiently by single-phase flow models. Consideration of realistic big jumps and high values of the primary and secondary two-phase flow variables lead to demanding conditions for the numerical simulator. The results are therefore sensitive to almost all parameters. Actual predictions need therefore a profound understanding of the material laws of compacting crushed salt and a precise description of the repository layout.

8 Concluding Remarks and Recommendations

8.1 Project Performance

In the investigations carried out in the DEBORA project, the most important issues were to determine how heat from the emplaced wastes will affect the rock surrounding the repository, how backfilled boreholes in a repository will be closed, and how the porosity / permeability of the backfill material is reduced under the effect of heat and rock stress. These are issues that are closely related to the most relevant parameters in assessments of radionuclide release from a repository in rock salt (Storck, 1993).

The scientific results are described in detail in the relevant Chapters 2 to 4. A brief summary of the knowledge gained is given in Chapter 7. This section discusses the conclusions and recommendations derived from the execution of the project, and an attempt is made to demonstrate the benefits of executing a project integrating in-situ experiments, laboratory studies, and modelling studies.

In the in-situ experiments the complex processes and the interactions between heating, room closure, and backfill compaction were studied, whereas in the laboratory tests single parameter values were determined that could not be measured exactly in situ. Moreover, in laboratory tests the measuring ranges could be extended to values which were not achievable in situ, for example, to very low porosities. These values were required to develop material models that are valid over a wide range. On the other hand, the laboratory generated values could be verified by evaluating in-situ measurements.

8.2 Recommendations for Future Work

A few items were found, related both to the experimental and the modelling studies, that require further research because they may have been the reasons for deviations between calculation results and measurements. They are discussed in Chapter 6 “Problems Encountered and Lessons Learned”. In a strongly compressed version these limitations to the outcome of the project can be summarized as follows:

- achieved backfill porosities did not match long-term repository conditions,

- two-dimensional THM codes are not sufficient to simulate three-dimensional experiment behaviour,

- instrumentation accuracy and reliability could not be checked in situ,

The recommendations derived from these items are discussed below.

The lowest porosities achieved in the in-situ experiments were considerably higher than the porosities expected in a repository. In view of the duration of the in-situ experiments performed in the DEBORA project and the fact that the porosity at the end of the experiments decreased very slowly, it is evident that residual porosities of about 1 % cannot be achieved in in-situ experiments in rock salt. To gain better understanding of the final stages of backfill compaction, laboratory tests should be performed in which backfill material samples taken from the experimental boreholes and drifts are compacted further. In these tests it would be advantageous to use drill cores or cutted samples from the preconsolidated backfill. Since, as shown in the laboratory tests (Chapter 3), very high pressures and/or temperatures are required to reach residual porosities, concurrently to the tests in an iterative process mathematical models should be used to extrapolate forward the test results to the final compaction stages.

Even at the lowest backfill porosities of about 1 % achieved in the laboratory tests, the permeability was still several orders of magnitude higher than that of intact rock salt. In order to study the transition from granulated material to intact salt, additional tests are required in which processes like chemical interactions in the presence of humidity and long-term creep of salt graines should be studied in detail. Since it is considered unfeasible to reach backfill compactions similar to that of rock salt at realistic compression pressures and using dry crushed salt, the transition presumably has to be investigated under moisted conditions. The tests should be supported by numerical simulations in which the consecutive steps in the consolidation process are predicted.

Most of the instruments performed well in the experiments. However, some failures occurred and some measurement results were difficult to interpret. To guarantee high measurement reliability, it is important already in the conceptual-design phase of an experiment to define and to rank the most important parameters to be investigated and to design the monitoring system accordingly. In the design not only the feasibility of redundancy, diversity, and symmetry should be taken into account, but also the

intrinsic maximum accuracy of the measurement system. In the experiment design concept also the effects of limited experiment dimensions, i.e., three - dimensional behaviour and boundary effects should be taken into account. Since during the experiment execution a drifting of the instruments' reading cannot be excluded, the measurement stability should be assessed by re-calibrating the instruments in-line, that is during the experiment execution, or after terminating the experiment.

Several tasks mentioned previously could only be accomplished by post test analyses which consisted of entering the experimental areas and dismantling the test set-up. In this programme, samples were taken from the backfill and instruments were retrieved for re-calibration. Additional components of a dismantling and validation programme were laboratory tests on the recovered backfill material. The post test analyses were found to be extremely useful since they helped to solve questions raised by deviating measuring and calculation results. In future in-situ experiments, a post-test analysis programme should therefore always be considered as a central component, already in the planning phase.

Numerical simulations of two-phase flow of gas and brine in backfilled HLW disposal boreholes suffered of missing parameter functions for relative permeability and capillary pressure of crushed salt. As a first attempt, existing data for common soil were used to perform an analysis of the considered processes and to conclude on their significance. In order to confirm the obtained results on dynamics and consequences of brine intrusion into an HLW repository, laboratory determination of the respective two-phase flow parameters is indispensable.

References

Albrecht, H., Hunsche, U., (1980): “Gebirgsmechanische Aspekte bei der Endlagerung radioaktiver Abfälle in Salzdiapiren unter besonderer Berücksichtigung des Fließverhaltens von Steinsalz”, Fortschr. Miner., 58(2): 212-247, Stuttgart.

Barnert, E., Brücher, H., Kroth, K., (1994): "Abschlußbericht zum Forschungsvorhaben "MAW- und HTR-BE-Versuchseinlagerung in Bohrlöchern - Teilprojekt Einlagerungs- und Bohrlochverschlußtechnik", KFA-Forschungszentrum Jülich GmbH, Jülich.

Bechthold, W., Rothfuchs, T., Poley, A., Ghoreychi, M., Heusermann, S., Gens, A., Olivella, S., (1999): “Backfilling and Sealing of Underground Repositories for Radioactive Waste in Salt (BAMBUS Project)”, EUR 19124 EN, CEC, Luxembourg

Breidenich, G., (1993): "Gekoppelte Berechnung der thermomechanischen Feldgrößen in einer Steinsalzformation infolge der Einlagerung radioaktiver wärmefreisetzender Abfälle", doctoral thesis, RWTH Aachen.

Cinar, Y., Müler, W., Pusch, G., Reitenbach, V., (1998): "Gas Migration in Salt, Part II: Experimental Work". In European Commission Report: Projects on the Effect of Gas in Underground Storage Facilities for Radioactive Waste (Pegasus Project), Proceedings of a progress meeting in Naantali, Finland, DOC XII/276/98-EN.

Duddeck, H., Guericke, B., (1995): "Der Einfluß des interaktiven Verhaltens von Gebirge und Deponat auf die geotechnische Standsicherheitsbeurteilung unterirdischer Entsorgungsanlagen", Proceedings of "Untertätige Entsorgung - Zweites Projektstatusgespräch des PTE zu BMBF-geförderten FuE-Vorhaben zur untertägigen Entsorgung chemisch-toxischer Abfälle am 5. und 6. Oktober 1995 in der Technischen Universität Freiberg", Forschungszentrum Karlsruhe GmbH, Karlsruhe.

Hein, H. J., (1991): "Ein Stoffgesetz zur Beschreibung des thermomechanischen Verhaltens von Salzgranulat", doctoral thesis RWTH Aachen.

Helmig, R., Braun, C., Emmert, M., (1994): "MUFTE - A numerical model for simulation of multiphase flow processes in porous and fractured-porous media", Programmdokumentation (HG 208). Technical Report 94/3, Institut für Wasserbau, Universität Stuttgart.

Hunsche, U., (1984): “Results and Interpretation of Creep Experiments in Rock Salt”. In: The Mechanical Behaviour of Salt, Proc. of the First Conf. Univ. Park (USA), Eds.: Hardy, H. R. Jr. & Langer, M., Trans Tech Publications, Clausthal, 159-167.

Jockwer, N., Rothfuchs, T., (1995): “Investigations and modelling of fluid release from rock salt at elevated temperature”, Proc. Workshop Testing and Modelling od Thermal, Mechanical and Hydrogeological Properties of Host Rocks for Deep Geological Disposal of Radioactive Waste, EUR 16219 EN, CEC, Brussels

Karman, P.C., (1956): “Flow of Gases through Porous Media”, Butterworths Scientific Publications, London.

Kröhn, K.-P., Fein, E., (1999): "Einfluß von Meßtoleranzen auf den Gesamtfehler bei der Bestimmung von Permeabilität und Porosität am Beispiel des DEBORA-Experiments 1", GRS-Bericht, (in Vorbereitung).

Leibholz, H., (1968): "Einführung in die Elastizitätstheorie", Reihe Wissenschaft und Technik, Verlag G. Braun, Karlsruhe.

Müller-Lyda, I., Birthler, H., Fein, E., (1999): "Ableitung von Permeabilitäts-Porositätsrelationen für Salzgrus", Gesellschaft für Anlagen- und Reaktorsicherheit (GRS) mbH, GRS-148, Köln

PSE: Projekt Sicherheitsstudien Entsorgung (PSE), (1985): "Entwicklung eines sicherheitsanalytischen Instrumentariums für das geologische Endlager für radioaktive Abfälle in einem Salzstock", zusammenfassender Abschlußbericht, Hahn Meitner Institut für Kernforschung, Berlin.

Rieckmann, M., (1970): "Untersuchungen von Turbulenzerscheinungen beim Fließen von Gasen durch Speichergesteine unter Berücksichtigung der Gleitströmung", Erdöl-Erdgas-Zeitschrift, Bd. 86, Heft 2.

Rothfuchs, T., Prij, J., Kröhn, K.-P., van den Horn, B.A., Wieczorek, K., (1996): "The DEBORA-Project Phase 1: Development of Borehole Seals for High-Level Radioactive Waste Repositories in Salt Formations", Final Report, EUR 16928 EN, CEC, Brussels.

Smailos, E., Schwarzkopf, W., Kienzler, B., Köster, R., (1992): "Corrosion of Carbon-Steel Containers for Heat-Generating Nuclear Waste in Brine Environments Relevant for a Rock-Salt Repository", Mat. Res. Soc. Symp. Vol. 257.

Spiers, C. J., Bzesowsky, R.H., (1993): "Densification Behaviour of Wet Granulat Salt: Theory versus Experiment", Universität Utrecht.

Storck, R., (1993): “Langzeitsicherheitsnachweise unter Berücksichtigung von Unsicherheiten”, Atomwirtschaft, 38, 285.

Swanson Analysis Systems, (1992): "ANSYS User's Manual, Houston".

Wallner, M., Caninenberg, C., Gonther, H., (1979): “Ermittlung zeit- und temperaturabhängiger mechanischer Kennwerte von Steinsalz”, Proc. 4th Int. Congress Rock Mechanic, Vol 1, Montreux, 313.

Wieczorek, K., Zimmer, U., (1998): "Untersuchungen zur Auflockerungszone um Hohlräume im Steinsalzgebirge", Abschlußbericht, Gesellschaft für Anlagen- und Reaktorsicherheit (GRS) mbH, GRS-A-2651, Köln

Zhang, C., Schmidt, M. W., Staupendahl, G., Heemann, U., (1993): "Entwicklung eines Stoffansatzes zur Beschreibung des Kompaktionsverhaltens von Salzgrus", Bericht Nr. 93-73 des Instituts für Statik der Technischen Universität Braunschweig, gemeinsame Veröffentlichung mit dem GSF-Institut für Tieflagerung Braunschweig.

List of Figures

List of Tables

Gesellschaft für Anlagen- und Reaktorsicherheit (GRS) mbH

Schwertnergasse 1
50667 Köln
Telefon +49 221 2068-0
Telefax +49 221 2068-888

Forschungsinstitute
85748 Garching b. München
Telefon +49 89 32004-0
Telefax +49 89 32004-300

Kurfürstendamm 200
10719 Berlin
Telefon +49 30 88589-0
Telefax +49 30 88589-111

Theodor-Heuss-Straße 4
38122 Braunschweig
Telefon +49 531 8012-0
Telefax +49 531 8012-200

www.grs.de

ISBN 3-931995-26-7